and radio frequency regions (chiral photon beams); spin-polarized electron beams; spin polarized neutrons; and so on. These will result in dichroism or differential scattering which may be attributed to the non-Newtonian effects of electroshearing.

6. Magnetic resonance phenomena may be utilized similarly to investigate non–Newtonian electroshearing. The symmetry argument in this instance constructs a chiral medium using a combination of shear and alternating electric field, and uses a chiral probe consisting of a static magnetic field combined with the same alternating electric field. Both probe and medium are negative to parity inversion and positive to time reversal, and both satisfy Barron's definition[279] of chirality. The apparatus can be imagined to consist of the electroshearing unit with good conducting electrodes such as brass or silver (nonmagnetic) embedded in a solenoid, or put between the pole pieces of a powerful magnet. The chiral probe field is a combination of the static magnetic field and alternating electric field applied between the (counterspinning) silver electrodes. The same ac electric field is used for the electric component of electroshearing, that is, to create the chiral medium. Thus, according to the handedness of the probe and medium, there will be asymmetric attenuation of the magnetic field, a kind of dichroism (and therefore birefringence) which could be detected through magnetic properties such as nuclear magnetic resonance and its relaxation. The NMR features would depend on the non–Newtonian nature of the sample's response to electroshearing. Conventional NMR technology could be implemented, the alternating electric field allowing fine tuning of the chirality of both probe and medium. The expected magnetic effects will be asymmetric in the handedness of the chiral probe, or alternatively of the medium, adding extra observables.

IX. NEW PUMP–PROBE LASER SPECTROSCOPIES: SYMMETRY AND APPLICATION TO ATOMIC AND MOLECULAR SYSTEMS

A. Basic Symmetry Concepts

We have seen in Sections VII and VIII that symmetry is one of the cornerstones of the scientific edifice, and in chemical spectroscopy has a particularly elegant historical facade. By the early 1840s Michael Faraday had convinced himself that there is an ineluctable link between electric and magnetic fields and light. In 1846 he proved this to the world[338] using static magnetic flux density (**B**) to rotate the plane of polarization of light passing through lead borate glass. In his own words, he had magnetized and electrified a ray of light. Maxwell's equations met the challenge of

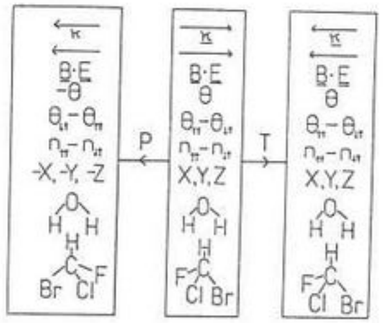

Figure 49. Schematic of motion-reversal symmetry.

Faraday's work, and shed light of their own.[339,340] Much of what we know still relies directly on the work of Faraday and Maxwell, with a little retrospective wisdom from the intervening years.

Some of this allows us to see now that if Faraday had attempted to rotate the plane of his ray of light with static electric field strength (**E**), he would have seen nothing.[341] (A diary entry, reviewed by Bragg[342] suggests that Faraday did indeed try the experiment with a static electric field, and briefly noted "no effect".) This has to do with two of the profound symmetry principles of physics,[343] those of reversality and parity inversion, first proposed in 1927 by Wigner.[344]

B. Complete Experiment Symmetry

1. *Wigner's Principle of Reversality* (T)

If a complete experiment is realizable in the laboratory frame (X, Y, Z), then it must also be so when all motions are reversed.

2. *Wigner's Principle of Parity Inversion* (P)

If a complete experiment is realizable in (X, Y, Z), then it must also be so in the frame ($-X$, $-Y$, $-Z$), with all position coordinates reversed.

These deceptively simple statements contain the key to why **B**, but not **E**, rotates the plane of polarization of electromagnetic radiation in an atomic or molecular ensemble. They also underline a central theme of this section, that if we were to find an influence, which we call **Π**, that has the same T and P symmetry as **B**, Wigner's Principles would allow it to rotate plane-polarized light, causing circular birefringence and dichroism.[345] We describe later how **Π** is generated by the conjugate product of a powerful circularly polarized "pump" laser, such as a neodymium-doped yttrium aluminium garnet (Nd:YAG) laser, or dye laser, propagating parallel to the "probe" light beam. The latter may be another, tunable, laser, or broad-band radiation from a contemporary interferometric spectrometer.

Figures 49 and 50 illustrate the application of Wigner's Principles to

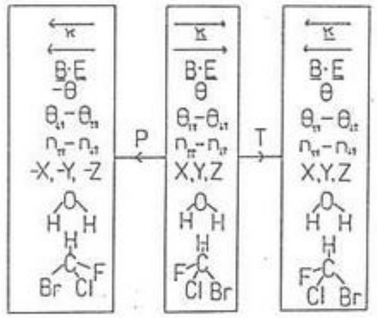

Figure 50. Schematic of parity-inversion symmetry.

the Faraday Effect. They contain the variables of the complete experiment: the propagation vector ($\boldsymbol{\kappa}$) of the probe laser, parallel or antiparallel to **B**; the laboratory frame of reference (X, Y, Z); the angle, $\Delta\theta$, through which the plane of polarization of the laser is rotated; and the molecular structure, which can be achiral or chiral. The former is represented by water, and the latter by an enantiomer of bromochlorofluoromethane. Figure 49 deals with the effect of T, which is motion reversal. Under T, the ray of light moves in the opposite direction, so that $\boldsymbol{\kappa}$ changes sign. Static magnetic flux density **B** is an axial vector which also reverses sign under T. It is the curl, $\nabla \times \mathbf{A}$, of the vector potential[286] **A**. The angle of rotation, the frame (X, Y, Z), and the molecular structures are unaffected by T, because they are motion-independent. The angle $\Delta\theta$ depends on the circular polarity of the light, a plane-polarized probe laser being made up in equal parts of right- and left-handed components, the mathematical descriptions of which are given later in this section. If a right-handed screw is reversed in motion, its pitch, or screw sense, is not changed by T. However, it is customary to define right circular polarity as clockwise rotation of the electric field vector as the propagation vector travels towards an observer. The effect of motion reversal, T, is to change clockwise motion to anticlockwise, so that T reverses circular polarity from right to left or vice versa. T also reverses the propagation vector, but clearly leaves the product of this with the circular polarity unchanged. It is this product that we have described as the "screw sense" of the electromagnetic wave. The result of applying T is shown in Fig. 49, the motion-reversed variables are relatively in the same configuration. For example, if $\boldsymbol{\kappa}$ had been parallel to **B**, it remains parallel, and has not become antiparallel. The vector product $\boldsymbol{\kappa} \cdot \mathbf{B}$ has not changed sign. Its symmetry representation, denoted $\Gamma(\boldsymbol{\kappa} \cdot \mathbf{B})$, has remained the same under T. Similarly, the sign of $\Delta\theta$ is the same, and also (X, Y, Z) and the achiral and chiral molecular structures. The Faraday effect is an "observable," because the motion-reversed experiment is realizable.

TABLE III
P and I Symmetries of $\boldsymbol{\kappa}$, **B**, and **E**

	P	T
$\boldsymbol{\kappa}$	−	−
B	+	−
E	−	+

In Fig. 50 the operator P is applied to the same variables as those of Fig. 49. P has the following effect on position, **q**, and momentum, **p** (Section V):

$$(\mathbf{q}, \mathbf{p}) \rightarrow (-\mathbf{q}, -\mathbf{p}) \tag{404}$$

and leaves the sign of time, t, unchanged. The propagation vector, $\boldsymbol{\kappa}$, being a photon momentum,[346] is reversed by P. The magnetic flux density **B** is not, essentially because it is generated[286] by a cylindrical current flow, whose sense of rotation is reversed by T but not by P. (In contrast, **E** is generated by two electrodes, one positively and the other negatively charged. Under P the positions of the plates are reversed, but the charges are not, so that **E** changes sign. T does not affect the stationary charges, so **E** does not change sign under T. It is invariant, i.e., positive, to T). P also makes a right-handed screw into a left-handed screw, and so reversed the circular polarity of the probe laser. It reverses the sign therefore, of $\boldsymbol{\kappa}$. It reverses the frame of reference, that is, $(X, Y, Z) \rightarrow (-X, -Y, -Z)$, and inverts the positions of all atoms of a molecule. It generates the opposite enantiomer, therefore, of a chiral molecule. These effects are summarized in Fig. 50. In the P-inverted experiment, everything has reversed in sign, but relative to each other, the variables have remained the same. The Faraday effect is again an "observable," because the P-inverted experiment is realizable.

The P and T symmetries of the variables $\boldsymbol{\kappa}$, **B**, and **E** are summarized in Table III. We see that $\boldsymbol{\kappa}$ is a "time odd, parity odd" variable; **B** is "time odd, parity even;" and **E** is "time even, parity odd."

It is known[342] that Faraday attempted to substitute **E** for **B** when examining the lead borate glass and recorded "no effect." How do these symmetry principles explain this? If we examine Figs. 49 and 50, it becomes clear that T has the effect

$$\Gamma(\boldsymbol{\kappa} \cdot \mathbf{E}) \xrightarrow{T} -\Gamma(-\boldsymbol{\kappa} \cdot \mathbf{E}) \tag{405}$$

on the vector product of $\boldsymbol{\kappa}$ and $\mathbf{E}$, showing immediately that $\mathbf{E}$ cannot rotate the plane of a light ray without violating the Wigner Reversality Principle. This is because the motion-reversed variables do *not* have the same relative sign, that is, $\boldsymbol{\kappa} \cdot \mathbf{E}$ is reversed, but the others are not. Therefore the *static* $\mathbf{E}$ equivalent of the Faraday effect is said to violate T. A $\Delta\theta$ observed under these conditions would be a "nonobservable", that is, a symmetry-violating observable.[346] Similarly P does not reverse the product $\boldsymbol{\kappa} \cdot \mathbf{E}$ (Table III), but reverses all the other variables in Fig. 50. The $\mathbf{E}$ equivalent of the Faraday effect also violates the Wigner Principle of Parity Inversion. Even if it did not violate T, it could only be observed, in consequence, in chiral ensembles. The group theory introduced later makes this point clearer.

It appears that $\Delta\theta$ has never been observed with $\mathbf{E}$ substituted for $\mathbf{B}$ in this context. If it were, unequivocally, it would signal the presence of a T-violating phenomenon (i.e., nonconservation of reversality), something which has been observed only once, and indirectly, in nuclear physics.[347] In contrast, the Wigner Principles allow the Faraday effect both in achiral and chiral ensembles, and this is what is observed experimentally.[286] P-violating phenomena were first predicted and observed in nuclear physics in the mid-1950s,[348] leading to the unification of the electromagnetic and weak forces,[349] the well-known CERN Experiment,[350] and to the expectation that P-violating phenomena pervade the whole of atomic and molecular spectroscopy,[351] one of the foremost achievements of science in this century. It is part of the purpose of this section to try to prepare theoretically for experiments to observe these P-violating phenomena spectroscopically.

C. The Symmetry of Cause and Effect: Group Theoretical Statistical Mechanics[352]

If an experiment conserves the Wigner P and T Principles, we can proceed with an investigation of the symmetries of cause and effect. These are subtle concepts, needing for clarity the language of group theory,[353] as described in Sections VII and VIII. The Neumann–Curie, or first, principle, as we have seen, holds for thermodynamic equilibrium when entropy is not changing systematically. In the rise transient condition[354] just after a field has been applied, for fall transients just after an applied field has been removed,[355] or in the steady state in the presence of an external field,[356] it is supplemented by a cause–effect principle which we have called the third principle of group theoretical statistical mechanics (gtsm).[352] The second principle is the equivalent of principle one applied[357] to a molecule-fixed frame of reference. The point groups of relevance refer, as we have seen, to the *ensemble* rather than the molecule itself,

the group $R_h(3)$ for achiral ensembles, and the group $R(3)$ for ensembles of chiral molecules. The former is the group[352] of all rotations and "reflections" (more accurately parity inversions) about an origin (or "point") in frame (X, Y, Z); and the latter is the group of all rotations only, because reflection in $R(3)$ would result in the opposite enantiomer, a different physical entity. In consequence, "reflection" (i.e., parity inversion) is not a valid group theoretical operation of $R(3)$.

The irreducible representations of $R_h(3)$ are the D symbols,[286] which are subscripted u or g, respectively, negative and positive to parity inversion. They are superscripted by a number ranging from 0 to n, indicating tensor order. The D symbols can be used to denote the symmetry of an ensemble average in $R_h(3)$ (Section VII). For example, the symmetry of $\langle m \rangle$, where m is a scalar quantity (zero rank tensor) such as mass, is $D_g^{(0)}(+)$. This is the totally symmetric irreducible representation (tsr), and principle one indicates that $\langle m \rangle$ is a finite quantity in frame (X, Y, Z). The plus sign in brackets denotes positive to T. The average $\langle \mathbf{v} \rangle$, where $\mathbf{v}$ is molecular center of mass velocity, vanishes in (X, Y, Z) by principle one, because its symmetry in $R_h(3)$ is $D_u^{(1)}(-)$, denoting an odd parity polar vector (a tensor of rank 1), which is negative to T. The average $\langle \boldsymbol{\omega} \rangle$, where $\boldsymbol{\omega}$ is molecular angular velocity, has the symmetry $D_g^{(1)}(-)$, and also vanishes by principle one because it does not contain the tsr of $R_h(3)$.

In the point $R(3)$ of chiral ensembles, the irreducible representations are D symbols without subscripts, because parity inversion in $R(3)$ is not a valid group theoretical operation, as we have seen. The symmetry of $\langle m \rangle$ in $R(3)$ is therefore $D^{(0)}(+)$, which is the tsr. The symmetries of $\langle \mathbf{v} \rangle$ and of $\langle \boldsymbol{\omega} \rangle$ are the same in $R(3)$: $\mathrm{D}^{(1)}$ $(-)$. This does not contain the tsr of R(3), and in consequence, both $\langle \mathbf{v} \rangle$ and $\langle \boldsymbol{\omega} \rangle$ vanish in a chiral ensemble at field-free equilibrium.

D. The D Symmetries of Natural and Magnetic Optical Activity

The rotation of plane-polarized electromagnetic radiation by $\mathbf{B}$, the Faraday effect, is often referred to as "magnetic optical activity."[286] It occurs both in $R_h(3)$ and $R(3)$, and its symmetry is that of $\mathbf{B}$ itself,[358] that is, $D_g^{(1)}(-)$ in $R_h(3)$ and $D^{(1)}$ $(-)$ in $R(3)$. It is therefore "time odd" and vanishes in the absence of an external influence which is also time odd. This may be $\mathbf{B}$, but, using principle three, may also be the conjugate product $\boldsymbol{\Pi}$ of a pump laser,[359–362] a simple statement with many consequences, some of which are described later in this review.

Rotation of plane-polarized radiation is observed in a chiral ensemble without $\mathbf{B}$ or $\boldsymbol{\Pi}$, and is called "natural optical activity." It is therefore a property of $R(3)$ only, and must also pass the test[286] of Wigner's Principles at field-free equilibrium. If we remove $\mathbf{B}$ from Fig. 49 it becomes clear

TABLE IV
Some Combined Field Symmetries

Tenor	$\hat{P}$	$\hat{T}$	$R_h(3)$	$R(3)$
E	−	+	$D_u^{(1)}$	$D^{(1)}$
Eκ	+	−	$D_g^{(0)} + D_g^{(1)} + D_g^{(2)}$	$D^{(0)} + D^{(1)} + D^{(2)}$
Bκ	−	+	$D_u^{(0)} + D_u^{(1)} + D_u^{(2)}$	$D^{(0)} + D^{(1)} + D^{(2)}$
B	+	−	$D_g^{(1)}$	$D^{(1)}$
EE	+	+	$D_g^{(0)} + D_g^{(1)} + D_g^{(2)}$	$D^{(0)} + D^{(1)} + D^{(2)}$
BB	+	+	$D_g^{(0)} + D_g^{(1)} + D_g^{(2)}$	$D^{(0)} + D^{(1)} + D^{(2)}$
EB	−	−	$D_u^{(0)} + D_u^{(1)} + D_u^{(2)}$	$D^{(0)} + D^{(1)} + D^{(2)}$
EBκ	+	+	$D_g^{(0)} + 3D_g^{(1)} + 2D_g^{(2)} + D_g^{(3)}$	$D^{(0)} + 3D^{(1)} + 2D^{(2)} + D^{(3)}$

that in the motion-reversed experiment, all variables for natural optical activity are reversed, that is, are relatively unchanged, and Wigner reversality is satisfied. In Fig. 50 with **B** missing, P has changed the sign of **κ**, has produced the opposite enantiomer of bromochlorofluoromethane, and has changed the sign of the angle of rotation. In a chiral ensemble, the P-inverted complete experiment is possible, because the relevant variables are relatively unchanged. In an achiral ensemble, however, P results in a water structure (Fig. 50) which is indistinguishable from the original. The molecular structure is plus to P, while all others are minus. In consequence, Wigner's P principle is not obeyed, and natural optical activity is not observable in an achiral ensemble at field-free equilibrium in the absence of parity violation[363] due to electroweak interactions.

The symmetry of natural optical activity is therefore that of a pseudoscalar in $R(3)$, denoted by $D^{(0)}(+)$, the tsr. By principle one its ensemble average is nonzero, and changes sign between enantiomers. It exists at equilibrium and is positive to T. It has no equivalent in the point group $R_h(3)$ in the absence of parity violation. In consequence, the symmetries of natural and magnetic optical activity are given different signatures.[364]

E. Application of gtsm—Combined Field Symmetries

The basic symmetries of Table III allow the definition of combined field symmetries.[364] Define the combined D symmetry of a tensor product[364] such as $\mathbf{E}_i\mathbf{B}_j$ as the complete product of their individual symmetry representations in the appropriate point group of the ensemble. This gives the results of Table IV where **κ** is the laser propagation vector, which is negative to P and T.[365] This may be the propagation vector of a probe or pump laser.

In classical electromagnetic field theory, rank zero natural optical rotation is $D^{(0)}(+)$ in $R(3)$ and $D_u^{(0)}(+)$ in $R_h(3)$. The equivalents for magnetic optical activity are $D^{(1)}(-)$ and $D_g^{(1)}(-)$, respectively, the quantities in brackets denoting positive or negative to motion reversal T. Table V is a summary of effects.

TABLE V
Summary of Field-Induced Optical Activity

Tensor	Occurrence of Signature			
	$D_u^{(0)}$ (+)	$D_g^{(1)}$ (−)	$D^{(0)}$ (+)	$D^{(1)}$ (−)
E	No	No	No	No
Eκ	No	Yes	No	Yes
Bκ	Yes	No	Yes	No
B	No	Yes	No	Yes
EE	No	No	Yes	No
BB	No	No	Yes	No
EB	No	No	No	Yes
EBκ	No	No	Yes	No

Ross et al. have given an equivalent analysis in terms of photon selection rules.[366] Their results can be obtained by this application of gtsm to **E**, **B**, and **κ**.

Table V shows, for example, that the application of a static electric field strength **E** produces neither natural nor magnetic optical activity, leading to no effect, as first noted by Faraday.[342] The magnetic flux density **B** produces magnetic optical activity; the product **Bκ** has been used by Barron[367] and the present author[297] to define the Wagnière–Meier effect (forward–backward birefringence[306–308] due to **B** coaxial with **κ** of an unpolarized probe laser). By reference to Table V this product contains the symmetry of natural optical activity. An interesting example[368] is the combined **EB** symmetry, which produces magnetic optical activity in chiral ensembles only, implying that a type of "Faraday effect" can be obtained in chiral ensembles with a combination of electric field strength and magnetic flux density. This is discussed in detail in Refs. 368 and 369.

F. Application of gtsm to Nonlinear Optical Activity

Nonlinear optics is an important part of chemical physics, and in classical terms, involves quantities nonlinear in the complex conjugates[297,370] of the electric and magnetic field components of the classical electromagnetic field from Maxwell's equations. In general, these have plus (+) and minus (−) complex conjugates, and are right or left circularly polarized:[297, 370]

$$\left.\begin{aligned}
\mathbf{E}_L^- &= E_0(\mathbf{i} + i\mathbf{j})e^{-i\theta_L}; & \mathbf{E}_L^+ &= E_0(\mathbf{i} - i\mathbf{j})e^{i\theta_L} \\
\mathbf{E}_R^- &= E_0(\mathbf{i} - i\mathbf{j})\mathbf{e}^{-i\theta_R}; & \mathbf{E}_R^+ &= E_0(\mathbf{i} + i\mathbf{j})\mathbf{e}^{i\theta_R} \\
\mathbf{B}_L^- &= B_0(\mathbf{j} - i\mathbf{i})e^{-i\theta_L}; & \mathbf{B}_R^- &= B_0(\mathbf{j} + i\mathbf{i})e^{-i\theta_R} \\
\mathbf{B}_L^+ &= B_0(\mathbf{j} + i\mathbf{i})e^{i\theta_L}; & \mathbf{B}_R^+ &= B_0(\mathbf{j} - i\mathbf{i})e^{i\theta_R} \\
\theta_L &= \omega t - \boldsymbol{\kappa}_L \cdot \mathbf{r}; & \theta_R &= \omega t - \boldsymbol{\kappa}_R \cdot \mathbf{r}
\end{aligned}\right] \tag{406}$$

In a laser propagating in Z of the laboratory frame (X, Y, Z), $\mathbf{i}$ and $\mathbf{j}$ here are unit vectors in X and Y, ω is the frequency of the field, and $\boldsymbol{\kappa}$ its wave vector. The position vector is denoted $\mathbf{r}$.

With these definitions,[297, 371] the electric dipole moment of a molecule in a strong laser field can be expressed as the double Taylor expansion[371]

$$\begin{aligned}
\mu_i = \mu_{0i} &+ \alpha_{1ij}E_j + \alpha_{2ij}B_j + \frac{1}{2!} \\
&\times (\beta_{1ijk}E_jE_k + \beta_{2ijk}E_j\beta_k + \beta_{3ijk}B_jE_k + \beta_{4ijk}B_jB_k) \\
&+ \frac{1}{3!}(\gamma_{1ijkl}E_jE_kE_l + \cdots + \gamma_{8ijkl}B_jB_kB_l) \\
&+ \cdots
\end{aligned} \tag{407}$$

in which all quantities are in general complex.[371] Similarly, the molecular magnetic dipole moment can be double Taylor expanded as

$$\begin{aligned}
m_i = m_{0i} &+ a_{1ij}B_j + a_{2ij}E_j + \frac{1}{2!} \\
&\times (b_{1ijk}B_jB_k + b_{2ijk}B_jE_k + b_{3ijk}E_jB_k + b_{4ijk}E_jE_k) \\
&+ \frac{1}{3!}(g_{1ijkl}B_jB_kB_l + \cdots + g_{8ijkl}E_jE_kE_l) \\
&+ \cdots
\end{aligned} \tag{408}$$

For example, the dynamic molecular property tensor α_{1ij} is the complex polarizability, α_{2ij} is the Rosenfeld tensor, and so on. The quantity μ_{0i} is the permanent molecular dipole moment in the absence of the laser field.

The accepted definition of rotational strength in linear optics is the Rosenfeld tensor α_{2ij}, which contains a tensor product of the molecular

TABLE VI
D Symmetries of Molecular Properties and Field Tensors for Optical Rotation: Point Group $R_h(3)^a$

Molecular Property		Field		Part of Dipole Moment	$D_u^{(0)}$	Order
α_2	$D_u^{(0)} + D_u^{(1)} + D_u^{(2)}(-)$	B	$B_g^{(1)}(-)$	μ	1	1
α_2		E	$D_u^{(1)}(+)$	m	1	1
β_1		EE	$D_g^{(0)} + D_g^{(1)} + D_g^{(2)}(+)$	μ	1	2
β_4	$D_u^{(0)} + 3D_u^{(1)} + 2D_u^{(2)} + D_u^{(3)}(+)$	BB	$D_g^{(0)} + D_g^{(1)} + D_g^{(2)}(+)$	μ	1	2
b_2		BE	$D_u^{(0)} + D_u^{(1)} + D_u^{(2)}(-)$	m	1	2
b_3		EB	$D_u^{(0)} + D_u^{(1)} + D_u^{(2)}(-)$	m	1	2
γ_2		EEB		μ	3	3
γ_3		EBE		μ	3	3
γ_5	$3D_u^{(0)} + 6D_u^{(1)} + 6D_u^{(2)}$	BEE	$D_g^{(0)} + 3D_g^{(1)} + 2D_g^{(2)} + D_g^{(3)}(-)$	μ	3	3
γ_8	$+3D_u^{(3)} + D_u^{(4)}(-)$	BBB		μ	3	3
g_2		BBE		m	3	3
g_3		BEB	$D_u^{(0)} + 3D_u^{(1)} + 2D_u^{(2)} + D_u^{(3)}(+)$	m	3	3
g_5		EBB		m	3	3

[a] For $R(3)$ remove g or u subscripts.

electric and magnetic dipole moments.[372] This can be seen at first order multiplying B_j in the expansion (407) of the electric dipole moment.

Applying gtsm we arrive at the classification scheme of Table VI.

From Table VI it can be deduced[371] that natural optical rotation to a given order in **E** and/or **B** occurs if the mediating property tensor contains the signature $D_u^{(0)}(\pm)$, with either a negative or positive T signature. The equivalent signature in $R(3)$ is $D^{(0)}(\pm)$. The possible nonlinear optical activities are summarized in Table VII.

A similar symmetry analysis can be made for "magnetic" optical activity.

Using Tables VI and VII, different classifications for the natural optical activity induced at different field orders become superfluous. We need only look to see if the relevant molecular property tensor contains $D_u^{(0)}$ with a plus or minus T signature coming from the opposite T signatures[286] of its real and imaginary parts. (The T signature, for example, of the real

TABLE VII
Known and New Optical Rotation Effects to Third Order with Suggested Nomenclature

Effect	Origin	Accompanies	Reference	Status
Rosenfeld optical rotation (First-order **B** rotation)	α_2 **B** part of $\boldsymbol{\mu}$	Polarization	372	Known
First-order **E** rotation	$\mathbf{a}_2\mathbf{E}$	**m** Magnetization	–	New
Second-order **EE** rotation	$\boldsymbol{\beta}_1\mathbf{EE}$	$\boldsymbol{\mu}$ Polarization	–	New
Magnetochiral birefringence (Second-order **BB** rotation)	$\boldsymbol{\beta}_4\mathbf{BB}$	$\boldsymbol{\mu}$ Polarization	306	Known
Inverse magnetochiral birefringence (Second-order **BE** and **EB** rotations)	$\mathbf{b}_2\mathbf{BE}$ $\mathbf{b}_3\mathbf{EB}$	**m** Magnetization	370	Known
Third-order **EEB** rotation	$\boldsymbol{\gamma}_2\mathbf{EEB}$	$\boldsymbol{\mu}$ Polarization		
Third-order **EBE** rotation	$\boldsymbol{\gamma}_3\mathbf{EBE}$	$\boldsymbol{\mu}$ Polarization		
Third-order **BEE** rotation	$\boldsymbol{\gamma}_5\mathbf{BEE}$	$\boldsymbol{\mu}$ Polarization		
Third-order **BBB** rotation	$\boldsymbol{\gamma}_8\mathbf{BBB}$	$\boldsymbol{\mu}$ Polarization	–	New
Third-order **BBE** rotation	$\mathbf{g}_2\mathbf{BBE}$	**m** Magnetization		
Third-order **BEB** rotation	$\mathbf{g}_3\mathbf{BEB}$	**m** Magnetization		
Third-order **EBB** rotation	$\mathbf{g}_5\mathbf{EBB}$	***m*** Magnetization		
Third-order **EEE** rotation	$\mathbf{g}_8\mathbf{EEE}$	***m*** Magnetization		

part of dynamic polarizability is plus and that of the imaginary part is minus. The P signature of both parts[286] is plus.)

Equations (407) and (408) and Tables VI and VII provide a summary for the unified treatment of the various linear and nonlinear optical effects. Within this framework, the magnetochiral effect[306] for example, is treated through the complex molecular property tensor $\boldsymbol{\beta}_4$, which contains $D_u^{(0)}$ (+). The effect is an electric dipole moment induced through $\boldsymbol{\beta}_4$ by the tensor product **BB** (or B_iB_j in Einstein notation) of the electromagnetic field. It can be thought of as the "second-order equivalent" of Rosenfeld rotation, characterized by $\alpha_{2ij}B_j$. The third-order equivalent in this sequence is $\gamma_{8ijkl}B_jB_kB_l$, whose $\boldsymbol{\gamma}_8$ tensor contains $D_u^{(0)}$ three times, signifying three independent third-order optical rotation effects. This analysis can be repeated for other sequences of optical rotatory effects, involving, for example, the inverse magnetochiral effect, recently proposed by Wagnière.[370]

G. Optical Activity Induced by a Pump Laser

A particularly useful nonlinear property of an intense pump laser is optical rectification, defined through vector cross products of the complex conjugate solutions to Maxwell's equations. These are referred to as conjugate products, and have been defined by Ward[373] in terms of Feynman diagrams of quantum perturbation theory. In this subsection the P and T symmetries of the conjugate product

$$\boldsymbol{\Pi} = \mathbf{E}_L^+ \times \mathbf{E}_L^- = -\mathbf{E}_R^+ \times \mathbf{E}_R^- = 2E_0^2 i\mathbf{k} \tag{409}$$

are discussed, and shown to be the same as that of magnetic flux density **B**. This leads to the important conclusion that $\boldsymbol{\Pi}$ of a pump laser can produce, theoretically, *all the effects of* **B**.

The conjugate product defined in Eq. (409) is nonzero *only in a circularly polarized laser*, and changes sign if the polarization is switched from right to left. It is a purely imaginary quantity, which is proportional to the laser electric field strength amplitude squared, E_0^2. Its interaction energy with an atom or molecule is therefore

$$\left.\begin{aligned} \Delta H &= -\frac{1}{2}\alpha_{1ij}\Pi_{ij} \\ &= \frac{\mathrm{i}}{2}\alpha''_{1k}\Pi_k \\ (\alpha_{1k} &\equiv \alpha'_{1k} - i\alpha''_{1k}) \end{aligned}\right] \tag{410}$$

where α''_{1k} is the axial vector (rank one tensor) representation of the antisymmetric, imaginary part, of the rank two dynamic polarizability tensor. The latter is T-negative from semiclassical theory,[286] and to obtain a T-positive scalar interaction energy, $\boldsymbol{\Pi}$ must be T-negative. This expectation is reinforced from first principles as follows.

We wish to prove that

$$\boldsymbol{\Pi} \xrightarrow{T} -\boldsymbol{\Pi} \tag{411}$$

that is, that the conjugate product is negative to motion reversal. Considering the four electric field strengths in Eq. (406) we expand $\mathbf{E}_L^-$ as

$$\left.\begin{aligned} \mathrm{Re}(\mathbf{E}_L^-) &= E_0(\mathbf{i}\cos\theta_L + \mathbf{j}\sin\theta_L) \\ \mathrm{Im}(\mathbf{E}_L^-) &= iE_0(\mathbf{j}\cos\theta_L - \mathbf{i}\sin\theta_L) \end{aligned}\right] \tag{412}$$

and apply T term by term as follows:

$$\left.\begin{aligned} \mathrm{Re}(\mathbf{E}_L^-) &\xrightarrow{T} E_0(\mathbf{i}\cos\theta_R - \mathbf{j}\sin\theta_R) \\ \mathrm{Im}(\mathbf{E}_L^-) &\xrightarrow{T} iE_0(\mathbf{j}\cos\theta_R + \mathbf{i}\sin\theta_R) \end{aligned}\right] \tag{413}$$

These follow because

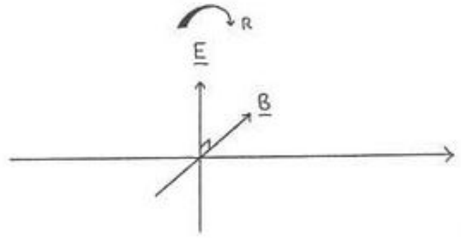

Figure 51. Basic elements of an electromagnetic wave. **E** and **B** are mutually perpendicular to the propagation vector, which is parallel to the conjugate product.

$$t \xrightarrow{T} -t; \qquad \omega \xrightarrow{T} \omega; \qquad \boldsymbol{\kappa}_L \xrightarrow{T} -\boldsymbol{\kappa}_R; \qquad \mathbf{r} \xrightarrow{T} \mathbf{r} \tag{414}$$

using the basic properties

$$\cos\theta_L \xrightarrow{T} \cos\theta_R; \qquad \sin\theta_L \xrightarrow{T} -\sin\theta_R \tag{415}$$

under T. These in turn follow because ω is a scalar angular frequency (a *number* of radians per unit time unaffected by motion reversal) and **r**, the position vector, is invariant to T by definition. The time t itself reverses by definition of T as motion reversal, because time is position **r** divided by velocity **v**, and the latter is reversed by the definition of motion reversal. Finally, $\boldsymbol{\kappa}$ the wave vector, is reversed in direction because the laser beam reverses direction with motion reversal. We have seen that T reverses the circular polarity of the laser (right to left or vice versa). Thus $\boldsymbol{\kappa}_L$ becomes $-\boldsymbol{\kappa}_R$ under T. Finally, Eq. (415) follows from the mathematical properties of the cosine and sine. Overall, therefore, T has the effect

$$\left.\begin{aligned} \mathbf{E}_L^- \xrightarrow{T} \mathbf{E}_R^+; \qquad \mathbf{E}_L^+ \xrightarrow{T} \mathbf{E}_R^- \\ (\mathbf{E}^+ \times \mathbf{E}^-)_L \xrightarrow{T} -(\mathbf{E}^+ \times \mathbf{E}^-)_R \end{aligned}\right] \tag{416}$$

and reverses the sign of the conjugate product when the laser is switched from left to right or vice versa. The conjugate product is therefore negative to T, as the Hamiltonian (Eq. 410) indicated.

The conjugate products $\boldsymbol{\Pi}_L$ and $\boldsymbol{\Pi}_R$ of a left and right circularly polarized pump laser, such as a Nd:YAG, have opposite signs. The quantity $\boldsymbol{\Pi}$ derives from the helical motion of conjugate electric field components of the pump laser and is given mathematically by the vector product of orthogonal conjugates. Figure 51 is an illustration of the fact that $\boldsymbol{\Pi}$ is an axial vector with the same T and P symmetries as **B**: minus to T and plus to P. Its forward direction is along the axis of the helix, and is therefore the direction of the propagation vector $\boldsymbol{\kappa}$ of the pump laser. The effect of

T is to reverse the direction of the laser beam, thus reversing both $\boldsymbol{\Pi}_L$ and $\boldsymbol{\Pi}_R$. However, $\boldsymbol{\Pi}$ is not reversed by P because it is the vector product of *two* P-negative electric field vectors.

From principle three, we expect $\boldsymbol{\Pi}$ to produce spectroscopic phenomena akin to **B**, because it has the same P and T symmetries. In the first instance, we expect an equivalent of the Faraday effect, that is, optical activity with $D_g^{(1)}(-)$ symmetry in $R_h(3)$ and $D^{(1)}(-)$ symmetry in $R(3)$. By substituting $\boldsymbol{\Pi}$ for **B** in Figs. (49) and (50) we can illustrate the conservation of Wigner reversality and parity inversion in achiral and chiral ensembles. Furthermore, wherever **B** appears in atomic and molecular spectroscopy, our five symmetry principles allow us to substitute $\boldsymbol{\Pi}$, *immediately yielding a variety of possible new phenomena*, for example: $\boldsymbol{\Pi}$-induced Zeeman splitting; $\boldsymbol{\Pi}$-induced nuclear resonance; and $\boldsymbol{\Pi}$-induced parity violating spectral features of profound interest. In the same way that **B** couples to orbital and spin-angular atomic and molecular properties, we expect $\boldsymbol{\Pi}$ to couple to fundamental properties of the same symmetry, both electronic and nuclear in nature. Our task is now to evaluate these possibilities theoretically, and, most importantly, to examine the theories experimentally. In this context we have the added advantage that $\boldsymbol{\Pi}$ of a pump laser which is focused and Q-switched can be enormous, allowing a great deal of latitude in the experimental investigation. Additionally, the frequencies of both pump and probe can be tuned to the frequency of the spectral feature under investigation, allowing resonances due to (1) the probe, (2) the pump, and (3) double resonance with consequent amplification of low-intensity spectral features such as P violating transitions which do not obey Laporte's Rule.[374] The symmetry allows $\boldsymbol{\Pi}$ to couple in the interaction Hamiltonian to a quantity akin to nuclear spin. This must be a nuclear "spin polarizability" because $\boldsymbol{\Pi}$ is proportional to pump-laser electric field strength ($\mathbf{E}_0^2$) squared. This would be a fundamentally new nuclear quantity akin to the nuclear magnetic dipole moment which links it to **B**. It would mediate the phenomenon of "nuclear electromagnetic resonance," a "symmetry clone" of NMR, opening up a multitude of new possibilities, theoretical and experimental.

Part of the purpose of this section is to try to estimate the likely order of magnitude of some of these new induced effects, in order to prepare the way for the all-important experimental investigation of the theory.

H. Some Expected Π-Induced Spectroscopic Effects

In this subsection we mention briefly some expected effects of $\boldsymbol{\Pi}$, using as a guideline the historical development of one or two of the spectroscopies which rely on **B**. This sets the theme for the variations that follow in other subsections.

I. Π-Induced Zeeman Splitting

A good account of conventional Zeeman splitting due to **B** is given by Barron[286] (p. 12 ff.). It was first observed by Zeeman[375] as the broadening of the two lines of the first principal doublet from a sodium flame placed between the poles of an electromagnet. The main features of the conventional (magnetic) Zeeman effect are described in contemporary theory in the A term of the electronic Faraday effect owing to **B**,[286] and therefore we will be able in this section to develop an analogous semiclassical theory of the A term of optical activity due to **Π**. The latter is expected therefore both in atomic and molecular ensembles, and later in this section an estimate is given of the magnitude of the splitting in terms of **Π** of the pump laser.

The hyperfine (nuclear) part of the optical Zeeman effect gives the exciting prospect of optical nuclear resonance in analogy with NMR. This analogy is developed quantum mechanically and classically later in this section.

J. Rayleigh–Raman Optical Activity Induced by Π

Radiation scattered from a chiral molecular ensemble is optically active, the Rayleigh and Raman spectral features of which provide specific information about fundamental molecular property tensors.[376] This is analogous with natural optical activity. Similarly, radiation scattered from a chiral or achiral ensemble to which **B** is applied shows magnetic optical activity. This leads to the expectation that radiation scattered from a probe laser will become optically active if **Π** from a pump laser is applied to the molecular ensemble which is the source of the scattered radiation. The semiclassical theory of this effect is developed in this section in terms of new molecular properties.

K. Forward–Backward Birefringence due to Π

In 1982, Wagnière and Meier[306] proposed another fundamental effect of **B** in the spectroscopy of chiral ensembles: forward–backward (FB) birefringence, the semiclassical theory of which was given later by Barron and Vrbancich[316] in terms of new molecular property tensors. FB birefringence due to **B** is measured with a probe laser whose propagation vector **κ** is parallel or antiparallel to **B**, as in the Faraday effect. However, Wagnière–Meier birefringence is a forward–backward asymmetry,[377] not a circular asymmetry as in the Faraday effect, and is measured with *unpolarized* probe radiation. We can apply the Wigner Principles to **B**-induced FB birefringence with reference, as usual, to Figs. 49 and 50, and replacing the observable of the Faraday effect (the angle of rotation) by

that of the Wagnière–Meier effect. The latter[378] is $(n^{\uparrow\uparrow} - n^{\uparrow\downarrow})$, where $n^{\uparrow\uparrow}$ denotes the real part of the refractive index with $\mathbf{B} \parallel \boldsymbol{\kappa}$; and $n^{\uparrow\downarrow}$ denotes $\mathbf{B} \uparrow\downarrow \boldsymbol{\kappa}$. Clearly, since T leaves the dot product $\mathbf{B} \cdot \boldsymbol{\kappa}$ unchanged, it has no effect on $(n^{\uparrow\uparrow} - n^{\uparrow\downarrow})$. The Wagnière–Meier effect therefore conserves Wigner Reversality. The Wigner P operation reverses the sign of the product $\boldsymbol{\kappa} \cdot \mathbf{B}$, and in consequence

$$(n^{\uparrow\uparrow} - n^{\uparrow\downarrow}) \xrightarrow{P} -(n^{\uparrow\uparrow} - n^{\uparrow\downarrow}) \tag{417}$$

that is, P reverses the sign of the variable in **B**-induced axial birefringence, which is observable in consequence in *chiral* ensembles only. Because of the forward–backward asymmetry of the effect, Barron[279] has suggested that it has the symmetry $D_u^{(1)}(-)$ of a time-odd polar vector in $R(3)$. Note that this has the same D symmetry as that of the Faraday effect (a time-odd axial vector symmetry) in $R(3)$. There is no Wagnière–Meier effect, however, in achiral ensembles, for example of atoms, without parity violation.[377] The optical equivalent with **B** replaced by **Π** therefore gives an excellent opportunity of observing P violation in atomic and achiral molecular ensembles by tuning the pump laser (for example a dye laser) to exact resonance.

Substituting **Π** for **B** we obtain the phenomenon of FB birefringence caused by a pump laser parallel or antiparallel to **κ** of a probe laser, whose semiclassical theory is developed, with order of magnitude estimates, in this section.

L. Parity Violation in Molecular Ensembles due to Π

The terra watt power levels achievable with contemporary pump lasers makes **Π**-induced *circular* bifringence (the **Π**-induced analogue of the Faraday effect) a candidate for the attempted observation in molecular ensembles of minute P violating phenomena due to electroweak interactions mediated by the neutral intermediate vector boson[279] whose existence was recently verified by the CERN experiment.[350] It is shown later, for example, that a focused and Q-switched Nd:YAG laser delivering $\mathbf{E}_0^2$ up to 10^{18} volts^2 m^{-2} is capable of rotating the plane of polarization of a probe laser at visible frequencies by about a million radians per meter of sample for $\mathbf{E}_0$ at a modest 10,000 volts cm^{-1}. By tuning the high power Nd:YAG pump to a P-violating transition (e.g., one that violates Laporte's Rule[374]) it may be possible to attain the enormous amplification needed to see clearly the P-violating spectral absorption.

M. The Optical Zeeman Effect—Quantization of the Imaginary Part of the Atomic or Molecular Polarizability (the Electronic Orbital–Spin Angular Polarizability)

It is well known that quantized angular momentum is described by important commutator relations and coupling coefficients such as those of Clebsch and Gordan.[379] It is proportional through the gyromagnetic ratio to the quantized magnetic dipole moment, which in general has orbital and spin components. Many important spectral phenomena, are induced by applied static magnetic flux density **B**. NMR depends on the availability of magnets of up to 14 Tesla, with a necessarily high degree of homogeneity. Imaging, medical, and Fourier transform NMR and ESR now pervade much of contemporary analytical chemistry. It would be interesting to supplement or replace the NMR magnet with **Π** of a circularly polarized and inexpensive laser.

The interaction Hamiltonian[410] describes the way in which the quantity **Π** interacts with an ensemble of atoms or molecules. The quantity $\mathbf{\Pi}_i$ is, as we have seen, a T-negative, P-positive axial vector, proportional to the square of the electric field strength of the laser. As such, it can be expressed mathematically as a rank two antisymmetric polar tensor[380]

$$\Pi_i = \epsilon_{ijk}\Pi_{jk} \tag{418}$$

where ϵ_{ijk} is the Levi Civita symbol (the rank three, totally antisymmetric, unit tensor). The interaction Hamiltonian in this representation is, mathematically, the tensor contraction on to the scalar[380]

$$\Delta H = \frac{i}{2}\alpha''_{1ij}\ \Pi_{ij} \equiv \frac{i}{2}(\alpha''_{1xx}\Pi_{xx} + \alpha''_{1xy}\Pi_{xy} + \cdots + \alpha''_{1yz}\Pi_{yz} + \alpha''_{1zz}\Pi_{zz}) \tag{419}$$

where α''_{1ij} is the rank two tensor representation of the imaginary part of the polarizability.[279,286] On the grounds of symmetry, this must also be an antisymmetric second-rank polar tensor in order to contract on to a scalar energy in Eq. (419) For a pump laser propagating in the Z direction, the tensor representation of its conjugate product is

$$\Pi_z \equiv \begin{bmatrix} 0 & 2iE_0^2 & 0 \\ -2iE_0^2 & 0 & 0 \\ 0 & 0 & 0 \end{bmatrix} \tag{420}$$

with XY and YX components being nonzero. By definition of the mathematical procedure of tensor contraction,[286,380] this implies that the imaginary part of the polarizability is

$$\left.\begin{aligned} \alpha''_{1i} &= \epsilon_{ijk}\alpha''_{1jk} \\ \alpha''_{1z} &= \alpha''_{1xy} - \alpha''_{1yx} \end{aligned}\right] \tag{421}$$

that is, either an axial vector with one Z component, or an antisymmetric polar tensor with XY and YX components. From semiclassical theory[286] these components are

$$\begin{aligned} \alpha''_{1xy} &= -\alpha''_{1yx} \\ &= -\frac{2}{\hbar}\sum_{j\neq n}\frac{\omega}{\omega_{jn}^2 - \omega^2}\,\mathrm{Im}(\langle n|\mu_x|j\rangle\langle j|\mu_y|n\rangle) \end{aligned} \tag{422}$$

where μ_x and μ_y are orthogonal electric dipole moment components defined by quantum states n and j, with transition frequency

$$\omega_{jn} = \omega_j - \omega_n \tag{423}$$

The angular frequency in radians s^{-1} of the pump laser is ω. It is immediately clear from Eq. (422) that the imaginary part of the dynamic polarizability vanishes as ω goes to zero. If the laser is tuned to the transition frequency,

$$\omega \doteqdot \omega_{jn} \tag{424}$$

the vector α''_{1i} is amplified enormously.

The axial vector α''_{1i} has the same P and T symmetries as angular momentum, and is therefore quantized in the same way. This allows an important analogy to be drawn between the properties of α''_{1i}, which we name *the electronic orbital-spin angular polarizability* (angular polarizability for short), and the magnetic dipole moment m_i.

The angular polarizability α''_{1i} is a quantized axial vector with positive P and negative T symmetries, the same P and T symmetries as m_i and angular momentum J_i. In relativistic quantum theory, the magnetic dipole moment is proportional through the gyromagnetic ratio (γ_e) to a sum of the orbital (**L**) and spin (2.002**S**) electronic angular momenta, neglecting for the moment the nuclear contribution proportional to the nuclear angular momentum

$$m_i = \gamma_e(L_i + 2.002S_i) \tag{425}$$

By a comparison of the Hamiltonians (Eq. 419) and

$$\Delta H_2 = -\gamma_e J_z B_z \tag{426}$$

we can immediately derive

$$\alpha''_{1z} \propto \left(\frac{\gamma_e}{B_0 c^2}\right) \tag{427}$$

showing that the angular polarizability is also proportional to the angular momentum. In analogy with Eq. (425) we have

$$\alpha''_{1i} = \gamma_\pi(L_i + 2.002S_i) \tag{428}$$

where γ_π is a new fundamental atomic or molecular property analogous to the gyromagnetic ratio, a *gyroptic* ratio.

Equation (428) leads to the important conclusion that *the angular polarizability has all the quantum mechanical properties of the angular momentum itself*.

Therefore it has the point-group symmetry in the molecule fixed frame of the well-known R symbols of the point-group character tables.[292] It has the commutator properties

$$\begin{aligned}[\alpha''_{1x}, \alpha''_{1y}] &= i\hbar\alpha''_{1z} \\ [\alpha''_{1y}, \alpha''_{1z}] &= i\hbar\alpha''_{1x} \\ [\alpha''_{1z}, \alpha''_{1x}] &= i\hbar\alpha''_{1y}\end{aligned} \tag{429}$$

Without having to solve the Schrödinger equation, and using the hermiticity of the commutator, it follows directly that angular polarizability of the commutator, it follows directly that angular polarizability is described by the angular momentum quantum numbers themselves. for orbital momentum these are L and its Z-axis projection, M

$$M = J, J-1, \ldots, -J \tag{430}$$

and by the spin-angular momentum quantum number S. These angular polarizability quantum numbers couple to others, such as the nuclear

angular momentum quantum number N, or the framework angular momentum quantum number O through the Clebsch Gordan, Racah, and Griffith equations.[381]

This leads to the expectation that a circularly polarized pump laser can generate all the spectroscopic properties customarily attributed to static magnetic flux density **B**, with a variety of useful analytical consequences, and with the important advantage of tuning to resonance (Eq. 424) with a natural frequency of the sample. One of these is named here the *optical Zeeman effect*, whose Hamiltonian can be expressed as

$$\Delta H = -\gamma_\pi(L_i + 2S_i)E_{0i}^2 \tag{431}$$

This puts the Hamiltonian in a form where it can be developed with vector coupling models, as in the conventional (magnetically induced) Zeeman effect.[382] It follows from Eq. (431) that the selection rules for transitions between energy levels in the optical Zeeman effect are

$$\left.\begin{aligned}\Delta J &= 0, \pm 1 \\ \Delta M &= 0, \pm 1\end{aligned}\right] \tag{432}$$

where M takes the values $J, \ldots, -J$.

A probe microwave (GHz frequency) field can be used to detect the optical Zeeman effect. When the probe is parallel to $\mathbf{\Pi}$ the selection rule is $\Delta M = 0$, giving the π components; and when the two fields are perpendicular, $\Delta M = \pm 1$, giving the σ components of the optical Zeeman effect. The pump laser is conveniently a circularly polarized narrow-width dye laser, and the sample may be sodium vapor[383–385] as in the original experiment by Zeeman.[375] This combination of GHz frequency probe and circularly polarized visible frequency dye laser can probably be used in the investigation of fine and nuclear (hyperfine) structure in the optical Zeeman effect.[386] The hyperfine structure is conveniently referred to as *optical electronic or nuclear spin resonance*.

For simple diatomic molecules, for example, the Hamiltonian (Eq. 431), initially neglecting hyperfine interactions, can be developed following Townes and Schawlow[382] in terms of the well-known Hund vector-coupling models. In the weak coupling limit, L_i and S_i precess about the molecular axis, which precesses about the total electronic angular momentum J_i. In the presence of the circularly polarized pump dye laser, tuned to resonance[383] with, for example, an atomic beam of diatomic molecules, J_i precesses about Π_i of the dye laser, with projection M_i in

the direction of Π_i. This allows the Hamiltonian (Eq. 431) to be rewritten as

$$\Delta H = -\frac{(\Lambda + 2 \cdot 002\Omega)\gamma_\pi M E_{0z}^2}{J(J+1)} \tag{433}$$

with Λ and Ω defined by

$$\Omega = \mathbf{k}_a \cdot \mathbf{J}; \qquad \Lambda = \mathbf{k}_a \cdot \mathbf{L} \tag{434}$$

where $\mathbf{k}_a$ is a unit vector in the molecular axis. We expect $(2J + 1)$ equally spaced *optical Zeeman lines* corresponding to the different values of M.

The extent of the splitting is determined by the ratio of the interaction energy $\alpha''_{1z}E_0^2$ to the reduced Planck constant $h/2\pi$. This ratio is increased dramatically in the resonance condition (Eq. 424).

Hund's case (b) can be written in direct analogy to Eq. (11–5) of Townes and Schawlow[382] as

$$\Delta H = -\frac{1}{2J(J+1)}\left\{\Lambda^2 \frac{(N(N+1) + S(S+1) - J(J+1))}{N(N+1)} + 2.002\,[J(J+1) + S(S+1) - N(N+1)]\right\} M\gamma_\pi E_0^2 \tag{435}$$

In general, the Hamiltonian of the optical Zeeman effect can be written in terms of the Landé factor g_J:

$$\Delta H = -g_J M \gamma_\pi E_0^2 \tag{436}$$

with g_J of the order of unity for molecules with net angular momentum, as in the conventional, **B**-induced, Zeeman effect. Otherwise g_J is dominated by the nuclear spin quantum number I. In general, g_J depends on the net electronic angular momentum J_i. In the optical Zeeman effect, if the Landé factors in states J_1 and J_2 are g_1 and g_2 respectively, and if the transition frequency (in Hz) between J_1 and J_2 is ν_0, the optical Zeeman spectrum will be a series of lines defined by

$$\nu = \nu_0 + (g_2 - g_1)M\gamma_\pi E_0^2/\hbar \tag{437}$$

for $\Delta M = 0$ (π components), and

$$\nu = \nu_0 + [(g_2 - g_1)M \pm g_1]\gamma_\pi E_0^2/\hbar \tag{438}$$

for $\Delta M = M_2 - M_1 = \pm 1$ (σ components), with M_1 the lower state quantum number. As the pump laser is swept across resonance with a natural transition frequency of the sample, the angular polarizability α''_{1i} will increase and decrease dramatically, and the spectral splittings will change accordingly. This pattern of change will be different for each natural transition frequency, giving plenty of scope for the development of useful new analytical methods based on the optical Zeeman effect.

In general, the g factors contain hyperfine (nuclear) and super hyperfine[387] contributions, which cause *nuclear electromagnetic resonance* as the GHz probe is swept across the same frequency as that of a transition frequency between hyperfine states. This is an optical equivalent of NMR.

For observation of the σ lines of the optical Zeeman effect, the electric field of the GHz electromagnetic probe should be perpendicular to Π_i of the circularly polarized pump laser (dye laser, Nd:YAG, CO_2 laser, etc.) so that the direction of propagation of the pump laser is parallel to the length or broadest faces of the waveguide carrying the GHz probe. *No optical Zeeman effect can be observed if the pump laser has not at least some degree of circular polarization*. This is useful in distinguishing it from the well-known Autler–Townes, or optical Stark, effect.[388–391] The latter depends on the *real* part of the polarizability (e.g., Eq. 2.59 of Ref. 388), whose symmetry is *T-positive*[388] from semiclassical theory, and which is a symmetric second-rank tensor with no axial vector equivalent. The optical Stark effect also has a zero frequency (DC) component,[388] whereas the optical Zeeman effect vanishes with vanishing ω from Eq. (422). The optical Stark effect has none of the quantization properties of the optical Zeeman effect, because the real part of the dynamical atomic or molecular polarizability is not proportional to angular momentum, having *opposite* T symmetry and being a *symmetric*-rank two tensor with no rank one axial vector equivalent.

It is important to bear in mind the opposite T and suffix symmetries[286] of the real and imaginary parts of the dynamic electronic polarizabilities. The fundamental difference between the Autler–Townes and optical Zeeman effects is a manifestation of these symmetry differences.

The general appearance of a simple type of optical Zeeman spectrum is expected to be similar to that sketched in Fig. (11-1) of the standard text by Townes and Schawlow[382] but will also depend, as mentioned, on resonance of type in Eq. (424). When nuclear hyperfine structure is considered, a Hamiltonian such as

$$\Delta H_2 = -\tfrac{1}{2}(\gamma_\pi g_J J_i \Pi_i + \gamma_{\pi n} g_I I_i \Pi_i) \tag{439}$$

must be used, where $\gamma_{\pi n}$ is the *nuclear gyroptic ratio* and I the nuclear spin quantum number. If this is much smaller than the hyperfine energy, so that Π_i does not disturb the coupling between J_i and I_i, the vector coupling model gives the Landé type Hamiltonian

$$\Delta H_2 = \{-\gamma_{\pi n} g_I [I(I+1) + F(F+1) - J(J+1)] - \gamma_\pi g_J [J(J+1) + F(F+1) - I(I+1)]\} \frac{M_F E_0^2}{2F(F+1)} \quad (440)$$

where F is the total angular momentum quantum number and M_F its projection on to Π_i of the circularly polarized pump laser. For a diamagnetic molecule, both terms of the optical Zeeman effect described by Eq. (440) are roughly equal in magnitude, giving considerable extra spectral detail for analytical purposes.

There appears to be another important potential advantage of the optical Zeeman effect over the conventional magnetic Zeeman effect. The pump laser of the former effect puts the molecule into an excited electronic state, in which there is net angular momentum imparted[392] to the molecule. The conjugate product Π_i spins a quantum state of the atom or molecule through the mediacy of α''_{1i}. This extra angular momentum results in a spectrum that is possible in the conventional Zeeman effect only in a molecule such as nitrous oxide, which is in a state with J number 3/2, so that the M_J states are 3/2, 1/2, −1/2, and −3/2, each of which is split into $M_J = 1, 0, -1$ states. Each M_J state would be expected to show hyperfine structure in optical Zeeman spectroscopy. Another example is that of oxygen, in which there would be an optical Zeeman splitting of the p-type triplets.

Symmetric and asymmetric tops would have more complicated optical Zeeman spectra, the case of HOD, for example, being interesting because its $4\bar{\nu}_{OH}$ state coincides with a circularly polarized Nd:YAG pump frequency.[393,394] The use of such coincidences between circularly polarized pump laser frequencies and natural transition frequencies is reminiscent of the well-developed techniques[395–397] of infrared and infrared–radio frequency double resonance, and of superhigh resolution saturation spectroscopy.[398] In each of these techniques, the circularly polarized pump laser (e.g., a narrow-width circularly polarized dye laser[392] would be used both for resonance, and for generation of Π_i, in analogy with the methods already in existence for multiphoton optical Stark splitting.[397]

One of the most sensitive techniques for optical Zeeman spectroscopy in atomic vapors would be possible with apparatus resembling that of Stroud and co-workers[397] utilizing circularly polarized visible dye lasers

and radio-frequency fields focused carefully on to an atomic beam of sodium vapor. Using this apparatus, Molander, Stroud, and Yeazell[398] have characterized what they termed "high angular momentum Stark states" using a process of two-photon absorption by a circularly polarized dye laser, using a circularly polarized radio frequency field to produce quantized angular momentum in the sodium atoms. In this way the sodium atoms were excited to the $n = 25$ manifold, that is, "dressed" by the circularly polarized radio frequency field at 200 MHz, 8 V cm^{-1} equivalent electric field strength. The "dressed" state was then excited by a sensitive resonant two-photon process, reminiscent of the method used by Whitley and Stroud[392] for one of the first unambiguous observations of the optical Autler–Townes effect. For observation of the optical Zeeman effect in sodium vapor, the dye laser of this apparatus would be intense and circularly polarized, possibly Q-switched and focused, and the MHz/GHz probe would not necessarily be circularly polarized. Another possibility would be the use of two radio-frequency fields, one intense and circularly polarized pump to produce Π_i, the other a weaker unpolarized probe. (The same concept of producing Π_i from a radio-frequency field would be potentially very interesting in a conventional NMR spectrometer, using a circularly polarized probe radio-frequency field to produce extra angular momentum, thus *electromagnetically Zeeman splitting the conventional NMR spectrum* and giving a large number of analytical possibilities.)

N. Semiclassical Theory of the Optical Zeeman Effect

It is well known in semiclassical theory[286] that the conventional (**B**-induced) Zeeman effect can be described as the A term of the quantum mechanical description of the Faraday effect,[338] first derived by Serber,[399] and rederived in terms of useful molecular property tensors by Buckingham and Stephens.[400] The semiclassical treatment depends on a Voigt–Born perturbation[286] of the appropriate molecular property by the applied field. In the **B**-induced Faraday effect

$$\alpha''_{1xy}(B_z) = \alpha''_{1xy} + \alpha^{(B)''}_{1xyz} B_z + \cdots \quad (441)$$

and in the **Π**-induced Faraday effect

$$\alpha''_{1xy}(\Pi_z) = \alpha''_{1xy} + \alpha^{(\pi)''}_{1xyz} \Pi_z + \cdots \quad (442)$$

both involving the imaginary part of the dynamic polarizability, the quantity, which, as we have seen, mediates the optical Zeeman effect. This is consistent with the fact that there is also an *optical Faraday effect*, whose A term is the quantum description of the optical Zeeman effect. The first

indications of the presence of an optical Faraday effect were obtained[401–403] by measuring the bulk magnetization due to a circularly polarized pulsed giant ruby laser, using[403] a simple inductance coil. The magnetization was easily observable[402,403] in a range of diamagnetic liquids through an electric current generated with the coil during a laser pulse, even though no resonance tuning–amplification was used. The optical Zeeman effect can be thought of as one of the numerous (and unexplored) spectral consequences of this magnetization by the circularly polarized pump laser. With resonance tuning, these effects appear well within the capability of ultrasensitive contemporary apparatus, such as that developed in other contexts by Stroud and co-workers.[397,398]

In semiclassical theory the angle of rotation of the optical Faraday effect can be expressed[286] as

$$\Delta\theta \doteq \frac{1}{2}\omega\mu_0 clN\langle\alpha''_{1xy}(f) + \alpha^{(\pi)''}_{1xyz}\Pi_z\rangle \tag{443}$$

$$\doteq \frac{1}{2}\omega\mu_0 cl\frac{N}{d_n}E_0^2\sum_n\left(\langle\alpha^{(\pi)''}_{1xyz}(f)\rangle + \frac{1}{kT}\langle\alpha''_{1zn}\,\alpha''_{1xy}(f)\rangle\right) \tag{444}$$

where ω is the measuring frequency (radians s^{-1}); μ_0 the permeability in vacuo in SI, c the velocity of light; l the sample length; N the number of molecules per unit volume; d_n the quantum state degeneracy; E_0^2 the square of the pump laser"s electric field strength; and kT the thermal energy per molecule. Here f is the dispersive line-shape function of semiclassical theory.[286] The ellipticity change in the probe is

$$\Delta\eta \doteq \frac{1}{2}\omega\mu_0 cl\frac{n}{d_n}E_0^2\sum_n\left(\langle\alpha^{(\pi)''}_{1xyz}(g)\rangle + \frac{1}{kT}\langle\alpha''_{1zn}\,\alpha''_{1xy}(g)\rangle\right) \tag{445}$$

where g is the absorptive lineshape function.[286]

The circular birefringence and dichroism due to Π_i can be written in formal analogy with the magnetic electronic A, B, and C terms, written in the molecule fixed frame, as follows:

$$\Delta\theta \doteq -\frac{\mu_0 clNE_0^2}{3\hbar}\left[\frac{2\omega_{jn}\omega^2}{\hbar}(f^2 - g^2)A + \omega^2 f\left(B + \frac{c}{kT}\right)\right] \tag{446}$$

$$\Delta\eta \doteq -\frac{\mu_0 clNE_0^2}{3\hbar}\left[\frac{4\omega_{jn}\omega^2}{\hbar}fgA + \omega^2 g\left(B + \frac{c}{kT}\right)\right] \tag{447}$$

for a quantum transition from n to j, where n is the state of lower energy, usually the ground state. The A, B, and C terms due to the pump laser"s conjugate product are

$$A = \frac{3}{dn}\sum_n(\alpha''_{1jz} - \alpha''_{1nz})\,\mathrm{Im}(\langle x|\mu_x|j\rangle\langle j|\mu_Y|n\rangle$$

$$B = \frac{3}{dn}\sum_n \mathrm{Im}\Bigg(\sum_{k\neq n}\frac{\langle k|\alpha''_{1z}|n\rangle}{\hbar\omega_{kn}}(\langle n|\mu_x|j\rangle\langle j|\mu_\gamma|k\rangle - \langle n|\mu_\gamma|j\rangle\langle j|\mu_x|k\rangle)$$

$$+\sum_{k\neq j}\frac{\langle j|\alpha''_{1z}|k\rangle}{\hbar\omega_{kj}}(\langle n|\mu_x|j\rangle\langle k|\mu_y|n\rangle - \langle n|\mu_y|j\rangle\langle k|\mu_x|n\rangle)\Bigg)$$

$$C = \frac{3}{dn}\sum_n \alpha''_{1zn}\,\mathrm{Im}(\langle n|\mu_x|j\rangle\langle j|\mu_y|n\rangle)$$

which represent a sum over transitions from component states of a degenerate set to an excited state ψ_j which itself could be a member of a degenerate set. Note that the A term, which describes the optical Zeeman effect in semiclassical theory, requires a definition of the angular polarizability α''_{1z} in states n and j. The definition in state n is Eq. (422), and that in state j is

$$\alpha''_{1\alpha\beta,j} = -\alpha''_{1\alpha\beta,j}$$

$$= -\frac{2}{\hbar}\sum_{k\neq j}\frac{\omega}{\omega_{kj}^2 - \omega^2}\mathrm{Im}(\langle j|\mu_\alpha|k\rangle\langle k|\mu_\beta|j\rangle) \tag{448}$$

where k denotes a quantum state higher in energy than j. In writing the A, B, and C terms in this way, weighted Boltzmann averaging[286] is used with the energy ratio $-\alpha''_{1z}\,E_0^2/kT$. A Q-switched and focused Nd:YAG laser produces E_0 of about 10^9 volt m^{-1}, and for an order of magnitude estimate[404] of about 10^{-41} $C^2\,m^2\,J^{-1}$ for α''_{1z} the ratio $\alpha''_{1z}E''_0/kT$ is of the order unity. It appears that this can easily be achieved by tuning to resonance with the transition frequencies ω_{nj} or ω_{jk}.

The A term is responsible for optical Zeeman splitting by the circularly polarized pump laser as measured by a suitable probe. A right circularly polarized pump laser delivers a photon with $-h$ projection in the propagation (κ) axis of the laser, producing a change $\Delta M = -1$ in the atomic or molecular quantum state. Conversely, the left circularly polarized pump laser delivers a photon with projection $+h$, with selection rule $\Delta M = 1$. In a linearly polarized pump there is no optical Zeeman effect, and the

selection rule is $\Delta M = 0$. This is accounted for classically in Eq. (409), where the left conjugate product is positive, and the right negative. The sign change produced by switching the pump"s polarity from left to right is equivalent to the change produced in the Faraday effect by switching the direction of **B** relative to the propagation vector of the probe.

As in the conventional, **B**-induced Faraday effect, the A term due to $\mathbf{\Pi}$ comes from the splitting of lines by $\mathbf{\Pi}$ into right and left circularly polarized components. The B term of the optical Faraday effect originates from the mixing of energy levels due to the pump laser, and the C term is a change of electronic population of the pump-laser-split ground states. In each case the magnetic dipole moment operator of the conventional Zeeman effect is replaced by the angular polarizability vector $\boldsymbol{\alpha}_1''$ with the same P and T symmetries and M quantum number selection rules. The angular polarizability can be greatly amplified by resonance as we have seen.

In the $\mathbf{\Pi}$-induced A and C terms, the vector polarizabilities in states n and j exist in general in the presence and absence of degeneracy, from the definitions (Eqs. 446 and 447). Therefore the A and C terms should be visible in molecules of lower symmetry than in the conventional **B**-induced equivalents.

O. Laser-Induced Electronic and Nuclear Spin Resonance

The above discussion leads to the theoretical expectation of electron and nuclear spin resonance due to optical rectification, of great potential value because lasers and circularly polarized radio frequency fields can ultimately[405] supplement interestingly the magnets of NMR and ESR spectrometers. The origin of electron spin resonance with $\mathbf{\Pi}$ is found in the quantum nature of the vector polarizability $\boldsymbol{\alpha}_1''$, which is proportional through Eq. (431) to the sum of the orbital and spin-angular momenta of the electron, the latter taking the values 1/2 and $-1/2$. If the probe is tuned to the resonance frequency ω_R it is absorbed when

$$\left.\begin{aligned}\hbar\omega_R &= E(1/2) - E(-1/2)\\ &= 2\hbar\gamma_\pi E_0^2\end{aligned}\right] \tag{449}$$

which is the condition for electron spin resonance due to optical rectification in a circularly polarized electromagnetic field. This depends on the $\Delta M = 1$ transition between the electron spin polarizability states 1/2 and $-1/2$. If the pump laser inputs the energy $\alpha_{1z}'' E_0^2$, the resonance frequency range is roughly $\alpha_{1z}'' E_0^2/\hbar$, which is in the MHz for an order of magnitude $10^{-41}\,\mathrm{C^2\,m^2\,J^{-1}}$ for the angular polarizability, and a pump laser electric

field strength of the order 10^6–$10^9\,\mathrm{volt\,m^{-1}}$. Conventional ESR spectrometers can therefore be adapted for use with the pump laser, using existing microwave probes. High-sensitivity apparatus is available similar to that developed[398] by Stroud and co-workers in another context. Resonance amplification of the angular polarizability can be utilized.

The most useful feature of conventional, **B**-induced, ESR is retained when **B** is substituted by $\mathbf{\Pi}$. This is coupling of electron and nuclear spins, caused by the $\mathbf{\Pi}$-induced transition between electron orientation states by the interaction of the spin-angular momenta of the electron with nuclei which have nonzero spin-quantum numbers I. This hyperfine resonance structure can be induced, under the right conditions, by $\mathbf{\Pi}$ of a pump laser, such as a dye laser. In the triphenyl methyl radical, for example, the **B**-induced hyperfine structure of one resonance peak contains no less than 196 lines, and similar detail is expected from $\mathbf{\Pi}$ used in place of **B**.

If a circular polarized pump laser is used to *supplement* the magnetic flux density of a conventional NMR spectrometer, the result is a Hamiltonian of the form

$$\Delta H_3 = -\gamma_n I_i B_i - \tfrac{1}{2}\gamma_\pi J_i \Pi_i \tag{450}$$

where γ_N is the nuclear gyromagnetic ratio, and the angular momentum J_i is the sum

$$J_i = L_i + 2.002 S_i \tag{451}$$

This Hamiltonian can be rewritten in the Landé form:

$$\begin{aligned}\Delta H_3 = &-\gamma_N\left(1 + \frac{I(I+1) - J(J+1)}{2J_T(J_T+1)}\right) J_{Ti} B_i\\ &-\frac{\gamma_\pi}{2}\left(1 - \frac{I(I+1) - J(J+1)}{2J_T(J_T+1)}\right) J_{Ti}\Pi_i\end{aligned} \tag{452}$$

where

$$J_T = J + I \tag{453}$$

is the total angular momentum quantum number. For $I \neq 0$ the customary NMR line, defined through the selection rule

$$\Delta M_I = \pm 1 \tag{454}$$

is split into a new pattern of lines dependent on the selection rule

$$\Delta M_{J_T} = 0, \pm 1 \tag{455}$$

and on the individual values of I and J. A convenient way of doing this is to increase the intensity and to circularly polarize the MHz probe radio-frequency field of the NMR spectrometer. *This has great potential application in analytical laboratories, because modifications to include* Π_i *can be made in standard NMR instruments, including 2-D (imaging), and Fourier transform NMR.*

P. Rayleigh–Raman Light-Scattering Optical Activity due to Optical Rectification

Magnetic Rayleigh–Raman optical activity was developed theoretically by Barron and Buckingham[406] and experimentally by Barron and co-workers. The radiation scattered from a probe laser becomes optically active by applying a magnetic field to the sample parallel to the incident probe laser. For 90° scattering

$$\Delta_X(90°) = \frac{2\,\mathrm{Im}(\alpha_{1XY}\,\alpha_1^*{}_{XX})}{\mathrm{Re}(\alpha_{1XX}\,\alpha_1^*{}_{XX} + \alpha_{1XY}\,\alpha_1^*{}_{XY})} \tag{456}$$

and

$$\Delta_Z(90°) = \frac{2\,\mathrm{Im}(\alpha_{1ZY}\,\alpha_1^*{}_{ZX})}{\mathrm{Re}(\alpha_{1ZX}\,\alpha_1^*{}_{ZX} + \alpha_{1ZY}\,\alpha_1^*{}_{ZY})} \tag{457}$$

where

$$\Delta = \frac{I^R - I^L}{I^R + I^L} \tag{458}$$

is the dimensionless circular intensity difference.[286] The scattering is described in Eqs. (456) and (457) by laboratory frame components of complex molecular polarizability tensors and complex conjugates described by a superscripted asterisk. The magnetic field **B** activates optical activity in several different ways, and in consequence so does **Π**. The latter activates the polarizability through a Voigt–Born expansion to first-order in Π_Z. Consequently, in analogy with the effect of **B**, there are several new

optically active scattering phenomena due to **Π** of a pump laser parallel to the incident probe. These can be subclassified into **Π**-induced Rayleigh and Raman effects associated with diagonal scattering transitions; and with off-diagonal transitions which probe the analogue of ground-state optical Zeeman splitting due to **Π**. There is also optically active resonance, as well as transparent, Raman scattering due to **Π**, together with the interesting prospect of double resonance, when both the pump and probe are tuned simultaneously. There is the additional advantage that **Π** is expected to have a much more direct influence on vibrational spectra than **B**, because **Π** is electromagnetic in origin, and Raman scattering in general is a phenomenon which depends on electronic states excited by electromagnetic fields.

Optical activity in scattered probe radiation due to **Π** of the pump laser (or circularly polarized radio-frequency field) conserves parity and reversality in all molecular ensembles (chiral and achiral) and the main contribution in Rayleigh scattering is due to interference between waves generated by polarizability tensor components respectively perturbed and unperturbed by **Π** of the pump laser. It is measured by scattered probe radiation at any scattering angle, but the theory simplifies considerably[407] for scattering at 90°.

The same considerations apply for Raman optical activity due to **Π**, but the interference is now between unperturbed symmetric transition polarizability components, $(\alpha_{ij})^s_{mn}$, and antisymmetric components $(\alpha_{ij})^a_{mn}$ perturbed by **Π**, and vice versa.[286]

In both Rayleigh and Raman contexts the Voigt–Born expansion in **Π** of the complex dynamic polarizability is

$$\alpha_{1ij}(\Pi_k) = \alpha'_{1ij} + \alpha^{(\pi)\prime}_{1ijk}\,\Pi_k - i(\alpha''_{1ij} + \alpha^{(\pi)\prime\prime}_{1ijk}\Pi_k) \tag{459}$$

and products such as $\alpha_{1xx}\alpha^*_{1xy}$ are Boltzmann-averaged[286] with the potential energy $\alpha''_{1Z}E_0^2/kT$. We obtain expressions for optically active scattering due to **Π** analogous with those for **B** given in Eqs. (3.5.45) and (3.5.53) of Ref. 286. The most general expression for the Stokes parameters for optically active scattered radiation due to **Π** are the analogues of those due to **B**[286] in Barron's Eq. (3.5.51), and in Barron, Meehan, and Vrbancich.[407] Here the superscripts R and L refer to the scattered probe radiation, whose electric field intensity is denoted $E_0^{(p)}$, and R is the distance from the scattering center:

$$\Delta\alpha = (I^R_\alpha - I^L_\alpha)/(I^R_\alpha + I^L_\alpha) \tag{460}$$

where

$$A = (\omega^4 \mu_0 E_0^{(p)2})/(16\pi^2 cR^2) \tag{461}$$

$$I_X^R - I_X^L = A\,\mathrm{Im}(\alpha_{1XX}\,\alpha_{XX}^*) \tag{462}$$

$$I_Z^R - I_Z^L = A\,\mathrm{Im}(\alpha_{1ZY}\,\alpha_{1ZX}^*) \tag{463}$$

$$I_X^R + I_X^L = \frac{A}{2}\,\mathrm{Re}(\alpha_{1XX}\,\alpha_{1XX}^* + \alpha_{1XY}\,\alpha_{1XY}^*) \tag{464}$$

$$I_Z^R + I_Z^L = \frac{A}{2}\,\mathrm{Re}(\alpha_{1ZX}\,\alpha_{1ZX}^* + \alpha_{1ZY}\,\alpha_{1ZY}^*) \tag{465}$$

The products of polarizabilities in these expressions are perturbed by $\mathbf{\Pi}$ of the pump laser. After Boltzmann averaging[286] for $\mathbf{\Pi}$ in the Z direction of the incoming probe beam, we have:[408–411]

$$\begin{aligned} I_X^R - I_X^L = 2AE_{0Z}^2\langle & \alpha'_{1XX}\,\alpha_{1XYZ}^{(\pi)''*} \\ & - \alpha''_{1XX}\,\alpha_{1XYZ}^{(\pi)'*} + \alpha_{1XXZ}^{(\pi)'}\,\alpha''^*_{1XZ} - \alpha_{1XXZ}^{(\pi)''}\,\alpha'^*_{1XY} \\ & + \frac{1}{kT}(\alpha'_{1XX}\,\alpha''^*_{1XY}\,\alpha''_{1XY} - \alpha''_{1XX}\,\alpha'^*_{1XY}\,\alpha''_{1XY})\rangle \end{aligned} \tag{466}$$

for the numerator of ΔX. It is seen that this is proportional to the square of the electric field intensities both of the pump and of the probe. In consequence, it appears that the effect can be easily large enough for observation with a suitable pump dye laser.

These Stokes parameters contain cross terms between and $(\alpha'_{1ij})^a_{mn}$ which are responsible for resonance Raman scattering from the probe due to $\mathbf{\Pi}$ of the circularly polarized pump. "Resonance" in this context refers to the probe frequencies. The Stokes parameters switch sign if the pump is switched from right to left for a given probe circular polarity. The effect can also be generated by a pump laser at any suitable angle to the probe, automatically removing the need to filter off scattered pump radiation.

In developing averages of the type shown in Eq. (466) use is made[408] of Boltzmann weighted averaging techniques to produce results in the laboratory frame such as

$$I_X^R - I_X^L = 2AE_0^2\langle\alpha_{1XX}\,\alpha_{1XY}^*\rangle_\pi \tag{467}$$

which transform into the molecule fixed frame[408] as follows:

$$\langle\alpha'_{1XX}\,\alpha_{1XYZ}^{(\pi)''*}\rangle = \alpha'_{1\gamma\delta}\alpha''_{1\epsilon\alpha\beta}\langle j_\alpha k_\beta i_\gamma i_\delta i_\epsilon\rangle$$

$$= \frac{1}{30}(2\alpha'_{1\alpha\beta}\epsilon_{\alpha\gamma\delta}\alpha''^*_{1\beta\gamma\delta} + \alpha'_{1\alpha\alpha}\epsilon_{\beta\gamma\delta}\alpha''_{1\gamma\delta\beta}) \tag{468}$$

using Greek subscripts to refer to molecule fixed-frame quantities. Stokes parameters such as

$$\begin{aligned} S_0^\alpha(0^0) = & -2KE_{0z}^2[2\alpha'_{1\alpha\beta}\,\epsilon_{\alpha\gamma\delta}\alpha''^*_{1\beta\gamma\delta} \\ & + \alpha'_{1\alpha\alpha}\epsilon_{\beta\gamma\delta}\alpha''^*_{1\gamma\delta\beta} + 2\alpha''_{1\alpha\beta}\epsilon_{\alpha\gamma\delta}\alpha'^*_{1\gamma\beta\delta} \\ & + \alpha''_{1\alpha\beta}\epsilon_{\alpha\beta\gamma}\alpha'^*_{1\delta\delta\gamma} + \frac{1}{kT}(2\alpha'_{1\alpha\beta}\epsilon_{\alpha\gamma\delta}\alpha''^*_{1\beta\gamma}\alpha''_{1\delta\mu} \\ & + \alpha'_{1\alpha\alpha}\epsilon_{\beta\gamma\delta}\alpha''^*_{1\gamma\delta}\alpha''_{1\beta\mu})]\rho\sin 2\eta \end{aligned} \tag{469}$$

can then be expressed conveniently in this frame of reference. These equations are formally identical with Barron"s Eqs. (3.5.45–3.5.47) of Ref. 286, but implement $\mathbf{\Pi}$ in place of $\mathbf{B}$ and the angular polarizability $\boldsymbol{\alpha}''_1$ in place of the magnetic dipole moment $\mathbf{m}$. As in scattered optical activity due to $\mathbf{B}$, that due to $\mathbf{\Pi}$ does not lead to a circularly polarized component in the light scattered at 90° if the pump and probe lasers are parallel. It can be generated when the circularly polarized pump laser is parallel with the scattered beam, and the intensity of the scattered probe radiation depends on the degree of circularity of the incident probe only when the pump is parallel with the probe.

The circular intensity differences for scattering of probe radiation at 0°, 180°, and 90° due to $\mathbf{\Pi}$ in a pump parallel to the probe are found in analogy with the theory of Barron and Buckingham[406] as

$$\begin{aligned} \Delta(0°) &= \Delta(180°) \\ &= -2E_0^2[2\alpha'_{1\alpha\beta}\epsilon_{\alpha\gamma\delta}\alpha''^*_{1\beta\gamma\delta} + \alpha'_{1\alpha\alpha}\epsilon_{\beta\gamma\delta}\alpha''^*_{1\gamma\delta\beta} \\ &\quad + 2\alpha''_{1\alpha\beta}\epsilon_{\alpha\gamma\delta}\alpha'^*_{1\gamma\beta\delta} + \alpha''_{1\alpha\beta}\epsilon_{\alpha\beta\gamma}\,\alpha'^*_{1\delta\delta\gamma} + \frac{1}{kT}(2\alpha'_{1\alpha\beta}\epsilon_{\alpha\gamma\delta}\alpha''^*_{1\beta\gamma}\alpha''_{1\delta\eta} \\ &\quad + \alpha'_{1\alpha\alpha}\,\epsilon_{\beta\gamma\delta}\alpha''^*_{1\gamma\delta}\alpha''_{1\beta\eta})]/(7\alpha'_{1\lambda\mu}\alpha'^*_{1\lambda\mu} + \alpha'_{1\lambda\lambda}\alpha'^*_{1\mu\mu} + 5\alpha''_{1\lambda\mu}\alpha''^*_{1\lambda\mu}) \end{aligned} \tag{470}$$

where the molecular property tensors are all expressed in the molecule fixed frame and where the tensor summation convention has been applied to repeated indices.

Q. Forward–Backward Birefringence due to Optical Rectification

Forward-backward birefringence due to a static magnetic field was introduced in 1982 by Wagnière and Meier,[306–308] and is another fundamentally important effect of **B** in atomic and molecular spectroscopy. From the third principle of gtsm we immediately have the possibility of an analogous effect due to **Π**, an effect which can be developed theoretically[409] in terms of the zeta tensor of semiclassical theory,[286] or alternatively,[408–411] directly from the Maxwell equation.

Forward–backward birefringence can be measured with *unpolarized* probe radiation. It is generated in the Wagnière–Meier effect, for example,[306,316] by reversing the direction of **B** with respect to **κ**, the propagation vector of the unpolarized probe. It is sustained *only in chiral ensembles*, and therefore, if observed in atoms, would be an indication of parity nonconservation.[290,412] It has been shown recently that forward–backward birefringence can be generated by a pump laser in at least two ways, called class one and two *spin-chiral birefringence*.[315] Class 1[412,413] is observed by switching the polarity of the pump from left to right, keeping the direction of its propagation constant. Class 2[412,413] keeps the circular polarity constant and reverses the direction of propagation. In both cases, **Π** plays the role of **B** of the Wagnière–Meier effect, and spin-chiral birefringence is sustained only in chiral ensembles, giving another good opportunity of investigating parity nonconservation in achiral ensembles. Both in class 1 and 2 spin-chiral effects, amplification by resonance is feasible by sweeping the frequency of the pump through natural transition frequencies of the chiral ensemble.

The semiclassical theory of spin-chiral birefringence for pump and probe directed in the Z axis relies on the following scalar elements of the zeta tensor:[316]

$$\zeta'_{XXZ} = \frac{2}{c}\left(\frac{\omega}{3} A''_{XXZ} + \alpha'_{2XY}\right) \tag{471}$$

and

$$\zeta'_{YYZ} = \frac{2}{c}\left(\frac{\omega}{3} A''_{YYZ} - \alpha'_{2YX}\right) \tag{472}$$

and on Voigt–Born perturbations linear in $\mathbf{\Pi}_z$ of the Rosenfeld tensor[316] and electric dipole – electric quadruple tensor[413]

$$\alpha'_{2XY}(\Pi_Z) = \alpha'_{2XY} + \alpha^{(\pi)\prime}_{2XYZ}\,\Pi_Z + \cdots \tag{473}$$

$$\alpha'_{2YX}(\Pi_Z) = \alpha'_{2YX} + \alpha^{(\pi)\prime}_{2YXZ}\,\Pi_Z + \cdots \tag{474}$$

$$A''_{XXZ}(\Pi_Z) = A''_{XXZ} + A^{(\pi)\prime\prime}_{XXZZ}\,\Pi_Z + \cdots \tag{475}$$

$$A''_{YYZ}(\Pi_Z) = A''_{YYZ} + A^{(\pi)\prime\prime}_{YYZZ}\,\Pi_Z + \cdots \tag{476}$$

subjected to Boltzmann averaging with the interaction energy

$$V(\Omega) = -E_0^2\,\alpha''_{1Z} \equiv -E_0^2(\alpha''_{1XY} - \alpha''_{1YX}) \tag{477}$$

The forward–backward birefringence of the class 1 effect is the difference

$$n'(\Pi_Z \uparrow\uparrow \kappa_Z) - n'(\pi_Z \uparrow\downarrow \kappa_Z) \tag{478}$$

where **κ** is the propagation vector of the probe laser. In a dilute solution for $E_0^2\,\alpha''_{1XY} \ll kT$ we have[413]

$$(n^{\uparrow\uparrow} - n^{\uparrow\downarrow}) \doteq 2\mu_0 c N E_0^2 \left\{ \frac{1}{3}\,\epsilon_{\alpha\beta\gamma}\alpha^{(\pi)\prime}_{2\alpha\beta\gamma}(f) + \frac{1}{30}\,kT\,[(4\delta_{\alpha\beta}\delta_{\gamma\delta} - \delta_{\alpha\gamma}\delta_{\beta\delta} - \delta_{\alpha\delta}\delta_{\beta\gamma})(\alpha'_{2\alpha\gamma}\alpha''_{1\beta\delta} - \alpha'_{2\beta\gamma}\,\alpha''_{1\alpha\delta})] + \frac{\omega}{45}\,(3A^{(\pi)\prime\prime}_{\alpha\alpha\beta\beta}(f) - A^{(\pi)\prime\prime}_{\alpha\beta\beta\alpha}(f) + \cdots \right\} \tag{479}$$

with tensor components defined in the molecule fixed frame. An order-of-magnitude estimate of this effect[413] produces

$$n^{\uparrow\uparrow} - n^{\uparrow\downarrow} \doteq 10^{-23} E_0^2 \tag{480}$$

which for a Q-switched and focused Nd:YAG laser delivering 10^{18} $(\text{volt/m})^2$ is of the order 10^{-5}, even without the added advantages of resonance tuning, in which condition the effect is amplified greatly. If a highly polarizable chiral material is chosen, such as a helical biomacromolecule or a cobalt complex, it is probable that the forward–backward birefringence can be increased to the point where it is easily observable even in a transparent part of the spectrum.

R. The Optical Faraday Effect — Order-of-Magnitude Estimate of the Angle of Rotation of a Plane-Polarized Probe

An expressison for the optical Faraday effect in the laboratory frame of reference can be obtained from the XY element of the perturbed polarizability, Eq. (441), which parallels the standard Voigt–Born perturbation in the semiclassical theory of the Faraday effect. The rotation of the plane of polarization of the probe laser can be derived[413] from Eq. (441) as the laboratory frame expression

$$\Delta\theta \doteqdot \frac{1}{2}\omega\mu_0 c|NE_0^2\left(\langle\alpha_{xyz}^{(\pi)\prime\prime}(f)\rangle + \frac{\langle\alpha_{1zn}''\,\alpha_{xy}''(f)\rangle}{kT}\right) \tag{481}$$

and where $\alpha_{xy}''(f)$ is the absorptive[286] part of the tensor component XY of the perturbed angular polarizability. In the molecule fixed frame, Eq. (481) becomes

$$\Delta\theta \doteqdot \frac{1}{6}\,\omega\mu_0\, clN\, E_0^2\,\alpha_{1\alpha\beta}''\frac{\alpha_{1\alpha\beta}''}{kT} + \cdots \tag{482}$$

for $\alpha_{1z}''E_0^2 \ll kT$ in dilute solution.

For a conservative order of magnitude $10^{-41}\,\mathrm{J^{-1}\,C^2\,m^2}$ for $\alpha_{1\alpha\beta}''(f)$, we obtain[413]

$$\Delta\theta \doteqdot 10^{-15}E_0^2\,\text{radian} \tag{483}$$

at 300 K for the angle of rotation due to the component of Eq. (482). This is easily within range of a contemporary laser spectropolarimeter,[414] even for an unfocused, CW dye laser operating out of resonance. As in the conventional Faraday effect, there will be an accompanying dichroism and optical rotatory dispersion in the visible and infrared frequency ranges. This type of spectrum provides unique and potentially useful analytical information for atomic and molecular ensembles, both chiral and achiral.

S. Electric Circular Birefringence and Dichroism

Faraday noted "no effect" when he attempted to see circular birefringence due to a static electric field. It is now known that such an effect would imply nonconservation of reversality. However, a nonzero time derivative of an electric field is negative to T, and can produce electric circular birefringence and dichroism in chiral ensembles. Recently, this effect has

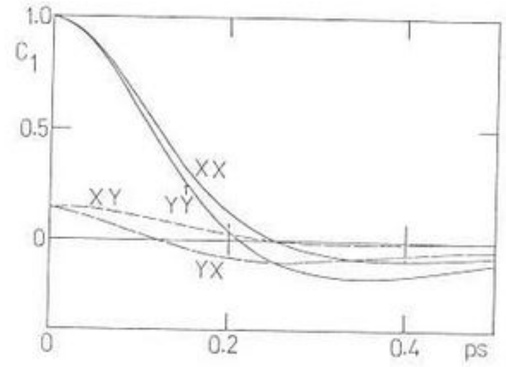

Figure 52. Diagonal (auto) and two off-diagonal (cross) correlation elements of the rotational velocity correlation function of the electric Faraday effect. The Fourier transform of the autocorrelation function is far infrared dichroism.

been supercomputer-simulated,[415] following a semiclassical treatment.[412] Electric circular dichroism was observed in the simulation through the Fourier transform of frequency spectra in the far infrared and dielectric range (Section I of the S enantiomer of bromochlorofluoromethane, using a Voigt–Born expansion of electric dipole moments:

$$\mu_{iR} = \mu_{0i} + \left(\alpha_{1ij} \pm \alpha_{1ijZ}\frac{\partial E_Z(t)}{\partial t}\right)E_j^R + \cdots \tag{484}$$

$$\mu_{iL} = \mu_{0i} + \left(\alpha_{1ij} \pm \alpha_{1ijZ}\frac{\partial E_Z(t)}{\partial t}\right)E_j^L + \cdots \tag{485}$$

induced respectively by a right and left circularly polarized probe field parallel to the electric field derivative. The latter was assumed to be cosinusoidal.[415] The electric circular dichroism observed in the far infrared range during the course of this simulation is illustrated in Fig. 52 for an input electric field derivative equivalent in energy to 7.0 kJ/mole. Figure 52 illustrates the difference in the rotational velocity correlation tensor (Sections I–VII) for right and left circularly polarized probe electromagnetic radiation. Electric-field-induced birefringence and dichroism is therefore accompanied by the appearance of asymmetric cross-correlation functions of the type seen in another context in Section VIII. It is accompanied, also, by anisotropy in the diagonal elements of the cross-correlation function. This produces spectral differences which are observable in principle with a modified Fourier transform spectrometer (Section II) with electrodes with central apertures to allow alternating left and right circularly polarized probe radiation from a piezoelectric modulator[416] or wire grid beam dividers[417] to pass through the chiral sample in the Z axis of the laboratory frame. The electrodes are used to apply the AC field derivative.

The orientational acf (Sections I to VII) exhibits the same type of

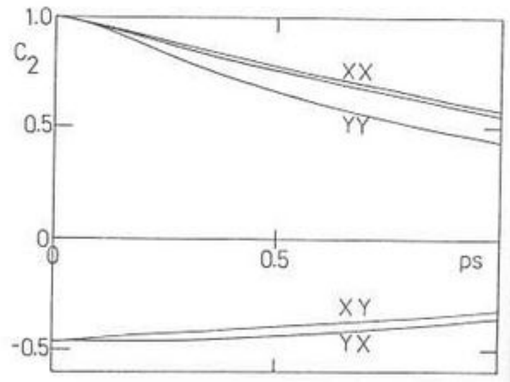

Figure 53. As for Fig. 52, orientational correlation function.

behavior (Fig. 53). However, in this case, the cross-correlation functions (XY and YX elements) are symmetric in time dependence. These are accompanied by the development of interesting new nonvanishing diagonal elements of the cross-correlation function between the linear and angular molecular momentum (Sections I–VII). These are much smaller in magnitude than the XY and YX ccf's of orientation and rotational velocity shown in Figs. 52 and 53, but nevertheless exist above the noise of the simulation. The ZZ element has a different time dependence from the XX and YY elements, which are approximately equal.

T. Frequency-Dependent Electric Polarization due to Optical Rectification in Chiral Ensembles

It has been shown recently by Evans and Wagnière[418] that **II** of the optical rectification effect can produce frequency-dependent electric polarization in chiral ensembles through the mediation of the angular polarizability. (This is the optical equivalent of **B**-induced electric polarization in a chiral ensemble capable of supporting the Rosenfeld tensor.) It should be carefully noted that this effect is again different from the well-known[388] A.C. Stark effect, or Autler–Townes effect, because the latter is mediated by the T-positive symmetric real part of the atomic or molecular polarizability and has a zero-frequency (DC) component.

It is convenient to discuss the new effect by Evans and Wagnière[418] in terms of the quantum mechanical expressions for optical rectification introduced by Ward[373] and used recently by Wagnière[370] to derive the inverse magnetochiral effect.

Optical rectification as discussed by Ward[373] leads to an expression for the DC electric polarization induced to second order by the electromagnetic field, and consists of double sums over all eigenstates of the unperturbed molecular system. The individual terms in these sums contain in

the numerators products of matrix elements of the system field interaction. In the denominators appear the transition energies of the system, the frequency of the radiation field, and appropriate damping factors. It is sufficient for our purposes to consider the numerators, which are of the general form

$$\boldsymbol{\mu}(\boldsymbol{\mu}' \cdot \mathbf{E}^-)(\boldsymbol{\mu}'' \cdot \mathbf{E}^+) \tag{486}$$

where $\boldsymbol{\mu}$,$\boldsymbol{\mu}'$, and $\boldsymbol{\mu}''$ designate matrix elements of the electric dipole moment operator and $\mathbf{E}^-$, $\mathbf{E}^+$ are the complex conjugate electric field strength vectors of the laser. Using isotropic averaging,[286,419] Eq. (486) splits up into a real part:

$$(\boldsymbol{\mu} \cdot \boldsymbol{\mu}' \times \boldsymbol{\mu}'')(\mathbf{E}^- \times \mathbf{E}^+) \tag{487}$$

The product $\mathbf{E}^- \times \mathbf{E}^+$ vanishes if the radiation is linearly polarized, and is purely imaginary (Eq. 409) for circularly polarized lasers. The induced DC electric polarization proportional to the product (Eq. 487) is therefore not directly observable, because it is purely imaginary.

However, at finite laser frequency ω in Eq. (422) the imaginary part of the polarizability is nonzero, and multiplies the imaginary product $\mathbf{E}^+ \times \mathbf{E}^-$ to give a *real* electric polarization which is mediated by a P-negative molecular property tensor.[418] *This means that a circularly polarized electromagnetic field produces electric polarization in ensembles of chiral molecules*. A particularly interesting aspect of this is the potential utilization of a circularly polarized radio-frequency field (from a waveguide) to produce linear and nonlinear[419] dielectric relaxation (Sections I–VII) in chiral liquids.

The first supercomputer simulation[418] and video animation[420] of this effect has recently been pursued with a torque (Sections IV–VI) of the type[421]

$$\langle T_q \rangle = \langle \beta_{ijk} E_j E_k \times E_j \rangle \tag{488}$$

and approximating the electromagnetic phase factor by

$$\theta_L \doteq \theta_R \doteq \omega t \tag{489}$$

The real part of this torque was incorporated into the code of the program TETRA (see Appendix) for 108 molecules of S-bromochlorofluoromethane, a chiral structure. The orientation and rotational velocity time-correlation functions of the ensemble were evaluated in the field-applied

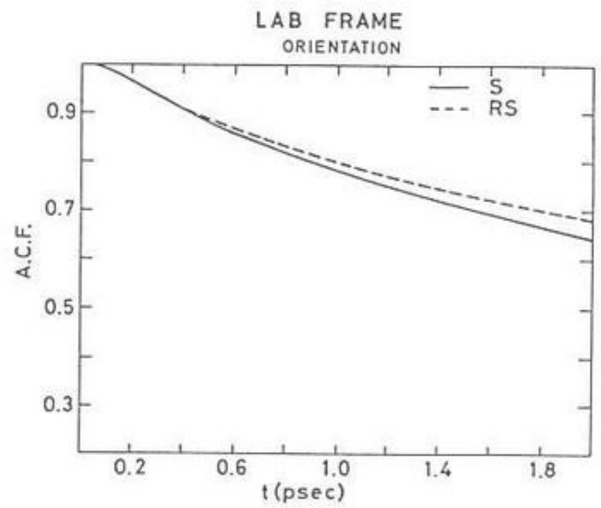

Figure 54. Orientational acf for (*S*)-bromochlorofluoromethane, (S), and the racemic mixture (RS), at field-free equilibrium.

steady state using two far infrared field frequencies of 10.0 and 1.0 THz respectively.

Figure 54 illustrates the orientational acf under field-free conditions for the *S* enantioner and racemic mixture. There are no orientational cross correlations. Figure 55 is the same correlation function for an applied field

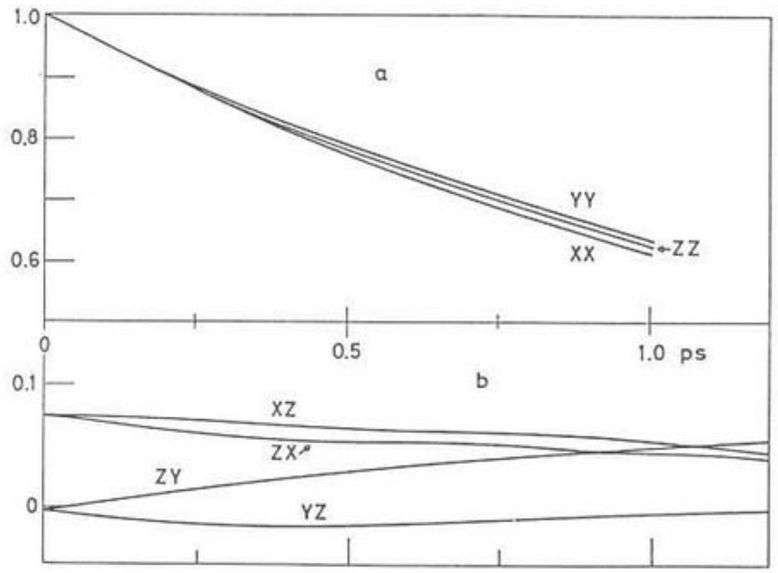

Figure 55. The effect of the conjugate product at a field-frequency of 10.0 THz. (*a*) Autocorrelation functions; (*b*) cross-correlation functions.

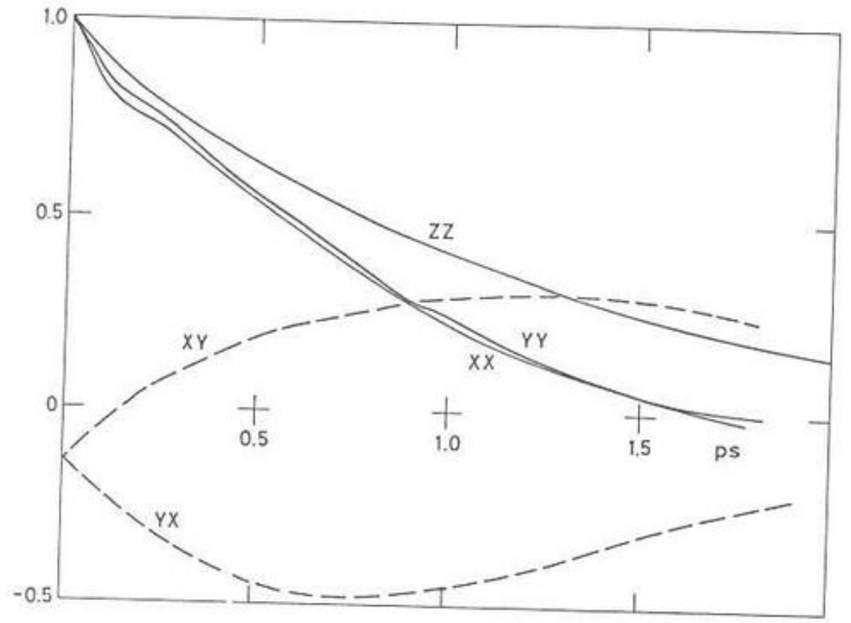

Figure 56. As for Fig. 55, frequency 0.01 THz.

of 1.0 THz, and Fig. 56 for 10.0 THz, each in the *S* enantiomer. At the lower frequency, anisotropy in the orientational acf components is clearly visible for a laser beam propagating in the *Z* axis. This is accompanied by the development of off-diagonal cross-correlation functions of orientation. At the higher frequency, Fig. 56, the anisotropy is lessened considerably, but the time dependencies of the orientational autocorrelation functions are clearly different from those at field-free equilibrium in Fig. 54. The Fourier transform of these acf elements is dielectric loss,[1,2] and this shows the presence of *laser-induced dielectric relaxation*[418] a potentially very useful phenomenon. In practice the THz fields of the simulation are replaced by GHz circularly polarized fields from a klystron or waveguide. Figure 55 also shows the presence of four off-diagonal orientational time-cross correlation functions in the presence of the circularly polarized electromagnetic field.

Figure 57–59 show the effect of the laser on the Fourier transform of the far infrared power absorption of the chiral liquid. There are interestingly asymmetric rotational velocity cross-correlation functions reminiscent of those simulated for shear (see Section VIII) by Evans and Heyes.[422] This shows that a circularly polarized radio-frequency field is capable, in a chiral liquid, of producing bandshape changes in the far infrared, providing new information on the molecular dynamics (Sections I–VII) of the liquid. The far infrared is of course the high-frequency adjunct (Section I) of the frequency range in which relaxational behavior has been investigated

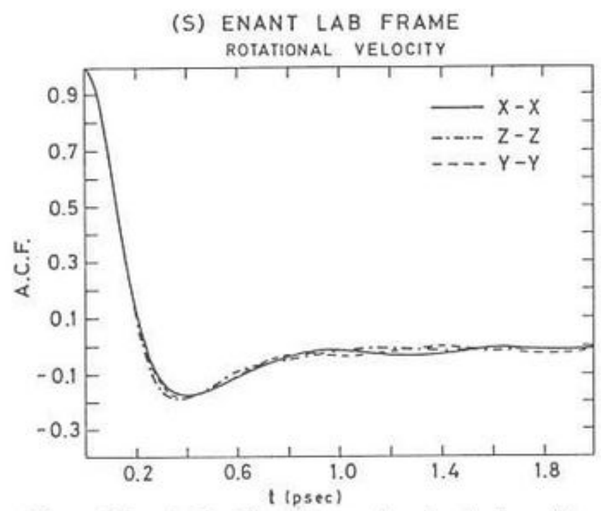

Figure 57. As for Fig. 55, rotational velocity acf's.

historically, and these results show the presence of *electromagnetically induced far infrared relaxational effects*.

The precise molecular dynamical nature of these have been animated on video at the Cornell National Supercomputer Facility and video copies are available on request from the Cornell Theory Center.

U. Symmetry of Laser-Induced Electric Polarization in Chiral Single Crystals

It is possible to express the induced electric polarization just described in terms of a P-negative molecular property tensor X_{ij} defined through

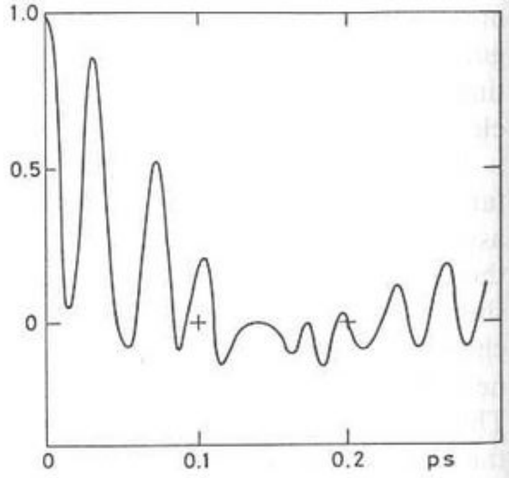

Figure 58. As for Fig. 57, 10.0 THz.

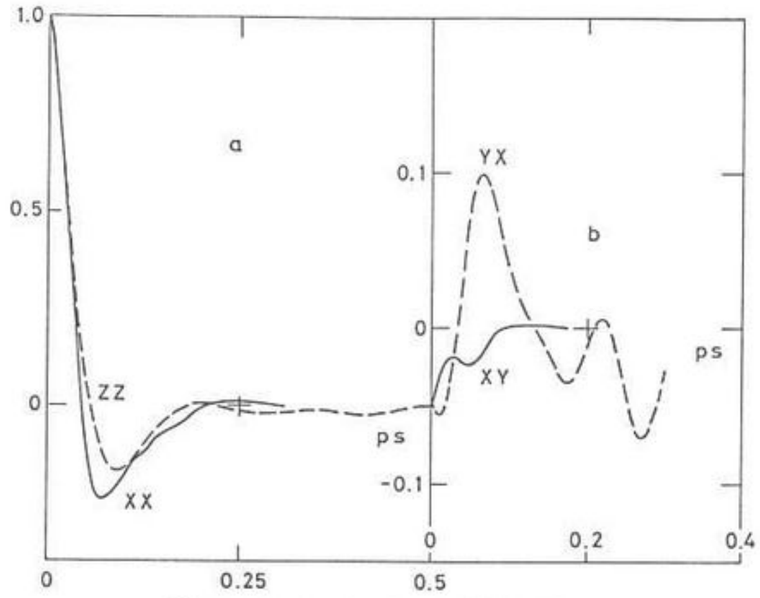

Figure 59. As for Fig. 57, 0.01 THz

$$\mu_i = X_{ij}\Pi_j \tag{490}$$

where μ_i is the induced electric dipole moment. It has been shown that X_{ij} is defined through the time-dependent Schrödinger equation by[432]

$$X_{\alpha\beta} = -\frac{2}{\hbar}\sum_{j\neq n}\frac{\langle n|\mu'_\alpha|j\rangle\langle j|\alpha''_\beta|n\rangle}{\omega_{jn}} \tag{491}$$

for a transition between quantum states n and j. Here μ'_α is the transition electric dipole moment. The angular polarizability is conveniently expressed by

$$\alpha''_{1\gamma} = \alpha''_{1\alpha\beta} - \alpha''_{1\beta\alpha} \tag{492}$$

through the tensor definition[422] of the T-negative, antisymmetric, part of the imaginary polarizability.

In this subsection, we consider the symmetry characteristics of X_{ij} in the 11 major chiral crystal point groups. This is important for ab initio computations and experimental investigations of X_{ij} in individual chiral molecules, and in chiral single crystals of material with useful nonlinear optical characteristics. In general, the symmetry of X_{ij} is

$$\Gamma(X_{ij}) = \Gamma(\mu'_i)\,\Gamma(\alpha''_{1j}) \tag{493}$$

TABLE VIII
Symmetry of X_{ij} in the Chiral Crystal Point Groups

Point Group		Finite Components of $X_{\alpha\beta}$	Orientation	Symmetry
Triclinic	C_1 (1)	All	Any	9A
Monoclinic	C_2 (2)	XX, YY, ZZ, XY, YX	$C^2 \parallel Z$	5A + 4B
Orthorhombic	D_2	XX, YY, ZZ	$C_2 \parallel X \parallel Y$	$3A_1 + 2B_1 + 2B_2 + 2B_3$
Trigonal	C_3 (3)	XX = YY, ZZ, XY − YX	$C_3 \parallel Z$	3A + 3E
	D_3(32)	XX = YY, ZZ	$C_3 \parallel Z$; $C_2 \parallel Y$	$2A_1 + A_2 + 3E$
Tetragonal	C_4 (4)	XX = YY, ZZ, XY − YX	$C_4 \parallel Z$	3A + 2B + 2E
	D_4	XX = YY, ZZ	$C_4 \parallel Z$; $C_2 \parallel Y$	$2A_1 + A_2 + B_1 + B_2 + 2E$
Hexagonal	C_6 (6)	XX = YY, ZZ, XY − YX	$C_6 \parallel Z$	$3A + 2E_1 + E_2$
	D_6 (622)	XX = YY, ZZ	$C_6 \parallel Z$; $C_2 \parallel Y$	$2A_1 + A_2 + E_2 + 2E_1$
Cubic	T (23)	XX = YY = ZZ	$C_4 \parallel Z$; $C_4 \parallel Y$	A + E + 2T
Chiral liquid		XX = YY = ZZ		$D^{(0)} + D^{(1)} + D^{(2)}$

which is a product of those of the electric dipole moment μ_i' and the angular polarizability α_{1j}''. In the point group R(3) of all rotations, the point group of a liquid ensemble of chiral molecules (Section VII), Eq. (493) can be expressed in terms of the irreducible D representations and D symmetries of Section VII as follows:

$$\Gamma(X_{ij}) = (D^{(0)} + D^{(1)} + D^{(2)})(-) \tag{494}$$

It is T- and P-negative, and must be activated by the T-negative influence $\mathbf{\Pi}$ to be observed, following the third principle of Section VII. It disappears at field-free equilibrium because the angular polarizability is essentially a projection of the imaginary part of the dynamic polarizability (Eq. 422) on to the Z axis. This is a finite ensemble average in a liquid ensemble only in the presence of $\mathbf{\Pi}$. It mediates a P-negative electric dipole moment μ_i produced by the P-positive influence Π_j, and in consequence can exist only in chiral media, such as chiral single crystals (Table VIII).

Note that this table can be used to characterize the equivalent molecular point groups, with the laboratory frame (X, Y, Z) replaced by the molecule fixed frame of the point group character tables.

In the triclinic crystal C_1 for example, there are nine independent components of X_{ij}, that is, the crystal supports all components in the laboratory frame (X, Y, Z). This is summarized by nine occurrences of the totally symmetric representation of the C_1 point group in the last column. Similarly, in a molecule of C_1 symmetry, all elements of X_{ij} exist in the molecule fixed frame. In the monoclinic there are five independent elements, in the trigonal C_3 there are three, and so on, thus summarizing the symmetry of the tensor X_{ij}, mediating laser-induced electric polarization in chiral crystals.

V. Electrodynamics of a Rotating Body—Some Spectral Consequences of the Lorentz Transformation

In the relativistic theory of classical electromagnetic fields[424] the Lorentz transformations relate **E** and **B** in the rest frame to their equivalents in a moving frame. The latter may translate or rotate with respect to the former. The Lorentz transformations show that the electromagnetic radiation reaching the rest frame of an earth-bound observer from a source in a distant galaxy, for example, receding along the X axis of the rest frame contains information about the velocity v at which the source is receding from the earth. The further away the galactic source in an expanding universe, the closer the fraction v/c approaches unity, where c is the constant velocity of light. This manifests itself in such well-known spectral phenomena as the stellar–galactic red shift.

The red shift is only one out of many optical phenomena which can be observed in the rest frame of the earth-bound observer with a contemporary laser spectropolarimeter, such as the one constructed by R. V. Jones,[414] attached to a telescope. It is shown in this subsection that circular birefringence in a chiral earth-bound sample is amplified relativistically when observed with the telescope–polarimeter. It is shown in Ref. 425 that the optical activity observed in this way with a source of electromagnetic radiation receding with a velocity v_Z (e.g., a star in a far galaxy) is amplified by the factor

$$R = (c + v_Z)/(c - v_Z) \tag{495}$$

the relativistic amplification.[425] This appears to be of interest in the amplification of the tiny parity nonconserving optical activity recently observed in atomic vapors.[426–430] The measurement proceeds in principle by gathering the stellar radiation with a powerful telescope, possibly in orbit, plane polarizing it, and analyzing the angle of rotation with the probe laser spectropolarimeter to microradian accuracy. This simultaneously provides information on the velocity of recession v_Z of the source, and amplifies relativistically the natural optical activity of the earth-bound sample.

Elegant use was made of a laser spectropolarimeter by R. V. Jones[414] in the first experimental demonstration of *rotational ether drag*, a circular birefringence of pure relatively origin generated in an achiral rotating glass rod by the Lorentz transformation.

It appears that J. J. Thompson[431] was the first to analyze ether drag, when, a few years after the first Michelson–Morley experiment, he considered light passing through a medium that is rotating about an axis parallel with the propagation axis of the electromagnetic beam. The angu-

lar drag per unit path length (the angle of rotation) was later obtained by Fermi[432] and was proportional to the ratio of the angular frequency of the rotating body (Ω_Z) to the velocity of light. Player[433] later extended Fermi's analysis to dispersive ether drag in a transparent rotating rod, which was measured meticulously by R. V. Jones, giving a result in good agreement with theory.[414]

The present author has extended the consideration by Player in several directions[434] to include the magnetization term of the Lorentz transformation, second-order effects, and polarization effects in a rotating rod of absorbing chiral material. In each case relativistic terms were found to give theoretical contributions to the angular rotation measurable in principle by a laser spectropolarimeter.[414]

These new effects were based on the Maxwell equation

$$\frac{1}{\mu_0}\nabla \times \mathbf{B} = \frac{\partial}{\partial t}(\epsilon_0 \mathbf{E} + \mathbf{P}) \tag{496}$$

Equation (496) is written in the approximation $\mathbf{M} \ll \mathbf{P}$, and $\mathbf{J} = 0$, where $\mathbf{M}$ is the bulk magnetization, $\mathbf{P}$ the polarization, and $\mathbf{J}$ the current density in the rest frame of the observer. Here ϵ_0 and μ_0 are respectively the frame invariant permittivity and permeability in vacuo. The time t is measured in the observer frame.

Consider the rod rotating at an angular velocity Ω_Z about the Z axis of the observer frame while radiation from a source in this frame propagates through it in the same Z axis. The quantities $\mathbf{P}$, $\mathbf{E}$, and $\mathbf{B}$ in Eq. (496) are now defined in the frame (x, y, z) which rotates with the rod. The inverse of the Lorentz transformation must be used to relate $\mathbf{P}$, $\mathbf{E}$, and $\mathbf{B}$ in frame (x, y, z) to their equivalents in the frame (X, Y, Z) of the static observer, the frame in which t is defined. In SI units,

$$[\mathbf{B}]_{(x,y,z)} = \left[\beta\left(\mathbf{B} - \frac{1}{c^2}\mathbf{v} \times \mathbf{E}\right)\right]_{(X,Y,Z)} \tag{497}$$

$$[\mathbf{E}]_{(x,y,z)} = [\beta(\mathbf{E} + \mathbf{v} \times \mathbf{B})]_{(X,Y,Z)} \tag{498}$$

$$[\mathbf{P}]_{(x,y,z)} = [\beta(\mathbf{P} - \epsilon_0\mu_0 \mathbf{v} \times \mathbf{M})]_{(X,Y,Z)} \tag{499}$$

where

$$\beta = \left(1 - \frac{v^2}{c^2}\right)^{-1/2} \tag{500}$$

and where the velocity v is defined[433] by

$$v_x = -\Omega_z y; \qquad v_y = \Omega_z X; \qquad v_z = 0 \tag{501}$$

where $\mathbf{R}$ is the radius of the rod. Note that $\mathbf{v}$ has the components

$$\mathbf{v} = \boldsymbol{\Omega} \times \mathbf{R}; \qquad \nabla \cdot \mathbf{v} = 0; \qquad \nabla \times \mathbf{v} = 2\boldsymbol{\Omega} \tag{502}$$

Therefore, the Maxwell equation (Eq. 496) becomes

$$\frac{1}{\mu_0}\left(\nabla \times \mathbf{B} - \frac{1}{c^2}\nabla \times (\mathbf{v} \times \mathbf{E})\right) = \epsilon_0 \frac{\partial}{\partial t}(\mathbf{E} + \mathbf{v} \times \mathbf{B}) + \frac{\partial}{\partial t}(\mathbf{P} - \epsilon_0\mu_0 \mathbf{v} \times \mathbf{M}) \tag{503}$$

with all quantities defined in the frame of the observer, the static laboratory frame (X, Y, Z).

Equation (503) has three extra terms of purely relativistic origin.[434] One of these is the Lorentz magnetization, $-\epsilon_0\mu_0 \mathbf{v} \times \mathbf{M}$, which introduces a contribution to the Thompson–Fermi–Player angle drag as described in Ref. 434, and also produces an interesting *relativistic forward–backward birefringence* which is measurable[435] in the Z axis with unpolarized light.

Player[433] considered a quasi-monochromatic optical disturbance in an isotropic medium of low absorption, where the displacement $\mathbf{D}$ was put directly proportional to the electric field strength $\mathbf{E}$, with no explicit consideration of the molecular nature of the polarization $\mathbf{P}$ and Lorentz magnetization. Molecular property tensors were employed in Refs. 434 and 435 to consider the relativistic effects of rotating a rod composed of molecular material. The displacement was accordingly

$$\mathbf{D} = \epsilon_0 \mathbf{E} + \mathbf{P} \tag{504}$$

with $\mathbf{E}$ and $\mathbf{P}$ defined respectively by Eqs. (498) and (499).

As in Player's analysis, the angular frequencies of the right and left circularly polarized components of the electromagnetic plane wave are affected by equal and opposite Doppler shifts, so that their frequencies in frame (X, Y, Z) appear to the observer to be[435]

$$\omega_R = \omega + \omega_1; \qquad \omega_L = \omega - \omega_1; \qquad \omega_1 = \left(\frac{\Omega_z R}{2c}\right)\omega \tag{505}$$

respectively, for right and left circular polarization of the probe laser. Accordingly, the frequency-dependent molecular property tensors are functions not of ω, but of these Doppler-shifted frequencies.

Without the Lorentz magnetization, the circular birefringence due to ether drag is found from Eq. (503) to be

$$n'_{LZ} - n'_{RZ'} = 3\Omega_z\left(\frac{1}{\omega - \Omega_D} + \frac{1}{\omega + \Omega_D}\right) \tag{506}$$

so that the angle of rotation is proportional to the ratio of Ω_z to the velocity of light, as found by both Player[433] and Fermi.[432] When Lorentz magnetization is accounted for in an absorbing chiral rod this result is supplemented[435] by

$$\langle n'_L - n'_R\rangle_{LM} = 2\Omega_Z Y\langle\alpha_{2ZY}\rangle\mu_0 N \tag{507}$$

which is proportional to the number of molecules per unit volume of the rotating rod N, and to the ensemble average over the Rosenfeld molecular property tensor component α_{2ZY}. There are also interesting second-order effects[434] which can be treated with molecular property tensors.

Relativistic forward–backward birefringence is present, furthermore, both in chiral and achiral rotating rods.[435] This effect is interestingly much larger in magnitude that ether drag, and is proportional to nonvanishing diagonal scalar components of ensemble-averaged molecular property tensors, giving information on them in a rotating chiral rod. In general, it can be expressed in terms of diagonal and off-diagonal elements of molecular property tensors through the magnetization term of the Lorentz transformation. It also depends on the X and Y velocity components of the rotating rod. If this is a chiral crystal, the Lorentz magnetization also makes a contribution, just described, to the rotational ether drag.

Defining $\mathbf{k}$ as a unit vector in the Z axis of the static observer frame, relativistic forward–backward birefringence is generated from the equation

$$\nabla(\mathbf{E}\cdot\mathbf{v}) = -\frac{\partial}{\partial t}(\mathbf{v}\times\mathbf{B}) + \mu_0\frac{\partial}{\partial t}(\mathbf{v}\times\mathbf{M}) \tag{508}$$

by comparing $\mathbf{k}$ coefficients in Eq. (503). Using the approximation

$$\nabla\times(\mathbf{v}\times\mathbf{E}) \sim \nabla(\mathbf{E}\cdot\mathbf{v}) - 2\mathbf{E}\times\boldsymbol{\Omega} \tag{509}$$

Ref. 435 derives the results

$$n'_{av} = \tfrac{1}{2}(\langle n'_{LZ}\rangle + \langle n'_{RZ}\rangle) \doteqdot 1 + \tfrac{1}{2}\mu_0 Nc\langle\alpha'_{2YY}\rangle \tag{510}$$

and

$$A''_{av} = \frac{\omega}{c}(\langle n''_{LZ}\rangle + \langle n''_{RZ}\rangle) \doteqdot \mu_0 Nc\langle\alpha''_{2YY}\rangle \tag{511}$$

for the average real refractive index n'_{av} and power absorption coefficient A''_{av} along the axis of the rotating rod in terms of the frequency-dependent diagonal elements $\langle\alpha'_{2yy}\rangle$ and $\langle\alpha''_{2yy}\rangle$ of the Rosenfeld tensor. Both $\langle\alpha'_{2yy}\rangle$ and $\langle\alpha''_{2yy}\rangle$ are visible therefore to *unpolarized* radiation, an interesting new effect of relativity. The latter also enters into consideration through the Doppler shifts of the frequency in the molecular property tensors. For example, the real and imaginary parts of the Rosenfeld tensor

$$\alpha'_{2YY} = \frac{\partial}{\hbar}\sum_{j\neq n}\frac{(\omega\pm\omega_1)_{jn}}{(\omega\pm\omega_1)^2_{jn} - (\omega\pm\omega_1)^2}\,\mathrm{Re}(\langle n|\mu_Y|j\rangle\langle j|m_Y|n\rangle) \tag{512}$$

and

$$\alpha''_{2YY} = -\frac{\partial}{\hbar}\sum_{j\neq n}\frac{(\omega\pm\omega_1)}{(\omega\pm\omega_1)^2_{jn} - (\omega\pm\omega_1)^2}\,\mathrm{Im}(\langle n|\mu_Y|j\rangle\langle j|m_Y|n\rangle) \tag{513}$$

Note that the former is negative to T and the latter is positive to T from semiclassical theory in a nonrotating medium. The rotation itself provides a vehicle for the "activation" of the real part of the Rosenfeld tensor, which becomes observable (Eq. 510) through the average refractive index measured by unpolarized radiation directed along the Z axis of the rotating rod. Further discussion of the role of bulk angular momentum in a nonrelativistic context is given in Ref. 436.

The above rotating rod method appears to be useful therefore in the

study of vibrational dichroism[437] without recourse to circularly polarized radiation.

W. Parity Nonconservation in New Laser Spectroscopies

Parity nonconservation is well known[279,438] to cause tiny optical rotations is atomic ensembles which are otherwise achiral. Several of the new laser spectroscopies developed in this section are mediated only in a chiral ensemble, examples being forward–backward birefringence due to (1) static magnetic flux density (the Wagnière–Meier effect), (2) the conjugate product $\mathbf{\Pi}$,[412,413] and, as we have just seen, (3) relativity in a rotating chiral rod. If any of these effects are observed in an achiral medium, such as water, it signals the presence of parity nonconservation in molecular matter.[438] Parity nonconservation applies whenever the Wigner Principle of Parity conservation is broken; another example would be the observation of circular birefringence and dichroism caused in an achiral medium by the time derivative of an electric field.

This is probably one of the most profound applications of the new spectroscopies introduced in this section, and further details of the ideas behind P and T nonconservation may be found in the interesting articles by Barron[279,438] and Mason.[439]

Acknowledgments

Part of this research was supported by the Center for Theory and Simulations in Science and Engineering (the Cornell Theory Center), which receives major funding from NSF (US); IBM (US), New York State, and Members of the Corporate Research Institute. Funding and support is also acknowledged from: IBM Kingston, New York State; the Universities of Zurich, London, Lancaster, and Wales; SERC (UK); the Leverhulme Trust; the Nuffield Foundation; and the Cornell National Supercomputer Facility.

Special thanks are due to Dr. Laura J. Evans.

References

1. M. W. Evans, G. J. Evans, W. T. Coffey, and P. Grigolini, *Molecular Dynamics and the Theory of Broad Band Spectroscopy*, Wiley Interscience, New York, 1982.
2. M. W. Evans, W. T. Coffey, and P. Grigolini, *Molecular Diffusion*, Wiley Interscience, New York, 1984; M.I.R., Moscow, 1988.
3. M. W. Evans, P. Grigolini, and G. Pastori-Parravicini, Eds., *Memory Function Approaches to Dynamical Problems in Condensed Matter*, vol. 62 of *Advances in Chemical Physics*, I. Prigogine and S. A. Rice, Eds., Wiley Interscience, New York, 1985.
4. Ibid., vol. 63, M. W. Evans, Ed., *Dynamical Processes in Condensed Matter*.
5. P. Debye, *Polar Molecules*, Chem. Catalog Co., New York, 1929.
6. A. Einstein, *Investigations on the Theory of the Brownian Movement*. R. Furth, Ed., Dover, New York, 1956.

7. N. Wax, Ed., *Selected Papers on Noise and Stochastic Processes*, Dover, New York, 1954.
8. J. Goulon, *Theories Stochastiques des Phenomènes de Transport*, Cas des Mouvements de Reorientations Moleculaires, Nancy, 1972.
9. P. Bordewijk and C. J. F. Böttcher, *Theory of Electric Polarization*, vols. 1 and 2, Elsevier, Amsterdam, 1973, 1979.
10. H. Fröhlich, *Theory of Dielectrics*, Oxford University Press, 1958.
11. J. B. Hasted, *Aqueous Dielectrics*, Chapman and Hall, London, 1973.
12. N. E. Hill, W. E. Vaughan, A. H. Price, and M. Davies, *Dielectric Properties and Molecular Behaviour*, van Nostrand, London, 1969.
13. B. K. P. Scaife, Ed., *Complex Permittivity*, English University Press, London, 1971.
14. C. P. Smyth, *Dielectric Behavior and Structure*, McGraw-Hill, New York, 1965.
15. A. D. Buckingham, Ed., *Organic Liquids, Structure, Dynamics, and Properties*, Wiley, New York, 1979.
16. A. Einstein, *Ann. Phys.* **17**, 549 (1905); **19**, 371 (1906).
17. P. Langevin, see Ref. 7.
18. M. von Smoluchowski, see Ref. 7.
19. P. Debye, Ref. 5.
20. J. L. Doob, *Stochastic Processes*, Wiley, New York, 1963.
21. J. Perrin, see Ref. 7.
22. A. Rahman, *Rev. Nuovo Cim.* **1**, 315 (1969).
23. H. Mori, *Prog. Theor. Phys.* **33**, 423 (1965); **34**, 399 (1965).
24. M. Davies Ed., *Dielectric and Related Molecular Processes*, vols. 1 to 3, Chemical. Society., London, 1972–1977.
25. R. A. Sack, *Physica* **22**, 917 (1956); *Proc. Phys. Soc.* **70**, 402, 414 (1957).
26. J. T. Lewis, J. R. McConnell, and B. K. P. Scaife, *Proc. R. Irish Acad.* **76A**, 43 (1976).
27. See C. Brot and G. Wyllie in Ref. 24.
28. K. D. Muller and W. D. Rothschild, *Far Infra red Spectroscopy*, Wiley Interscience, New York, 1971.
29. G. Chantry, *Submillimetre Spectroscopy*, Academic, New York, 1971.
30. N. E. Hill, *Proc. Phys. Soc.* **82**, 723 (1963).
31. G. Wyllie, reviewed in Ref. 24.
32. I. Larkin and M. W. Evans, *J. Chem. Soc., Faraday Trans.* **2**, 70, 477 (1974).
33. J. H. Calderwood and W. T. Coffey, *Proc. R. Soc., A* **356**, 269 (1977).
34. M. W. Evans, Ref. 24, **3**, 1 (1977).
35. M. W. Evans, W. T. Coffey, G. J. Evans, and G. Wegdam, *J. Chem. Soc., Faraday Trans.* **2**, 74, 1310 (1977).
36. W. T. Coffey and M. W. Evans, *Mol. Phys.* **35**, 975 (1978).
37. M. W. Evans, W. T. Coffey, and G. J. Evans, ibid. **38**, 477 (1978).
38. E. Kestermont, F. Hermans, R. van Loon, G. J. Evans, and M. W. Evans, *Chem. Phys. Lett.* **52**, 521 (1978).
39. M. W. Evans, A. R. Davies, and G. J. Evans, in *Advances in Chemial Physics*, vol. 44, I. Prigogine and S. A. Rice, Eds., Wiley Interscience, New York, 1980, pp. 255–481.

40. M. W. Evans, W. T. Coffey, and G. J. Evans, *Adv. Mol. Rel. Int. Proc.* **20**, 11 (1981).
41. W. T. Coffey, P. Corcoran, and M. W. Evans, *Proc. R. Soc., A* **410**, 61 (1987).
42. W. T. Coffey, P. Corcoran, and M. W. Evans, *Mol. Phys.* **61**, 1 (1987).
43. Ibid., p. 15.
44. M. W. Evans, *Chem. Phys. Lett.* **39**, 601 (1976).
45. M. W. Evans and G. J. Evans, *J. Mol. Liq.* **36**, 293 (1987).
46. B. J. Berne and R. Pecora, *Dynamical Light Scattering with Reference to Physics, Chemistry and Biology*, Wiley Interscience, New York, 1976.
47. J. P. Ryckaert, A. Bellemans, and G. Ciccotti, *Mol. Phys.* **44**, 979 (1981).
48. M. W. Evans, *Phys. Rev. Lett.* **50**, 351 (1983).
49. For a review, see Ref. 4, M. W. Evans and G. J. Evans.
50. M. W. Evans, *Phys. Rev. Lett.* **55**, 1551 (1985).
51. M. W. Evans and G. J. Evans, ibid., p. 818.
52. M. W. Evans, *Phys. Rev. A* **34**, 468 (1986).
53. M. W. Evans and G. J. Evans, ibid. **33**, 1903 (1985).
54. D. H. Whiffen, *Mol. Phys.* **63**, 1053 (1988).
55. M. W. Evans, K. N. Swamy, G. C. Lie, and E. Clementi, *Mol. Sim.* **1**, 187 (1988).
56. M. W. Evans, *Phys. Rev. A* **34**, 2302 (1986).
57. M. W. Evans, ibid. **35**, 2989 (1987).
58. M. W. Evans, *Physica* **168**, 9 (1991).
59. A. H. Price and P. Maurel, *J. Chem. Soc., Faraday Trans.* 2, **69**, 1486 (1973).
60. For a review, see Ref. 12.
61. J. Chamberlain, *The Principles of Interferometric Spectroscopy*, Wiley, Chichester, 1978.
62. For example, Bruker Spectrospin, *Quart. Rev.*
63. M. W. Evans, M. Davies, and I. W. Larkin, *J. Chem. Soc., Faraday Trans.* 2, **69**, 1011 (1973).
64. J. Goulon, D. Canet, G. J. Davies, and M. W. Evans, *Mol. Phys.* **30**, 973 (1975).
65. G. J. Davies and M. W. Evans, *J. Chem. Soc., Faraday Trans.* 2, **71**,1275 (1975).
66. Ibid. **72**, 727 (1976).
67. Ibid., p. 1206.
68. G. J. Davies, G. J. Evans, and M. W. Evans, ibid., p. 1901.
69. M. W. Evans, *Spectrochim. Acta* **30**, 79 (1974).
70. M. W. Evans, *J. Chem. Soc., Faraday Trans.* 2, **69**, 763 (1973).
71. Ibid. **71**, 843 (1975).
72. A. I. Baise, ibid. **69**, 1907 (1972).
73. J. H. Colpa and J. A. A. Ketelaar, *Mol. Phys.* **1**, 873 (1958).
74. M. W. Evans, *Mol. Phys.* **29**, 1345 (1975).
75. M. W. Evans, *Spectrochim. Acta* **32**,1259 (1976).
76. R. Balescu, *Equilibrium and non-Equilibrium Statistical Mechanics*, Wiley, New York, 1975.
77. D. A. McQuarrie, *Statistical Mechanics*, Harper and Row, New York, 1975.
78. R. C. Tolman, *The Principles of Statistical Mechanics.*, Oxford University Press, 1938.

79. G. J. Evans, C. J. Reid, and M. W. Evans, *J. Chem. Soc., Faraday Trans.* **2**, 74, 343 (1978).
80. C. J. Reid, R. A. Yadav, G. J. Evans, and M. W. Evans, ibid. **74**, 2143 (1978).
81. C. J. Reid, G. J. Evans, and M. W. Evans, *Chem. Phys. Lett.* **56**, 529 (1975).
82. C. J. Reid and M. W. Evans, *J. Chem. Soc., Faraday Trans.* 2, **75**, 1218 (1975).
83. Ibid. **76**, 286 (1980).
84. Ibid., *Mol. Phys.* **40**, 1357 (1980).
85. Ibid., in *Molecular Interactions*, W. J. Orville-Thomas, Ed., Wiley, Chichester, 1982.
86. M. W. Evans, *Spectrochim. Acta* **36A**, 929 (1980).
87. M. W. Evans, *Acc. Chem. Res.* **14**, 253 (1981), The Meldola Lecture.
88. M. W. Evans, *Chem. Phys.* **62**, 481 (1981).
89. M. W. Evans, G. J. Davies, and M. Veerappa, ibid. **61**, 73 (1981).
90. G. J. Evans and M. W. Evans, *Infra red Phys.* **18**, 455 (1978).
91. D. M. Heyes and D. Fincham, in Ref. 4.
92. J. P. Hansen and I. R. McDonald, *Theory of Simple Liquids*, 2nd. ed., Academic, New York, 1986.
93. L. Verlet, *Phys. Rev.* **159**, 98 (1967).
94. K. Singer, J. V. L. Singer, and A. J. Taylor, *Mol. Phys.* **37**, 1239 (1979).
95. M. W. Evans, G. J. Evans, and G. Wegdam. *Mol. Phys.* **33**, 180 (1977).
96. M. W. Evans, *Chem. Phys. Lett.* **58**, 518 (1978).
97. C. Brot, G. Bossis, and C. Hesse-Bezot, *Mol. Phys.* **40**,1053 (1980).
98. D. Kivelson and P. Madden, *Mol. Phys.* **30**, 1749 (1975).
99. B. K. P. Scaife, in Ref. 24, vol. 1.
100. J. G. Kirkwood, *J. Chem. Phys.* **7**, 911 (1939).
101. A. M. Stoneham, *Handbook of Interatomic Potentials*, A.E.R.E., Harwell, 1981.
102. *The Information Quarterly for MD and MC Simulations*, S.E.R.C., Daresbury, U.K.
103. E. K. Eliel, N. L. Allinger, S. J. Angyal, and G. A. Morrison, *Conformational Analysis*, Wiley, New York, 1965.
104. G. C. Lie and E. Clementi, *Phys. Rev. A* **33**, 2679 (1986).
105. M. Wojcik and E. Clementi, *J. Chem. Phys.* **85**, 3544 (1986).
106. M. W. Evans, G. C. Lie, and E. Clementi, *J. Chem. Phys.* **89**, 6399 (1988).
107. M. W. Evans and C. J. Reid, ibid. **76**, 2576 (1982).
108. Ibid., *Spectrochim. Acta* **38A**, 417 (1982).
109. M. W. Evans, G. C. Lie, and E. Clementi, *J. Chem. Phys.* **87**, 6040 (1987).
110. G. C. Lie and E. Clementi, ibid. **64**, 2314 (1976).
111. M. D. Morse and S. A. Rice, ibid. **76**, 650 (1982).
112. M. G. Sceats and S. A. Rice, in *Water, A Comprehensive Treatise*, vol. 7, F. Francks, Ed., Plenum, New York, 1982.
113. For example the Specialist Periodical Reports of the London Chemical Society.
114. P. N. Brier and A. Perry, *Adv. Mol. Rel. Int. Proc.* **13**, 46 (1978).
115. P. van Konynenberg and W. A. Steele, *J. Chem. Phys.* **56**, 4775 (1972).
116. A. M. Amorim da Costa, M. A. Norman, and J. H. P. Clarke, *Mol. Phys.* **29**, 191 (1975).

117. P. A. Lund, O. Faurskov-Nielsen, and E. Praestgaard, *Chem. Phys.* **28**, 167 (1978).
118. J. F. Dill, T. A. Litovitz, and J. A. Bucaro, *J. Chem. Phys.* **62**, 3839 (1975).
119. C. K. Cheung, D. R. Jones, and C. H. Wang, *J. Chem. Phys.* **64**, 3567 (1976).
120. S. Claesson and D. R. Jones, *Chim. Scripta* **9**, 103 (1976).
121. A. E. Boldeskal, S. S. Esman, and V. E. Pogornelov, *Opt. Spectrosc.* **37**, 521 (1974).
122. V. M. Baranov, *Vopt. Mol. Spektrosk.* **89**, 348 (1974).
123. M. W. Evans, W. Luken, G. C. Lie, and E. Clementi, *J. Chem. Phys.* **88**, 2685 (1988).
124. J. Anderson, I. J. Ullo, and S. Yip, *J. Chem. Phys.* **86**, 4078 (1987).
125. M. W. Evans, G. C. Lie, and E. Clementi, *J. Mol. Liq.* **40**, 89 (1989).
126. P. A. Egelstaff, *An Introduction to the Liquid State*, Academic, New York, 1967.
127. M. W. Evans and M. Ferrario, *Adv. Mol. Rel. Int. Proc.* **22**, 245 (1982).
128. Ibid., p. 75.
129. Ibid., *Chem. Phys.* **72,** 141 and 147 (1982).
130. M. W. Evans, M. Ferrario, P. Marin, and P. Grigolini, *J. Mol. Liq.* **26**, 249 (1983).
131. M. W. Evans, G. C. Lie, and E. Clementi, *Phys. Lett A* **130**, 289 (1988).
132. M. W. Evans and A. A. Hasanein, *J. Mol. Liq.* **29**, 45 (1984).
133. C. Brot and I. Darmon, *Mol. Phys.* **21**, 785 (1971).
134. M. W. Evans and M. Ferrario, *Adv. Mol. Rel. Int. Proc.* **24**, 139 (1982).
135. M. W. Evans, G. J. Evans, and V. K. Agarwal, *J. Chem. Soc., Faraday Trans.* 2, **79**, 153 (1983).
136. M. W. Evans and G. J. Evans, ibid. **79**, 767 (1983).
137. M. W. Evans, *J. Mol. Liq.* **25**,149 (1983).
138. M. W. Evans and G. J. Evans, ibid. **26**, 63 (1983).
139. M. W. Evans, *Phys. Rev. A* **30**, 2062 (1984).
140. M. W. Evans, *J. Chem. Soc., Faraday Trans.* 2, **81**, 1463 (1985).
141. M. W. Evans, *Phys. Scripta* **31**, 419 (1985).
142. M. W. Evans, *Physica* **131B&C**, 273 (1985).
143. M. W. Evans, G. C. Lie, and E. Clementi, *Chem. Phys. Lett.* **138**, 149 (1987).
144. M. W. Evans, G. C. Lie, and E. Clementi, *Phys. Rev. A* **36**, 226 (1987).
145. D. J. Evans, *Computer Phys. Rep.* **1**, 299 (1984).
146. A van der Avoird, F. Mulder, P. E. Wormer, and P. M. Berns, in *Topics in Current Chemistry*, M. J. S. Dewar, Ed., Springer Verlag, Berlin, 1980.
147. Ref. 1. p. 818.
148. H. S. Sandhu, *J. Am. Chem. Soc.* **97**, 6284 (1975).
149. Ibid., p. 830.
150. M. Woijik and E. Clementi, *J. Chem. Phys.* **85**, 3544 (1986).
151. O. Matsuoka, E. Clementi, and M. Yoshimine, *J. Chem. Phys.* **64**, 1351 (1976).
152. S. Toxvaerd, *Phys. Rev. Lett.* **51**, 1971 (1983).
153. K. N. Swamy and E. Clementi, IBM Technical Report, Dept. 48B/428, Kingston, New York, 1987.
154. E. Clementi and K. N. Swamy, in *Structure and Dynamics of Proteins, Nucleic Acids and Membranes*, E. Clementi and S. Chin, Ed., Plenum, New York, 1986.
155. Summarized in Chapter 5 of Ref. 3.

156. M. W. Evans, K. N. Swamy, K. Refson, G. C. Lie, and E. Clementi, *Phys. Rev. A*, **36**, 3935 (1987).
157. M. W. Evans, *Phys. Rev. A* **31**, 3947 (1985).
158. M. W. Evans, *Phys. Scripta* **30**, 94 (1984).
159. M. W. Evans, *J. Mol. Liq.* **26**, 49 (1983).
160. M. W. Evans, *J. Chem. Phys.* **79**, 5403 (1983); **78**, 925 (1983).
161. For example, volumes in *Advances in Chemical Physics*, I. Prigogine and S. A. Rice, Eds., Wiley Interscience, New York.
162. M. W. Evans, G. Wegdam, and G. J. Evans, *Adv. Mol. Rel. Int. Proc.* **11**, 295 (1977).
163. T. Occelli, B. Quentrec, and C. Brot, *Mol. Phys.* **36**, 257 (1978).
164. B. J. Alder, H. Strauss, and G. Weiss, *J. Chem. Phys.* **59**, 1002 (1973).
165. M. W. Evans and G. J. Evans, *J. Mol. Liq.* **39**, 25 (1988).
166. M. W. Evans, G. C. Lie, and E. Clementi, ibid. **40**, 89 (1989).
167. R. Zwanzig, *Ann. Rev. Phys. Chem.* **16**, 67 (1965).
168. B. J. Alder and T. E. Wainright, *Phys. Rev.* **1A**, 18 (1970).
169. J. J. Erpenbeck and W. W. Wood, *J. Stat. Phys.* **24**, 455 (1981).
170. W. W. Wood, *Fundamental Problems in Statistical Mechanics, Part* 3, E. G. D. Cohen, Ed., Plenum, New York, 1975, p. 331.
171. D. J. Evans and G. P. Morriss, *Phys. Rev. Lett.* **51**, 1776 (1983).
172. Summarized in Chapter 5 of Ref. 1.
173. E. L. Hannon, G. C. Lie, and E. Clementi, *Phys. Lett. A* **119**, 174 (1986).
174. M. W. Evans, *J. Chem. Soc. Faraday Trans.* 2, **82**, 653 (1986).
175. M. W. Evans, *J. Mol. Struct.* **80**, 389 (1982).
176. M. W. Evans, *Adv. Mol. Rel. Int. Proc.* **22**, 1 (1982).
177. M. W. Evans, J. K. Vij, C. J. Reid, G. J. Evans, and M. Ferrario, *Adv. Mol. Rel. Int. Proc.* **22**, 245 (1982).
178. M. W. Evans and M. Ferrario, ibid. **24**, 139 (1982).
179. Ibid. **24**, 139 (1982).
180. M. W. Evans, ibid. **23**, 113 (1982).
181. J. S. Rowlinson and M. W. Evans, *Chem. Soc. Ann. Rep.* **72**, 5 (1975).
182. A. D. Buckingham, *Chem. Soc. Quart. Rev.* **63** (1959).
183. C. Brot, in Ref. 24, vol. 2, 1975.
184. L. D. Landau and E. M. Lifshitz, *Quantum Mechanics, Non-Relativistic Theory*, Pergamon, Oxford, 1958.
185. C. A. Chatzidimitriou–Dreismann in M. W. Evans, Ed., *J. Mol. Liq.* Orville–Thomas Issue, 1988.
186. M. F. Herman and E. Kluck in Ref. 4.
187. See Ref. 1, p. 235.
188. E. Fatuzzo and P. R. Mason, *Proc. Phys. Soc.* **90**, 729 (1967).
189. D. Kivelson and P. A. Madden, *Mol. Phys.* **30**, 1749 (1975).
190. A. Gerschel, I. Darmon, and C. Brot, ibid. **33**, 527 (1977).
191. M. W. Evans, *Spectrochim. Acta* **31A**, 609 (1975).
192. S. Kielich in Ref. 24, vol. 1, 1972.

193. M. W. Evans, *J. Chem. Soc. Faraday Trans.* 2, **71**, 843 (1975).
194. P. Madden, *Mol. Phys.* **36**, 365 (1978).
195. P. van Konynenberg and W. A. Steele, *J. Chem. Phys.* **56**, 4776 (1972).
196. M. W. Evans, *J. Mol. Liq.* **25**, 211 (1983).
197. M. W. Evans and G. J. Evans, ibid. **25**, 177 (1983).
198. Ibid. **25**, 149 (1983).
199. M. W. Evans, G. J. Evans, and V. K. Agarwal, *J. Chem. Soc. Faraday Trans.* 2, **79**, 137 (1983).
200. M. W. Evans and G. J. Evans, ibid. **79**, 153 (1983).
201. M. W. Evans, ibid. **79**, 719 (1983).
202. M. W. Evans, G. J. Evans, C. J. Reid, P. Minguzzi, G. Salvetti, and J. K. Vij, *J. Mol. Liq.* **34**, 269 (1987).
203. M. W. Evans, ibid. **34**, 269 (1987).
204. M. W. Evans, G. C. Lie, and E. Clementi, *Phys. Rev. A* **36**, 226 (1987).
205. M. W. Evans, K. N. Swamy, G. C. Lie, K. Refson, and E. Clementi, ibid. **36**, 3935 (1986).
206. M. W. Evans, G. C. Lie, and E. Clementi, *Phys. Lett. A* **130**, 289 (1988).
207. M. W. Evans, J. K. Vij, and C. J. Reid, *Mol. Phys.* **50**, 1247 (1983).
208. M. W. Evans, K. N. Swamy, G. C. Lie, and E. Clementi, *Mol. Sim.* **1**, 187 (1988).
209. M. W. Evans, *J. Chem. Soc. Faraday Trans.* 2, **79**, 1811 (1983).
210. M. W. Evans, *J. Mol. Liq.* **27**, 19 (1983).
211. M. W. Evans, P. L. Roselli, and C. J. Reid, ibid. **29**, 1 (1984).
212. M. W. Evans, *Phys. Scripta* **39**, 94 (1984).
213. M. W. Evans, C. J. Reid, P. L. Roselli, and J. K. Vij, *J. Mol. Liq.* **29**, 11 (1984).
214. M. W. Evans, *Phys. Rev. A* **30**, 2062 (1984).
215. M. W. Evans, G. J. Evans, and J. Baran, *J. Mol. Liq.* **25**, 261 (1983).
216. M. W. Evans and G. J. Evans, *Chem. Phys. Lett.* **96**, 416 (1983).
217. M. W. Evans, G. J. Evans, and J. Baran, *J. Chem. Soc. Faraday Trans.* 2, **79**, 1473 (1983).
218. M. W. Evans, *J. Mol. Liq.* **26**, 229 (1983).
219. M. W. Evans, *J. Chem. Soc. Faraday Trans.* 2, **81**, 1463 (1985).
220. D. Hennequin, P. Glorieux, E. Arimondo, and M. W. Evans, ibid. **83**, 463 (1987).
221. M. W. Evans, G. C. Lie, and E. Clementi, IBM Technical Report, KGN 142, Kingston, New York, 1987.
222. R. C. Tolman, *The Principles of Statistical Mechanics*, Oxford University Press, 1938.
223. W. T. Coffey and B. V. Paranjape, *Proc. R. Irish Acad.* **78A**, 17 (1978).
224. M. Morse and H. Feschbach, *Methods of Theoretical Physics*, McGraw-Hill, New York, 1953.
225. M. S. Beevers, J. Crossley, D. C. Garrington, and G. Williams, *J. Chem. Soc. Faraday Trans.* 2, **72**, 1482 (1976).
226. M. Gregson and J. Parry–Jones in Ref. 24.
227. M. S. Beevers and J. Khanarian, *Aust. J. Chem.* **32**, 263 (1979); **33**, 2585 (1980).
228. M. W. Evans, *J. Chem. Phys.* **76**, 5473, 5480 (1982); ibid. **77**, 4632 (1983).

229. W. T. Coffey, C. Rybarsch, and W. Schroer, *Phys. Lett. A* **88**, 331 (1982); ibid., *Chem. Phys. Lett.* **92**, 245 (1982).
230. M. W. Evans, G. C. Lie, and E. Clementi, *Phys. Lett. A* **130**, 289 (1988).
231. M. W. Evans, P. Grigolini, and F. Marchesoni, *Chem. Phys. Lett.* **95**, 544 (1983).
232. Ibid., p. 548.
233. P. Grigolini, *Mol. Phys.* **31**, 1717 (1976).
234. M. S. Beevers and D. A. Elliott, *Mol. Cryst. Liq. Cryst.* **26**, 411 (1979).
235. M. W. Evans, G. C. Lie, and E. Clementi, *Phys. Rev. A* **36**, 226 (1987).
236. M. W. Evans, G. C. Lie, and E. Clementi, IBM Technical Report, KGN 153, (1988).
237. M. W. Evans, G. C. Lie, and E. Clementi, *Phys. Rev. A* **37**, 2551 (1988).
238. M. W. Evans, *J. Mol. Liq.* **38**, 175 (1988).
239. M. W. Evans and D. M. Heyes, *Mol. Phys.* **69**, 241 (1990).
240. M. W. Evans, G. C. Lie, and E. Clementi, *Z. Phys. D* **7**, 397 (1988).
241. B. J. Berne and R. Pecora, *Dynamical Light Scattering with Reference to Physics, Chemistry and Biology*, Wiley Interscience, New York, 1976.
242. D. H. Whiffen, *Mol. Phys.* **63**, 1053 (1988).
243. M. W. Evans, *J. Chem. Phys.* **86**, 4096 (1987).
244. J. A Salthouse and M. J. Ware, *Point Group Character Tables*, Cambridge University Press, 1972.
245. L. D. Landau and E. M. Lifshitz, *Mechanics*, Pergamon Press, Oxford, 1976.
246. M. R. Spiegel, *Vector Analysis*, Schaum, New York, 1959.
247. D. W. Condiff and J. S. Dahler, *J. Chem. Phys.* **44**, 3988 (1966).
248. L. P. Hwang and J. H. Freed, *J. Chem. Phys.* **63**, 118, 4017 (1975).
249. P. G. Wolynes and J. M. Deutch, *J. Chem. Phys.* **67**, 733 (1977).
250. G. T. Evans, *Mol. Phys.* **36**, 1199 (1978).
251. U. Steiger and R. F. Fox, *J. Math. Phys.* **23**, 296 (1982).
252. G. van der Zwan and J. T. Hynes, *Physica* **121A** 224 (1983).
253. E. Dickinson, *Ann. Rep. Chem. Soc.* **140**, 421 (1985).
254. N. K. Ailawadi and B. J. Berne, *Faraday Symp.* **11** (1976).
255. B. J. Berne and J. A. Montgomery, *Mol. Phys.* **32**, 363 (1976).
256. M. W. Evans, G. C. Lie, and E. Clementi, *IBM Tech. Rep.*, KGN 131 (1988).
257. M. W. Evans, W. Luken, G. C. Lie, and E. Clementi, *J. Chem. Phys.* **88**, 2685 (1988).
258. G. C. Lie and E. Clementi, *Phys. Rev. A* **33**, 2679 (1986).
259. R. J. Bartlett, I. Shavitt, and G. D. Purvis, *J. Chem. Phys.* **71**, 281 (1979).
260. W. F. van Gunsteren, H. J. C. Berendsen, and J. A. C. Rullman, *Faraday Disc. Chem. Soc.* **66**, 58 (1978).
261. M. W. Evans, G. C. Lie, and E. Clementi, *J. Chem. Phys.* **88**, 5157 (1988).
262. M. G. Sceats and S. A. Rice, in *Water, a Comprehensive Treatise*, vol. 7, F. Franks, Ed., Plenum, New York, 1982.
263. C. A. Angell, ibid., Chapter 1.
264. O. C. Bridgman and E. W. Aldrich, *J. Heat Transfer* **87**, 26 (1965).
265. M. H. Price and J. M. Walsh, *J. Chem. Phys.* **26**, 824 (1957).
266. G. W. F. Pardoe, Ph.D. Thesis, University of Wales, 1969.

267. M. W. Evans, *J. Chem. Soc., Faraday Trans.* 2, **72**, 2138 (1976).
268. M. W. Evans, *J. Chem. Phys.* **86**, 4096 (1987).
269. F. H. Stillinger and A. Rahman, *J. Chem. Phys.* **60**, 1545 (1974).
270. M. W. Evans, G. C. Lie, and E. Clementi, *J. Chem. Phys.* **89**, 6399 (1988).
271. M. W. Evans, G. C. Lie, and E. Clementi, *J. Chem. Phys.* **87**, 6040 (1987).
272. M. W. Evans, *J. Chem. Soc. Faraday Trans.* 2, **82**, 1967 (1986).
273. H. Friedmann and S. Kimel, *J. Chem. Phys.* **47**, 3589 (1967).
274. G. Ewing, *Acc. Chem. Res.* **2**, 168 (1969).
275. M. Doi and S. F. Edwards, *J. Chem. Soc., Faraday Trans.* 2, **74**, 918 (1978).
276. D. Frenkel and J. F. Maguire, *Mol. Phys.* **49**, 503 (1983).
277. M. W. Evans, G. C. Lie, and E. Clementi, *J. Mol. Liq.* **39**, 1 (1988).
278. F. E. Neumann, *Vorlesungen uber die Theorie Elastizitat der Festen Korper und des Lichtathers*, Teubner, Leipzig, 1885.
279. L. D. Barron, *Chem. Soc. Rev.* **15**, 189 (1986).
280. P. Curie, *J. Phys.* (*Paris*) **3**, 393 (1894).
281. S. F. Mason, *Molecular Optical Activity and the Chiral Discriminations*, Cambridge University Press, 1982.
282. L. Pasteur, *Rev. Sci.* **7**, 2 (1884).
283. H. Primas, *Chemistry, Quantum Mechanics, and Reductionism*, Springer-Verlag, Berlin, 1981.
284. E. P. Wigner, *Z. Phys.* **43**, 624 (1927).
285. R. P. Feynman, R. B. Leighton, and M. Sands, *The Feynman Lectures in Physics*, Addison-Wesley, Reading, MA, 1964.
286. L. D. Barron, *Molecular Light Scattering and Optical Activity*, Cambridge University Press, 1982.
287. R. R. Birss, *Symmetry and Magnetism*, North-Holland, Amsterdam, 1966.
288. A. V. Shubnikov and V. A. Koptsik, *Symmetry in Science and Art*, Plenum, New York, 1974.
289. W. Heisenberg, *Introduction to the Unified Theory of Elementary Particles*, Wiley, New York, 1966.
290. T. D. Lee, *Particle Physics and Introduction to Field Theory*, Harwood, Chur, 1981.
291. E. Bright-Wilson, Jr., J. C. Decius, and P. G. Cross, *Molecular Vibration*, McGraw-Hill, New York, 1955.
292. R. L. Flurry, Jr., *Symmetry Groups, Theory and Applications*, Prentice-Hall, Englewood Cliffs, NJ, 1980.
293. J. A. Salthouse and M. J. Ware, *Point Group Character Tables*, Cambridge University Press, 1972.
294. D. S. Urch, *Orbitals and Symmetry*, Penguin, Harmondsworth, 1970.
295. F. A. Cotton, *Chemical Applications of Group Theory*, Wiley Interscience, New York, 1963.
296. M. W. Evans, *Phys. Lett. A* **134**, 409 (1989).
297. M. W. Evans, *Phys. Rev. A* **39**, 6041 (1989).
298. M. W. Evans, G. C. Lie, and E. Clementi, *J. Mol. Liq.* **37**, 231 (1988).
299. M. W. Evans, *Mol. Phys.* **67**, 1195 (1989).
300. M. W. Evans and D. M. Heyes, *Mol. Phys.* **65**, 1441 (1988).

301. M. W. Evans and D. M. Heyes, *Phys. Rev. B.* **42**, 4363 (1990).
302. J. Harris, *Rheology of non-Newtonian Flow*, Longmans, London, 1977.
303. W. R. Schowalter, *Mechanics of non-Newtonian Fluids*, Pergamon, Oxford, 1978.
304. D. M. Heyes, *J. non-Newtonian Fluid Mech.* **27**, 47 (1988).
305. Ibid., *J. Chem. Soc. Faraday Trans.* 2, **82**, 1365 (1986).
306. G. Wagnière and A. Meier, *Chem. Phys. Lett.* **93**, 78 (1982).
307. G. Wagnière, *Z. Naturforsch* **39A**, 254 (1984).
308. G. Wagnière and A. Meier, *Experientia* **39**, 1090 (1983).
309. D. Radulesu and J. Moga, *Bull. Soc. Chim. Romania* **1**, 2 (1939).
310. G. P. Morriss and D. J. Evans, *Phys. Rev. A* **35**, 792 (1987).
311. D. J. Evans and G. P. Morriss, *Computer Phys. Rep.* **1**, 297 (1984).
312. L. D. Barron, *Chem. Phys. Lett.* **135**, 1 (1987).
313. H. Zocher and C. Torok, *Proc. Natl. Acad. Sci., U.S.A.* **39**, 681 (1953).
314. P. G. de Gennes, *C. R. Hebd. Seances Acad. Sci. Ser. B* **270**, 891 (1970).
315. M. W. Evans, *Chem. Phys. Lett.* **152**, 33 (1988).
316. L. D. Barron and J. Vrbancich, *Mol. Phys.* **51**, 715 (1984).
317. M. W. Evans, *Chem. Phys.* **135**, 187 (1989).
318. W. Maier and A. Saupe, *Z. Naturforsch.* **13A**, 564 (1958).
319. P. G. de Gennes, *The Physics of Liquid Crystals*, Oxford University Press, 1974.
320. G. R. Luchurst and G. Zannoni, *Proc. Roy. Soc.* **343A**, 389 (1975).
321. J. H. Freed, *J. Chem. Phys.* **66**, 3428 (1977).
322. A. de Vries, *Mol. Cryst. Liq. Cryst.* **49**, 1 (1978).
323. M. W. Evans, *Chem. Phys.* **127,** 413 (1988).
324. M. W. Evans and D. M. Heyes, *J. Chem. Soc. Faraday Trans.* 2, **86**, 1041 (1990).
325. D. J. Evans and G. P. Morriss, *Computer Phys. Rep.* **1**, 297 (1984).
326. D. M. Heyes, ibid. **8**, 71 (1988).
327. D. J. Evans, *Mol. Phys.* **42**,1355 (1981).
328. L. D. Landau and E. M. Lifshitz, *Statistical Physics*, Pergamon, Oxford, 1978.
329. D. M. Heyes, *J. Chem. Soc. Faraday Trans.* 2, **84**, 705 (1988).
330. D. J. Evans and G. P. Morriss, *Phys. Rev. Lett.* **56**, 2172 (1985).
331. D. M. Heyes, *J. Chem. Soc. Faraday Trans.* 2, **82** 1365 (1986).
332. P. N. Pusey and R. J. A. Tough, in R. Pecora, *Dynamical Light Scattering, Applications of Photon Correlation Spectroscopy*, Ed., Plenum. New York, 1985.
333. P. A. Madden, *Mol. Phys.* **36**, 365 (1978).
334. B. J. Berne and R. Pecora, *Dynamical Light Scattering with Reference to Physics, Chemistry and Biology*, Wiley Interscience, New York, 1976.
335. D. M. Heyes and R. Szczepanski, *J. Chem. Soc. Faraday Trans.* 2, **83**, 319 (1987).
336. D. J. Evans and J. F. Ely, *Mol. Phys.* **59**, 1043 (1986).
337. M. W. Evans and D. M. Heyes, *Mol. Sim.* **4**, 339 (1990).
338. M. Faraday, *Phil. Mag*, **28**, 294 (1846).
339. P. W. Atkins, *Molecular Quantum Mechanics*, Oxford University Press, 1982.
340. L. D. Landau and E. M. Lifshitz, *The Classical Theory of Fields*, Pergamon, Oxford, 1975.
341. G. E. Stedman, *Diagrammatic Group Theory*, Cambridge University Press, 1990.

342. W. H. Bragg, *Rev. Mod. Phys.* **3**, 449 (1931).
343. E. P. Wigner, *Group Theory*, Academic, New York, 1959.
344. E. P. Wigner, *Z. Phys.* **43**, 624 (1927).
345. M. W. Evans, *Phys. Lett. A* **146**, 475 (1990).
346. M. W. Evans, *Phys. Lett. A* **147**, 364 (1990).
347. J. H. Christenson, J. W. Cronin, V. L. Fitch, and R. Turlay, *Phys. Rev. Lett.* **13**, 138 (1964).
348. C. S. Wu, E. Ambler, R. W. Hayward, D. D. Hoppes, and R. P. Hudson, *Phys. Rev.* **105**, 1413 (1957).
349. E. Fermi, *Z. Phys.* **88**, 161 (1934).
350. K. Gottfried and V. F. Weisskopf, *Concepts of Particle Physics*, Clarendon, Oxford, 1984.
351. M. A. Bouchiat and L. Pottier, *Sci. Am.* **250(6)**, 76 (1984).
352. M. W. Evans and D. M. Heyes, *Phys. Scripta* **42**, 196 (1990).
353. M. W. Evans, *Mol. Phys.* **71**, 193 (1990).
354. M. W. Evans and D. M. Heyes, *Phys. Rev. B*, **42**, 4363 (1990).
355. M. Ferrario, P. Grigolini, A. Tani, R. Vallauri, and B. Zambon, in Ref. 3, Chapter 6, p. 225.
356. M. W. Evans and D. M. Heyes, *Comp. Phys. Comm.*, Thematic Issue, **62**, 249 (1991).
357. M. W. Evans and D. M. Heyes, *J. Mol. Liq.* **44**, 27 (1989).
358. E. Verdet, *Comp. Rendues* **39**, 548 (1854).
359. G. H. Wagnière and J. B. Hutter, *J. Opt. Soc. Am. B* **6**, 693 (1989).
360. N. Bloembergen, *Non-Linear Optics*, Benjamin, New York, 1965.
361. Y. R. Shen, *The Principles of Non-Linear Optics*, Wiley, New York, 1984.
362. J. A. Giordmaine, *Phys. Rev.* **138**, 1599 (1965).
363. M. W. Evans, *J. Mod. Opt.*, **37**, 1655 (1990).
364. M. W. Evans, *Phys. Lett. A* **146**, 185 (1990).
365. G. E. Stedman, *Adv. Phys.* **34**, 513 (1985).
366. H. J. Ross, B. S.. Sherbourne, and G. E. Stedman, *J. Phys. B, At. Mol. Opt. Phys.* **22**, 459 (1989).
367. L. D. Barron, *Bio-Systems* **20**, 7 (1987).
368. M. W. Evans, *J. Chem. Phys.* **93**, 2328 (1990).
369. M. W. Evans, *Int. J. Quant. Chem.*, Clementi Issue, in press, (1991).
370. G. Wagnière, *Phys. Rev. A* **40**, 2437 (1989).
371. M. W. Evans, *Phys. Rev. A* **41**, 4601 (1990).
372. G. Wagnière, *Chem. Phys. Lett.* **110**, 546 (1984).
373. J. F. Ward, *Rev. Mod. Phys.* **37**, 1 (1965).
374. O. Laporte, *Z. Phys.* **51**, 512 (1924).
375. P. Zeeman, *Phil. Mag*, **43**, 226 (1986).
376. L. D. Barron, *Mol. Phys.* **31**, 129 (1976).
377. G. Wagnière, *Z. Phys. D* **8**, 229 (1988).
378. M. W. Evans, *J. Mod. Opt.*, in press (1991).
379. J. S. Griffith, *The Irreducible Tensor Method for Molecular Symmetry Groups*, Prentice Hall, Englewood Cliffs, NJ, 1962.

380. U. Fano and G. Racah, *Irreducible Tensorial Sets*, Academic, New York, 1959.
381. S. B. Piepho and P. N. Schatz, *Group Theory in Spectroscopy with Applications to Magnetic Circular Dichroism*, Wiley, New York, 1983.
382. C. H. Townes and A. L. Schawlow, *Microwave Spectroscopy*, McGraw-Hill, New York, 1955.
383. J. E. Borkholm and P. F. Liao, *Opt. Commun.* **21**, 132 (1977).
384. A. Schabert, R. Keil, and P. E. Toschek, *Opt. Commun.* **13**, 265 (1975).
385. C. Delsart and J. C. Keller, *J. Phys. B.* **9**, 2769 (1978).
386. M. W. Evans, *J. Mol. Spect.*, **146**, 143 (1991).
387. Ch. Salomon, CH. Breant, A. van Lerberghe, G. Camy, and C. U. Bordé, *Appl. Phys. B* **29**, 153 (1982).
388. D. C. Hanna, M. A. Yuratich, and D. Cotter, *Non-Linear Optics of Free Atoms and Molecules*, Springer, New York, 1979.
389. S. H. Autler and C. H. Townes, *Phys. Rev.* **100**, 703 (1955).
390. S. Feneuille, *Rep. Prog. Phys.* **40**, 1257 (1977).
391. S. E. Moody and M. Lambropoulos, *Phys. Rev. A* **15**, 1497 (1977).
392. H. R. Gray and C. R. Stroud, Jr., *Opt. Commun.* **25**, 359 (1978).
393. F. Fleming Krim, A. Sinha, and M. C. Hsiao, *J. Chem. Phys.* **92**, 6333 (1990).
394. W. Worthy, *Chem. Eng. News* **68**(26), 24 (1990).
395. C. Reiser, J. I. Steinfeld, and H. W. Galbraith, *J. Chem. Phys.* **74**, 2189 (1981).
396. E. Arimondo, P. Glorieux, and T. Oka, *Phys. Rev. A* **17**, 1 375 (1978).
397. R. M. Whitley and C. R. Stroud, Jr., *Phys. Rev. A* **14**, 1488 (1976).
398. W. A. Molander, C. R. Stroud, Jr., and J. A. Yeazell, *J. Phys. B.* **19**, L461 (1986).
399. R. Serber, *Phys. Rev.* **41**, 489 (1932).
400. A. D. Buckingham and P. J. Stephens, *Ann. Rev. Phys. Chem.* **17**, 399 (1966).
401. P. S. Pershan, *Phys. Rev.* **130**, 19 (1963).
402. J. P. van der Ziel, P. S. Pershan, and L. D. Malmstrom, *Phys. Rev. Lett.* **15**, 190 (1965).
403. P. S. Pershan, J. P. van der Ziel, and L. D. Malmstrom, *Phys. Rev.* **143**, 574 (1966).
404. S. Kielich, in M. Davies (Sen. Rep.), *Dielectric and Related Molecular Processes*, vol. 1, Chem. Soc., London, 1972.
405. M. W. Evans, *J. Mol. Liq.* in press (1991).
406. L. D. Barron and A. D. Buckingham, *Mol. Phys.* **20**, 1111 (1971).
407. L. D. Barron, C. Meehan, and J. Vrbancich, *J. Raman Spect.* **12**, 251 (1982).
408. M. W. Evans, *J. Mol. Spect.*, **143**, 327 (1990).
409. M. W. Evans, *Spectrochim. Acta*, **46A**, 1475 (1990).
410. M. W. Evans, *Chem. Phys.*, **150**, 197 (1991).
411. M. W. Evans, *Phys. Lett. A*, **149**, 328 (1990).
412. M. W. Evans, *Phys. Rev. Lett.* **64**, 2909 (1990).
413. M. W. Evans, *Opt. Lett.* **15**, 836 (1990).
414. R. V. Jones, *Proc. Roy. Soc.* **349A**, 423 (1976).
415. M. W. Evans, *J. Mol. Liq.*, **47**, 109 (1990).
416. T. B. Freedman, M. Germana Paterlini, Nam Soo Lee, and L. A. Nafie, *J. Am. Chem. Soc.* **109**, 4727 (1987).

417. P. L. Polavarapu, P. G. Quincey, and J. R. Birch, *Infra red Phys.* **30**, 175 (1990).
418. M. W. Evans and G. Wagnière, *Phys. Rev. A*, **42**, 6732 (1990).
419. Ref. 404, vols. 2 and 3.
420. Video animation (with narration) by C. Pelkie, B. Land, and M. W. Evans, Cornell National Supercomputer Facility, based on the code TETRA (see Appendix).*
421. See appendix of Ref. 371 for more details.
422. M. W. Evans and D. M. Heyes, Proceedings of the NATO Conference on Complex Flows, Brussels, 1989, published 1991.
423. M. W. Evans, *J. Phys. Chem.*, **95**, 2256 (1991).
424. E. B. Cullwick, *Electromagnetism and Relativity*, Longmans, Green, and Co., London, 1957.
425. M. W. Evans, *J. Mod. Opt.*, in press (1991).
426. P. G. H. Sandars, in K. Crowe, J. Ducios, G. Fiorentini, and G. Torelli, Eds., *Fundamental Interactions and Structure of Matter*, Plenum, New York, 1980.
427. E. N. Fortson and L. Wilets, *Adv. At. Mol. Phys.* **16**, 319 (1980).
428. L. D. Barron, in *New Developments in Molecular Chirality*, P. Mezey, Ed., Reidel, Netherlands, 1990.
429. M. A. Bouchiat and C. Bouchiat, *J. Phys.* (*Paris*) **35**, 899 (1974).
430. M. Quack, *Angew. Chem. Int. Ed. Engl.* **28**, 571 (1989).
431. J. J. Thompson, *Proc. Camb. Phil. Soc.* **5**, 250 (1886).
432. E. Fermi, *Rend. Lincei* **32**, 115 (1923).
433. M. A. Player, *Proc. Roy. Soc.* **349A**, 441 (1976).
434. M. W. Evans and A. Lakhtakia, *Phys. Rev. A*, in press (1991).
435. M. W. Evans, *Phys. Lett. A*, in press (1991).
436. M. W. Evans, *Spec. Sci. Tech.*, in press (1991).
437. S. J. Cianciosi, K. M. Spencer, T. B. Freedman, L. A. Nafie, and J. E. Baldwin, *J. Am. Chem. Soc.* **111**, 1913 (1989).
438. L. D. Barron, in *Theoretical Models of Chemical Bonding*, Z. B. Maksic, Ed., Springer, Berlin, 1990.
439. S. F. Mason, *Bio Systems* **20**, 27 (1987).

* Judged best animation in the Natural Sciences and Mathematics Category of the IBM 1990 Supercomputer Competition and Conference; to be distributed by "Media Magic," California in video cassette format; see also M. W. Evans and C. R. Pelkie, Conference Proceedings and *J. Opt. Soc. Am., B*, in press.

APPENDIX: MOLECULAR DYNAMICS SIMULATION ALGORITHM "TETRA"

This appendix provides FORTRAN code for the molecular dynamics simulation algorithm "TETRA," evolved gradually from work by Schofield, Singer, Ferrario, and Evans. It integrates the classical equations of motion for an ensemble of asymmetric tops diffusing in three dimensions. The version shown is for liquid water, with a facility for applying a right-handed circularly polarized laser.

This code formed the basis for much of the simulation work reported in this article, and copies on magnetic tape are available from the author upon request.

A library of molecular dynamics simulation algorithms has been set up at the United Kingdom's Science and Engineering Research Council Daresbury Laboratory, CCP5 Group, Daresbury, Warrington WA4 4AD, UK. These algorithms are available for individual research scientists and are described regularly in the CCP5 Quarterly Newsletter. They are supplied with detailed descriptive documentation, and are available for many different areas of computer simulation. Algorithms for the test molecule dichloromethane are available from the same source, and were set up during the pilot project of the European Molecular Liquids Group (EMLG).

The following TETRA code is not meant as a substitute for a comprehensive description, but illustrates the stages involved in the computer simulation of an asymmetric top molecule diffusing in three dimensions.

```
      PROGRAM TETRA
C---- MOL DYNAMICS PROGRAM FOR WATER -------
C
      IMPLICIT REAL*8 (A-H,O-Z)
C
C  ATOMIC COORDINATES: XAT,YAT,ZAT, I.LE.IA.LE 432
C
      REAL*8 M(6),JX(108),JY(108),JZ(108),IN(6),TM
      REAL*8 KB,NAV,JCON,NINE,NTEN,NITF,NTTF
      INTEGER TITLE(80),INDEX(25),BIND(6)
      CHARACTER*4 TIND(6),TII(8)
      DIMENSION
     1    TXA(108),TYA(108),TZA(108),EXO(3,108),EYO(3,108),EZO(3,108)
     2,RI(6),ODDT(6),EDDDX(6),EDDDY(6),EDDDZ(6)
      DIMENSION O(6),OSQ(6),OM(6),OMSQ(6),ODOT(6)
     1,SQE(3),CO(6),EEX(6),EEY(6),EEZ(6),EXN(6),EYN(6)
     2,EZN(6),ELX(6),ELY(6),ELZ(6),EDDX(6),EDDY(6),EDDZ(6)
     3,TE(6),OP(101),EDOX(6),EDOY(6),EDOZ(6)
      DIMENSION  SIG(6,6),EPS(6,6),BSIG(36),EP(36),BSIGSQ(36),
     *ACR(36),CHA(6),BCHA(36)
      DIMENSION G(6,100),GR(6,100)
      COMMON /ATT/ XAT(648),YAT(648),ZAT(648),XA(648),YA(648),ZA(648)
```

```
C
C  CENTRE OF MASS COORD.: XC,XCN(NEW),XCO(OLD);C.O.M. VEL. VXC...
C
      COMMON /CMT/ XC(108),YC(108),ZC(108),XCO(108),YCO(108),ZCO(108),
     &XCN(108),YCN(108),ZCN(108),VXC(108),VYC(108),VZC(108)
C
C  UNIT VECTORS ALONG THE PRINCIPAL AXES: EX,EY,EZ; EXN; EXO,ETC.
C  EX(L,IC)  L=1,2,3 SPECIFIES THE AXIS; IC(1-108)
C  SPECIFIES  THE  MOLECULE
C
      COMMON /CMO/ EX(3,108),EY(3,108),EZ(3,108)
C
C  ANGULAR MOMENTUM JX,...
C
      COMMON /CMJ/ JX,JY,JZ,IN,TM,KB,NAV
C
C  FORCES: FXC,FYC,FZC ION C.O.M.,FAX,FAY,FAZ: ON ATOMS.
C  TORQUES: TX.TY,TZ; TXN(NEW).....TXO(OLD)....
C
      COMMON /FOR/ FXC(108),FYC(108),FZC(108),TX(108),TY(108),TZ(108),
     &FAX(648),FAY(648),FAZ(648),TXO(108),TYO(108),TZO(108)
C
C    PHYSICAL CONSTANT ...
C
      COMMON /N/ NOM,NOMM1,NORM,NT,NOFST,NTINC,INOF
C
                                                  COMMON        /PHY/
     TEMP,VOL,DT,BOXL,FACTOR,CONFAC,CUT,RTKTM,RKTF,FF,DTF
C
      COMMON /NTR/ TRIG
C
C    LENNARD JONES POTENTIAL PARAMATERS ...
C
C    SIG=MATRIX OF DISTANCE PARAMETERS
C    EP=MATRIX OF ENERGY PARAMETERS
C
C  PRINCIPAL MOMENTS OF INERTIA IN(1-3);THEIR RECIPROCALS RI(1-3)
C
C
C O=ANGULAR VELOCITIES ABOUT PRINCIPAL AXES OSQ=O*O
C.....LOCAL  VARIABLES=EX;  EDDX,  ETC.  SECOND  DERIVATIVES  OF
     ELX.....
C  TE=SCALAR PRODUCTS OF TORQUES WITH UNIT VECTORS E,....
C  SUMI(1)=I(1)+I(2)-2I(3) ETC.
C
C   PAIR DISTRIBUTION FUNCTION ... GR(SITE)
```



```
C
      DATA G,GR/1200*0.0D0/
C
C     ----- IBM ERRSET -----
C
      CALL ERRSET(201,256,-1,1,1,1)
      CALL ERRSET(208,  0,-1,1,1,1)
C
      KB=1.3807D-00
      NAV=6.0223D+23
      ELSQ=2.3071138D+05
      NATM=5

      DATA INDEX/1,2,1,3,3,2,4,2,5,5,1,2,1,3,3,3,5,3,6,6,
     *3,5,3,6,6/
      DATA TI1/'CH2 ','CL2 ','OUT ','LJ+C','HARG','T=   ','293K','VOL='/
      DATA TIND/'H-H ','H- O','H-Q ','O- O','O- Q','Q-Q '/
      DATA BIND/4,4,8,1,4,4/
      DATA ONE,TWO,THREE,SIX,PTFI/1.0D0,2.0D0,3.0D0,6.0D0,0.5D0/
      DATA FOUR,ELEV,TWLE,EITE/4.0D0,11.0D0,12.0D0,18.0D0/
      DATA FIVE,SEVE,NINE,NTEN,TWFO/5.0D0,7.0D0,9.0D0,19.0D0,24.0D0/

                                                              DATA
     ZOFST,RSTKE,RSRKE,RTQTE,RRQTE,RTPE,RTPR,RTQP,RQTEN,RTEN,
     &RTMO,RTJM,RQEK,RVT,RVIR,RTRTE/16*0.0D0/
      DATA  ZER0,SSTKE,SSRKE, TQTE, RQTE, TPE, TPR, TQP,QTOTE,TTEN,
     &TTMO,TTJM,TQEK,TVT,TVIR,TTRTE/16*0.0D0/
      CALL DATE(DAT)
      CALL TIME(TRIG)


      X=RAND(1)
      READ(5,3) (TITLE(I),I=1,80)
    3 FORMAT(80A1)
      READ(5,4) NOM,NMAX,NT,NTINC,NDUMP,MM,MODE,MTIME,IPRINT
    4 FORMAT(10I8)
      READ(5,10) TEMP,VOL,DT,FCC,CUT,DFFT,TMAX
   10 FORMAT(8D10.3)
    6 FORMAT(10X,5X,80A1////)
    8 FORMAT(1X,' NUMERICAL SIMULATION RUN CONDITION'/10X,
     &'NUMBER OF MOLECULES = ',I5,' INTEGRATION TIME STEP = ',G12.5
     &,' POTENTIAL CUT-OFF DISTANCE = ',G12.5/)
    7 FORMAT(1X,' THERMODYNAMICAL CONDITION '/3X,' TEMPERATURE
     = '
     &,F10.5,'  MOLAR VOLUME = ',G12.5//)
      NZ=0
      PYE=(DACOS(-1.0D0))
```

```
AK1=TWO*PYE/FCC
ANINT=100.0D0
ROOT2=DSQRT(TWO)
RR2=ONE/ROOT2
ROOT3=DSQRT(THREE)
CONFAC=NAV/(DFLOAT(NOM))
BOXL=(VOL/CONFAC)**(ONE/THREE)
FACTOR=TWO/BOXL
DELGR=CUT/(FACTOR*ANINT)
TKIN=ZER0
TROT=ZER0
RDT=ONE/DT
DTSQ=DT**2
DTCU=DT**3
DTF=DT*FACTOR
NAT=NOM*NATM
NOMM1=NOM-1
GRFAC=BOXL**3/(TWO*PYE*NOM*NOMM1*DELGR)
INOF=0
FF=FACTOR**2
FF24=TWFO*FF
FITW=FIVE/TWLE
TWTH=TWO/THREE
ONTW=ONE/TWLE
ONSI=ONE/SIX
ONTF=ONE/TWFO
FITF=FIVE/TWFO
NITF=NINE/TWFO
NTTF=NTEN/TWFO
STWT=SEVE/TWLE
VCON=1.0D+02
PCON=1.0D-25
FCON=1.0D-13
ECON=1.0D-23
JCON=1.0D-35
CUTF=CUT/FACTOR
PRINT 6,(TITLE(I),I=1,80)
PRINT 7,TEMP,VOL
PRINT 8,NOM,DT,CUTF
CUTSQ=CUT**2
CALL LENJO(SIG,EPS,BSIG,BSIGSQ,EP,KB,FACTOR)
CALL CHARGE(CHA,BCHA,ELSQ,FACTOR,TWFO)
CALL RANGE(PSI,PELR,CUT,NOM,ACR,EP,BSIGSQ)
CALL KINET(NAV,FACTOR,M,TM,IN,RI)
RKTF=KB*TEMP*FF
RMTT=DTSQ/TM
```



```
      RTKTM=DSQRT(KB*TEMP/TM)
      IF(MM .EQ. 1) GO TO 89
      XX=DFLOAT(MM)
      PRINT 2345,DFLOAT(MM)
 2345 FORMAT(G14.6)
      CALL LATFCC(FCC)
      GO TO 90
   89 CONTINUE
C
C     ***  READ INITIAL CONDITION FROM DISK FILE  ***
C
      IF(MODE.NE.3)  GO TO 731
      ZOFST=ZER0
      READ(7)
      READ(7)
      GO TO 734
  731 CONTINUE
      READ(7) ZOFST,SRKE,STKE,SSTKE,SSRKE,TQTE,RQTE
     &       ,TPE,TPR,TQP,QTOTE,TTMO,TTJM,TQEK,TVIR,TVT
      READ(7) G
  734 CONTINUE
      READ(7) XCN,YCN,ZCN,XC,YC,ZC,VXC,VYC,VZC
      READ(7) JX,JY,JZ,EX,EY,EZ
      READ(7) TX,TY,TZ,TXO,TYO,TZO,TXA,TYA,TZA
C
C     ***  ----------------------------------  ***
C
      PRINT 432,ZOFST
  432 FORMAT(1X,'  SIMULATION RUN START FROM TIME STEP  = ',F10.3)
      MM=1
      DO 9 I=1,2
      PRINT 431,XCN(I),YCN(I),ZCN(I),EX(1,I),EY(1,I),EZ(1,I),
     &JX(I),JY(I),JZ(I),XC(I),YC(I),ZC(I)
  9   CONTINUE
      CALL ZERO(FCC)
      IF(MODE.NE.2) GO TO 90
      PRINT 433,MTIME,TEMP
  433  FORMAT(1X//,3X,' C.O.M. VELOCITIES AND ANGULAR MOMENTUM
RESCA',
     &'LED INITIALLY AND EVERY ',I3,' STEPS. TEMPERATURE = ',F10.3)
      CALL TSCAL(1,TRTE,ROTE)
  90  CONTINUE
      PRINT 431,DTSQ,DTCU,FACTOR,CONFAC,RTKTM
      PRINT 431,FF,EP(1),BSIG(2),TM
      NOFST=INT(ZOFST)
      IF(NOFST.LT.NT) WRITE(1) TI1,VOL
```

```
      IF(NOFST.LT.NT) GO TO 300
      NSTO=(NOFST-NT)/NDUMP + 10
      DO 737 J=1,NSTO
      KJ=J
      READ(1,END=847)
  737 CONTINUE
  847 PRINT 849,KJ
  849 FORMAT(10X,'  NUMBER OF RECORDS SKIPPED = ',I10,' READY ',
     &' TO WRITE THE NEW ONES',1X///)
  300 CONTINUE
      PE=ZER0
      VIR=ZER0
      VIRT=ZER0
C  START OF LOOP
      SUMEX=0.0
      SUMEY=0.0
      SUMEZ=0.0
      SUMVX=0.0
      SUMVY=0.0
      SUMVZ=0.0


      INOF=INOF+1
      NOFST=NOFST+1
      ZOFST=ZOFST+ONE
C
C
      DO 369 IC=1,NOM
      UX=TWO*DINT(XCN(IC))
      UY=TWO*DINT(YCN(IC))
      UZ=TWO*DINT(ZCN(IC))
      XCO(IC)=XC(IC)-UX
      YCO(IC)=YC(IC)-UY
      ZCO(IC)=ZC(IC)-UZ
C
C  CENTRE OF MASS POSITIONS COMPUTED NEXT
C
      XC(IC)=XCN(IC)-UX
      YC(IC)=YCN(IC)-UY
      ZC(IC)=ZCN(IC)-UZ
C
C
C
  369 CONTINUE
      CALL ATPOS(NATM)
C
```



```
C     ATPOS DOES NOT AFFECT CENTRE OF MASS POSITIONS XC,YC,ZC
C
C  FORCES  LOOP
C
      DO 150 I=1,NOM
      FXC(I)=ZER0
      FYC(I)=ZER0
      FZC(I)=ZER0
      DO 151 IA=1,NATM
      I4=NATM*(I-1)
      L=I4+IA
      FAX(L)=ZER0
      FAY(L)=ZER0
  151 FAZ(L)=ZER0
  150 CONTINUE
      SK1=ZER0
      DO 152 IC=1,NOM
      AK=TWO*AK1*(XC(IC)+YC(IC)+ZC(IC))
  152 SK1=SK1+DCOS(AK+PYE)
      DO 350 IC=1,NOMM1
      XCI=XC(IC)
      YCI=YC(IC)
      ZCI=ZC(IC)
      I4=NATM*(IC-1)
      J=IC+1
      DO 340 JC=J,NOM
      J4=NATM*(JC-1)
C     COORD DIFFERENCES BETWEEN C.O.M.S
C
C       POTENTIAL CUT-OFF ON C.O.M DISTANCES TO HELP WITH CHARGES
C
      DCX=XCI-XC(JC)
      DCY=YCI-YC(JC)
      DCZ=ZCI-ZC(JC)
      DCX=DCX-DINT(DCX)*TWO
      DCY=DCY-DINT(DCY)*TWO
      DCZ=DCZ-DINT(DCZ)*TWO
      RCSQ=DCX*DCX+DCY*DCY+DCZ*DCZ
      IF(RCSQ.GT.CUTSQ) GO TO 340
      DO 351 IA=1,NATM
      K=I4+IA
      IA5=5*(IA-1)
      XATK=XAT(K)
      YATK=YAT(K)
      ZATK=ZAT(K)
      FAXK=ZER0
```

```
      FAYK = ZER0
      FAZK = ZER0
      DO 341 JA = 1,NATM
      L = J4 + JA
      DATX = XATK-XAT(L)
      DATY = YATK-YAT(L)
      DATZ = ZATK-ZAT(L)
      DAAX = DCX + DATX
      DAAY = DCY + DATY
      DAAZ = DCZ + DATZ
      DAAX = DAAX-TWO*(DFLOAT(IDINT(DAAX)))
      DAAY = DAAY-TWO*(DFLOAT(IDINT(DAAY)))
      DAAZ = DAAZ-TWO*(DFLOAT(IDINT(DAAZ)))
      RSQ = DAAX**2 + DAAY**2 + DAAZ**2
      RDIJ = DSQRT(RSQ)
      RRSQ = ONE/RSQ
      IJ = IA5 + JA
      NDF = IDINT(RDIJ*ANINT) + 1
      IF(NDF .GT. 100) GO TO 342
      NIND = INDEX(IJ)
      GR(NIND,NDF) = GR(NIND,NDF) + ONE
  342 CONTINUE
      ALJ = (RRSQ*BSIGSQ(IJ))**3
      BLJ = ALJ*ALJ
      AEL = BCHA(IJ)/RDIJ
      FLJ = EP(IJ)*(BLJ + BLJ-ALJ) + AEL
      PE = PE + EP(IJ)*(BLJ-ALJ) + SIX*AEL
      VIR = VIR-FLJ
      A = FLJ*RRSQ
C     A = A-ACR(IJ)
      VIRT = VIRT + (DAAX*DATX + DAAY*DATY + DAAZ*DATZ)*A
      FAAX = A*DAAX
      FAAY = A*DAAY
      FAAZ = A*DAAZ
      FAX(L) = FAX(L)-FAAX
      FAXK = FAXK + FAAX
      FAY(L) = FAY(L)-FAAY
      FAYK = FAYK + FAAY
      FAZ(L) = FAZ(L)-FAAZ
      FAZK = FAZK + FAAZ
  341 CONTINUE
      FAX(K) = FAXK + FAX(K)
      FAY(K) = FAYK + FAY(K)
      FAZ(K) = FAZK + FAZ(K)
  351 CONTINUE
  340 CONTINUE
```



```
  350 CONTINUE
      DO 355 IC = 1,NOM
      I4 = NATM*(IC-1)
      DO 356 IA = 1,NATM
      K = I4 + IA
      FXC(IC) = FXC(IC) + FAX(K)
      FYC(IC) = FYC(IC) + FAY(K)
      FZC(IC) = FZC(IC) + FAZ(K) + CHA(IA)*0.0
  356 CONTINUE
  355 CONTINUE
      DO 354 IA = 1,NAT
      FAX(IA) = FAX(IA)*FF24
      FAY(IA) = FAY(IA)*FF24
      FAZ(IA) = FAZ(IA)*FF24
  354 CONTINUE
      PE = TWO*TWO*PE
      VIR = TWFO*VIR
      VIRT = VIRT*TWFO
      SPE = PE + PELR
      SVIR = VIR
      SVIRT = VIRT
      RTPE = RTPE + SPE
C
C     PE AND VIR SHOULD BE S.I. UNITS;FORCES CONTAIN FACTOR
C
      DO 353 IC = 1,NOM
      FXC(IC) = FXC(IC)*FF24
      FYC(IC) = FYC(IC)*FF24
      FZC(IC) = FZC(IC)*FF24
  353 CONTINUE
C     THE ABOVE LOOP COMPUTES NET FORCES
      TKE = ZER0
      XMO = ZER0
      YMO = ZER0
      ZMO = ZER0
C     MD LOOP
C       XCI ETC. UPDATED FROM XC(I) ETC TO COMPUTE VELOCITIES
C       XC(I), YC(I), ZC(I) DUMPED TO WRITE (1)
C
      DO 360 I = 1,NOM
      XCI = TWO*XC(I)-XCO(I) + FXC(I)*RMTT
      YCI = TWO*YC(I)-YCO(I) + FYC(I)*RMTT
      ZCI = TWO*ZC(I)-ZCO(I) + FZC(I)*RMTT
      VXC(I) = PTFI*(XCI-XCO(I))
      VYC(I) = PTFI*(YCI-YCO(I))
      VZC(I) = PTFI*(ZCI-ZCO(I))
```

```
C
C  CENTRE OF MASS LINEAR VELOCITIES, LAST POINT BEFORE DUMP
C
      XMO = XMO + VXC(I)
      YMO = YMO + VYC(I)
      ZMO = ZMO + VZC(I)
      TKE=TKE+VXC(I)**2+VYC(I)**2+VZC(I)**2
      XCN(I)=XCI
      YCN(I)=YCI
      ZCN(I)=ZCI
360   CONTINUE
      TMO = DSQRT( XMO*XMO + YMO*YMO + ZMO*ZMO )*TM/DTF
      STKE=(TKE/(DTF**2))*PTFI*TM
      TRTE=TWTH*STKE/(KB*NOM)
      RTMO = RTMO + TMO
      RSTKE = STKE + RSTKE
      RTQTE = RTQTE + TRTE*TRTE
C         ROTATION
C       PRINCIPAL MOMENTS OF INERTIA ARE IN(1)-IN(3)
C       RECIPROCALS  RI(1)-RI(3)
C       CALCULATE ANGULAR MOMENTUM
C       IF NOFST=2 NO INITIAL MODIFICATION NECESSARY
C
      XJI=ZER0
      YJI=ZER0
      ZJI=ZER0
      ROTKE=ZER0
      DO 361 IC=1,NOM
      I4=NATM*(IC-1)
      TXI=ZER0
      TYI=ZER0
      TZI=ZER0
      DO 362 IA=1,NATM
      K=I4+IA
      TXI=TXI+YAT(K)*FAZ(K)-ZAT(K)*FAY(K)
      TYI=TYI+ZAT(K)*FAX(K)-XAT(K)*FAZ(K)
362   TZI=TZI+XAT(K)*FAY(K)-YAT(K)*FAX(K)
      E0=100.00
      OMX= 0.05
      WT=OMX*NOFST
      TXI=E0*(DSIN(WT)*EY(1,IC)-DCOS(WT)*EZ(1,IC))+TXI
      TYI=-E0*DSIN(WT)*EX(1,IC)+TYI
      TZI=E0*DCOS(WT)*EX(1,IC)+TZI
C       INITIALISATION REQUIRED.
      IF(NOFST.GT.3) GO TO 374
      IF(NOFST.EQ.3) GO TO 373
```



```
      IF(NOFST.EQ.2) GO TO 372
C     FIRST STEP  ZERO ORDER ALGORITHM FOR J
      JX(IC)=JX(IC)+DT*TXI
      JY(IC)=JY(IC)+DT*TYI
      JZ(IC)=JZ(IC)+DT*TZI
      GO TO 371
C     SECOND STEP FIRST ORDER ALGORITHM FOR J
372   JX(IC)=JX(IC)+PTFI*(TXI+TX(IC))*DT
      JY(IC)=JY(IC)+PTFI*(TYI+TY(IC))*DT
      JZ(IC)=JZ(IC)+PTFI*(TZI+TZ(IC))*DT
      DTORX=(TXI-TX(IC))*RDT
      DTORY=(TYI-TY(IC))*RDT
      DTORZ=(TZI-TZ(IC))*RDT
      GOTO 375
C     THIRD STEP SECOND ORDER ALGORITHM FOR J
373   JX(IC)=JX(IC)+DT*(FITW*TXI+TWTH*TX(IC)-ONTW*TXO(IC))
      JY(IC)=JY(IC)+DT*(FITW*TYI+TWTH*TY(IC)-ONTW*TYO(IC))
      JZ(IC)=JZ(IC)+DT*(FITW*TZI+TWTH*TZ(IC)-ONTW*TZO(IC))
      DTORX=(THREE*TXI+TXO(IC)-FOUR*TX(IC))*PTFI*RDT
      DTORY=(THREE*TYI+TYO(IC)-FOUR*TY(IC))*PTFI*RDT
      DTORZ=(THREE*TZI+TZO(IC)-FOUR*TZ(IC))*PTFI*RDT
      GO TO 376
C     NORMAL ALGORITHM THIRD ORDER INTEGRATION
                                                                    374
      JX(IC)=JX(IC)+DT*(NITF*TXI+NTTF*TX(IC)-FITF*TXO(IC)+ONTF*TXA(IC))

      JY(IC)=JY(IC)+DT*(NITF*TYI+NTTF*TY(IC)-FITF*TYO(IC)+ONTF*TYA(IC))

      JZ(IC)=JZ(IC)+DT*(NITF*TZI+NTTF*TZ(IC)-FITF*TZO(IC)+ONTF*TZA(IC))

      DTORX=(ELEV*TXI-EITE*TX(IC)+NINE*TXO(IC)-TWO*TXA(IC))*ONSI*RDT

      DTORY=(ELEV*TYI-EITE*TY(IC)+NINE*TYO(IC)-TWO*TYA(IC))*ONSI*RDT

      DTORZ=(ELEV*TZI-EITE*TZ(IC)+NINE*TZO(IC)-TWO*TZA(IC))*ONSI*RDT
376   TXA(IC)=TXO(IC)
      TYA(IC)=TYO(IC)
      TZA(IC)=TZO(IC)
375   TXO(IC)=TX(IC)
      TYO(IC)=TY(IC)
      TZO(IC)=TZ(IC)
371   TX(IC)=TXI
      TY(IC)=TYI
      TZ(IC)=TZI
361   CONTINUE
370   CONTINUE
```

```
C       THE ANGULAR MOMENTUM HAS BEEN ADVANCED
      SUMC=ZER0
      DO 377 IC=1,NOM
      DO 345 L=1,3
      ELX(L)=EX(L,IC)
      ELX(L+3)=ELX(L)
      ELY(L)=EY(L,IC)
      ELY(L+3)=ELY(L)
      ELZ(L)=EZ(L,IC)
      ELZ(L+3)=ELZ(L)
      OM(L)=(JX(IC)*ELX(L)+JY(IC)*ELY(L)+JZ(IC)*ELZ(L))*RI(L)
      OM(L+3)=OM(L)
      OMSQ(L)=OM(L)**2
      OMSQ(L+3)=OMSQ(L)
      TE(L)=TX(IC)*ELX(L)+TY(IC)*ELY(L)+TZ(IC)*ELZ(L)
345   CONTINUE
      XJI=XJI+JX(IC)
      YJI=YJI+JY(IC)
      ZJI=ZJI+JZ(IC)
      ROTKE=ROTKE+PTFI*(IN(1)*OM(1)**2+IN(2)*OM(2)**2+IN(3)*OM(3)**2)
      DO 346 L=1,3
      O(L)=OM(L+1)*OM(L+2)
      OSQ(L)=OMSQ(L+1)+OMSQ(L+2)
      O(L+3)=O(L)
      OSQ(L+3)=OSQ(L)
      ODOT(L)=(TE(L)+(IN(L+1)-IN(L+2))*O(L))*RI(L)
      ODOT(L+3)=ODOT(L)
      EDOX(L)=OM(L+1)*ELX(L+2)-OM(L+2)*ELX(L+1)
      EDOX(L)=-EDOX(L)
      EDOX(L+3)=EDOX(L)
      EDOY(L)=OM(L+1)*ELY(L+2)-OM(L+2)*ELY(L+1)
      EDOY(L)=-EDOY(L)
      EDOY(L+3)=EDOY(L)
      EDOZ(L)=OM(L+1)*ELZ(L+2)-OM(L+2)*ELZ(L+1)
      EDOZ(L)=-EDOZ(L)
      EDOZ(L+3)=EDOZ(L)
346   CONTINUE
C       TE(1)-(3)=T.EA
C       O(1)-(3)=OMA,OMB/IC ETC.
      DO 385 L=1,3
C
C  MIXED ALGORITHM,ONLY OMEGA DOT TERMS IN ACCELERATION
C  OF E VECTORS
      EDDX(L)=ODOT(L+2)*ELX(L+1)-ODOT(L+1)*ELX(L+2)
     &+EDOX(L+1)*OM(L+2)-EDOX(L+2)*OM(L+1)
      EDDY(L)=ODOT(L+2)*ELY(L+1)-ODOT(L+1)*ELY(L+2)
```



```
     &+EDOY(L+1)*OM(L+2)-EDOY(L+2)*OM(L+1)
      EDDZ(L)=ODOT(L+2)*ELZ(L+1)-ODOT(L+1)*ELZ(L+2)
     &+EDOZ(L+1)*OM(L+2)-EDOZ(L+2)*OM(L+1)
      EDDX(L+3)=EDDX(L)
      EDDY(L+3)=EDDY(L)
      EDDZ(L+3)=EDDZ(L)
      EDDDX(L)=ZER0
      EDDDY(L)=ZER0
      EDDDZ(L)=ZER0
385   CONTINUE
      IF(NOFST.EQ.1) GOTO 386
      DO 388 L=1,3
      DTE=DTORX*ELX(L)+DTORY*ELY(L)+DTORZ*ELZ(L)
      TEDOT=TX(IC)*EDOX(L)+TY(IC)*EDOY(L)+TZ(IC)*EDOZ(L)
      TEDD=JX(IC)*EDDX(L)+JY(IC)*EDDY(L)+JZ(IC)*EDDZ(L)
      ODDT(L)=DTE+TWO*TEDOT+TEDD
      ODDT(L+3)=ODDT(L)
388   CONTINUE
      DO 382 L=1,3

EDDDX(L)=EDDX(L+1)*OM(L+2)-EDDX(L+2)*OM(L+1)+TWO*(EDOX(L+1)*ODOT

&(L+2)-EDOX(L+2)*ODOT(L+1))+ELX(L+1)*ODDT(L+2)-ELX(L+2)*ODDT(L+1)

EDDDY(L)=EDDY(L+1)*OM(L+2)-EDDY(L+2)*OM(L+1)+TWO*(EDOY(L+1)*ODOT

&(L+2)-EDOY(L+2)*ODOT(L+1))+ELY(L+1)*ODDT(L+2)-ELY(L+2)*ODDT(L+1)

EDDDZ(L)=EDDZ(L+1)*OM(L+2)-EDDZ(L+2)*OM(L+1)+TWO*(EDOZ(L+1)*ODOT

&(L+2)-EDOZ(L+2)*ODOT(L+1))+ELZ(L+1)*ODDT(L+2)-ELZ(L+2)*ODDT(L+1)
382   CONTINUE
386   DO 384 L=1,3

EXN(L)=ELX(L)+DT*EDOX(L)+PTFI*DTSQ*EDDX(L)+ONSI*DTCU*EDDDX(L)

EYN(L)=ELY(L)+DT*EDOY(L)+PTFI*DTSQ*EDDY(L)+ONSI*DTCU*EDDDY(L)

EZN(L)=ELZ(L)+DT*EDOZ(L)+PTFI*DTSQ*EDDZ(L)+ONSI*DTCU*EDDDZ(L)
      EX(L,IC)=EXN(L)
      EY(L,IC)=EYN(L)
      EZ(L,IC)=EZN(L)
      EXN(L+3)=EXN(L)
      EYN(L+3)=EYN(L)
      EZN(L+3)=EZN(L)
      EEX(L)=EXN(L)
```

```
      EEX(L+3)=EEX(L)
      EEY(L)=EYN(L)
      EEY(L+3)=EEY(L)
      EEZ(L)=EZN(L)
      EEZ(L+3)=EEZ(L)
384   CONTINUE
C  ORTHONORMALISATION
      IF (NOFST.LE.4) GOTO 387
      IF (NOFST.NE.(5*NOFST/5)) GOTO  377
387   CONTINUE
C  ORTHOGONALISATION
      DO 391 L=1,3
      CO(L)=EEX(L+1)*EEX(L+2)+EEY(L+1)*EEY(L+2)+EEZ(L+1)*EEZ(L+2)
391   CO(L+3)=CO(L)
      DO 393 L=1,3
      EXN(L)=EEX(L)-PTFI*(CO(L+2)*EEX(L+1)+CO(L+1)*EEX(L+2))
      EYN(L)=EEY(L)-PTFI*(CO(L+2)*EEY(L+1)+CO(L+1)*EEY(L+2))
      EZN(L)=EEZ(L)-PTFI*(CO(L+2)*EEZ(L+1)+CO(L+1)*EEZ(L+2))
      EEX(L)=EXN(L)
      EEY(L)=EYN(L)
      EEZ(L)=EZN(L)
393   CONTINUE
C     NORMALISATION
397    DO 390 L=1,3
      SQE(L)=EXN(L)**2+EYN(L)**2+EZN(L)**2-ONE
      CORR=SQE(L)*(THREE*PTFI/TWO*SQE(L)-PTFI)+ONE
      EEX(L)=EXN(L)*CORR
      EEY(L)=EYN(L)*CORR
      EEZ(L)=EZN(L)*CORR
      EEX(L+3)=EEX(L)
      EEY(L+3)=EEY(L)
      EEZ(L+3)=EEZ(L)
390   CONTINUE
392   DO 394 L=1,3
      EX(L,IC)=EEX(L)
      EY(L,IC)=EEY(L)
      EZ(L,IC)=EEZ(L)
394   CONTINUE
      SUMEX=SUMEX+EX(1,IC)
      SUMEY=SUMEY+EY(1,IC)
      SUMEZ=SUMEZ+EZ(1,IC)
      SUMVX=SUMVX+VXC(IC)
      SUMVY=SUMVY+VYC(IC)
      SUMVZ=SUMVZ+VZC(IC)
377   CONTINUE
      TJMI=DSQRT( XJI*XJI + YJI*YJI + ZJI*ZJI )/FACTOR
```



```
      ROTKE=ROTKE/FF
      RTJM = RTJM + TJMI
      SRKE=ROTKE
      ROTE=TWTH*SRKE/(NOM*KB)
      TOTEN=STKE+SPE+SRKE
      RTEN=RTEN+TOTEN
      RSRKE=RSRKE+SRKE
      RQEK=RQEK+(SRKE+STKE)*(SRKE+STKE)
      RRQTE =RRQTE + ROTE*ROTE
      RTRTE=RTRTE + ROTE*TRTE
      RVIR=RVIR+SVIR+SVIRT+PSI
      RVT=RVT+(SVIR+SVIRT+PSI)*(TRTE+ROTE)
      PRESS=(STKE+SRKE-SVIR-SVIRT-PSI)/THREE
      PRESS=PRESS/(.101325D-01*(VOL/CONFAC))
      RTPR = RTPR + PRESS
      RTQP = RTQP + PRESS*PRESS
      RQTEN = RQTEN + TOTEN*TOTEN
      IF (NOFST .LT. NT) GO TO 379
      NTT=NOFST-NT
      IF(NTT .NE. NDUMP*(NTT/NDUMP)) GO TO 379
      ZDUMP=DFLOAT(NTT/NDUMP) + ONE
      WRITE(1) ZDUMP,XC,YC,ZC,VXC,VYC,VZC,JX,JY,JZ,EX,EY,EZ,
     AFXC,FYC,FZC,TX,TY,TZ,XA,YA,ZA


 379 CONTINUE



      SUMEX=SUMEX/108.0
      SUMEY=SUMEY/108.0
      SUMEZ=SUMEZ/108.0
      SUMVX=SUMVX/108.0
      SUMVY=SUMVY/108.0
      SUMVZ=SUMVZ/108.0
      PRINT 513,SUMEX,SUMEY,SUMEZ,SUMVX,SUMVY,SUMVZ
513   FORMAT(6E14.7)
      IF(NOFST.NE.(NOFST/IPRINT)*IPRINT) GO TO 378
      PRINT 501,NOFST,STKE,SRKE,SPE,TOTEN,PRESS,TMO,TJMI,SK1
501   FORMAT(1X,/,' TIME STEP=',I5,' KIN.EN=',G12.5,' ROT.EN=',G12.5
     &' POT.EN=',G12.5,' TOT.EN=',G12.5,' PRESSURE=',G12.5/
     &' TOT.P=',G12.5,' ANG.MOM.=',G12.5,'        S(KX) = ',G12.5)
500   FORMAT(' TR.TEMP=',F12.2,5X,'ROT.TEMP=',F12.2/)
      PRINT 500 ,TRTE,ROTE

      IF(NOFST.NE.NT) GO TO 233
```

```
      NZ=INOF
      DO 222 L2=1,6
      DO 222 L1=1,100
  222 GR(L2,L1) = ZER0
      RSTKE = ZER0
      RSRKE = ZER0
      RQEK  = ZER0
      RTQTE = ZER0
      RRQTE = ZER0
      RTRTE = ZER0
      RTPE  = ZER0
      RTPR  = ZER0
      RTQP  = ZER0
      RQTEN = ZER0
      RTMO  = ZER0
      RTJM  = ZER0
      RVIR  = ZER0
      RVT   = ZER0
      RTEN  = ZER0
  233 CONTINUE
C
C  TEMP.SCALING
C
  378  CONTINUE
C
      IF((INOF-NZ).NE.((INOF-NZ)/NTINC)*NTINC) GO TO 415
      IF (NOFST .LE. NT) GO TO 417
      SUBAVK=(RSTKE-TKIN)*TWTH/(NTINC*KB*NOM)
      SUBAVR=(RSRKE-TROT)*TWTH/(NTINC*KB*NOM)
      IF(DABS(SUBAVR+SUBAVK-TWO*TEMP) .LT. DFFT) GO TO 417
      CALL TSCAL(3,SUBAVK,SUBAVR)
  417 TKIN=RSTKE
      TROT=RSRKE
      GO TO 416
  415 IF(MODE.NE.2) GO TO 416
      IF(NOFST.NE.MTIME*(NOFST/MTIME)) GO TO 416
      CALL TSCAL(1,TRTE,ROTE)
      CALL ZERO(FCC)
  416 CONTINUE


 431  FORMAT(2X,3E13.5,1X,3E13.5/2X,3E13.6,1X,3E13.5)
      IF (NOFST.GT.NMAX) GO TO 400
      IF (NOFST.LT.NMAX) GOTO 300

  400 CONTINUE
```



```
      INOF  = INOF - NZ
      RNOF  = ONE / ( DFLOAT ( INOF ) )
      IF(NOFST .LT. NT) GO TO 334
      SSTKE = SSTKE + RSTKE
      SSRKE = SSRKE + RSRKE
      TQEK  = TQEK  + RQEK
      TQTE  = TQTE  + RTQTE
      RQTE  = RQTE  + RRQTE
      TTRTE = TTRTE + RTRTE
      TPE   = TPE   + RTPE
      TPR   = TPR   + RTPR
      TQP   = TQP   + RTQP
      QTOTE = QTOTE + RQTEN
      TTMO  = TTMO  + RTMO
      TTJM  = TTJM  + RTJM
      TVIR  = TVIR  + RVIR
      TVT   = TVT   + RVT
      DO 333 L2=1,6
      DO 333 L1 = 1,100
  333 G(L2,L1)=G(L2,L1)+GR(L2,L1)
  334 CONTINUE
      DO 223 L2 =1,6
      R = -DELGR/TWO
      DO 223 L1 = 1,100
      R = R + DELGR
  223 GR(L2,L1)=GR(L2,L1)*RNOF*GRFAC/(BIND(L2)*R**2)
C
C  ***     DUMP FINAL CONFIGURATION TO DISK FOR RESTART   ***
C
      WRITE(8) ZOFST,SRKE,STKE,SSTKE,SSRKE,TQTE,RQTE
     &       ,TPE,TPR,TQP,QTOTE,TTMO,TTJM,TQEK,TVIR,TVT
      WRITE(8) G
      WRITE(8) XCN,YCN,ZCN,XC,YC,ZC,VXC,VYC,VZC
      WRITE(8) JX,JY,JZ,EX,EY,EZ
      WRITE(8) TX,TY,TZ,TXO,TYO,TZO,TXA,TYA,TZA

     ***     ----------------------------------------  ***

      RSTKE = RSTKE * RNOF * (ECON*CONFAC)
      RSRKE = RSRKE * RNOF * (ECON*CONFAC)
      RQEK  = RQEK  * RNOF * (ECON*CONFAC)**2
      RTQTE = RTQTE * RNOF
      RRQTE = RRQTE * RNOF
      RTRTE = RTRTE * RNOF
      RTPE  = RTPE  * RNOF * (ECON*CONFAC)
      RTPR  = RTPR  * RNOF
```

```
      RTQP  = RTQP  * RNOF
      RTEN  = RTEN  * RNOF * (ECON*CONFAC)
      RQTEN = RQTEN * RNOF * (ECON*CONFAC)**2
      RTMO  = RTMO  * RNOF * (PCON*CONFAC)
      RTJM  = RTJM  * RNOF * (JCON*CONFAC)
      RVIR  = RVIR  * RNOF * (ECON*CONFAC)
      RVT   = RVT   * RNOF  * (ECON*CONFAC)
      TRTE  = RSTKE * TWTH / (KB*NAV*ECON)
      ROTE  = RSRKE * TWTH / (KB*NAV*ECON)
      PRINT 988,INOF
  988 FORMAT(1H1,'  RUN AVERAGED QUANTITIES. ',I8,'-TIME STEPS FOR
THIS
     &,' JOB.'//)
                                                          PRINT
989,RSTKE,TRTE,RSRKE,ROTE,RQEK,RTQTE,RRQTE,RTPE,RTPR,RTQP,
     &RTEN,RQTEN,RTMO,RTJM,RVIR,RVT,RTRTE
  989 FORMAT(1X,' < KIN.TRA.EN. > = ',G12.5,20X,' < TRA.TEMP. > = ',
     &G12.5,//,1X,' < KIN.ROT.EN. > = ',G12.5,20X,' < ROT.TEMP. > = ',
     &G12.5,//,1X,' < (KIN.TOT.EN.)**2 > = ',G12.5,/,1X,' < (TRA.TEMP.)
     &,'**2 > = ',G12.5,/1X,' < (ROT.TEMP.)**2 > = ',G12.5,/,1X,
     &' < POT.EN. > = ',G12.5,/,1X,' < PRESSURE > = ',G12.5,20X,
     &' < (PRESSURE)**2 > = ',G12.5,//,1X,' < TOTAL ENERGY > = ',G12.5,
     &20X,' < (TOT.EN.)**2 > = ',G12.5,//,1X,' < C.O.M. IMPULSE > = ',
     &G12.5,10X,' < ANG. MOM. > = ',G12.5//1X,
     &' < VIRIAL > = ',G12.5,' < VIR.*TEMP. > = ',G12.5,
     &' < TRA.TEMP*ROT.TEMP > = ',G12.5/)
      PRINT  999,(TIND(IJ),IJ=1,6)
      R= -DELGR/TWO
      DO 244 L1=1,100
      R=R+DELGR
  244 PRINT 1999,L1,R,(GR(J,L1),J=1,6)
 1999 FORMAT(4X,I4,4X,G10.3,6(2X,G12.5))
  999 FORMAT(1H ,' ATOM-ATOM PAIR DISTRIBUTION G(R) '/15X
     &,'R',4X,7(9X,A5)/)
      IF( NOFST .LT. NT ) GO TO 7000
      RZOF = ONE /  ( DFLOAT ( NOFST - NT ) )
      IF(NOFST.LT.NT) RZOF=ONE/(DFLOAT(NOFST))
      SSTKE = SSTKE * RZOF * (ECON*CONFAC)
      SSRKE = SSRKE * RZOF * (ECON*CONFAC)
      TQEK  = TQEK  * RZOF * (ECON*CONFAC)**2
      TQTE  = TQTE  * RZOF
      RQTE  = RQTE  * RZOF
      TTRTE = TTRTE * RZOF
      TPE   = TPE   * RZOF * (ECON*CONFAC)
      TPR   = TPR   * RZOF
      TQP   = TQP   * RZOF
```



```
      TTEN  = (TPE+SSTKE+SSRKE)
      QTOTE = QTOTE * RZOF * (ECON*CONFAC)**2
      TTMO  = TTMO  * RZOF * (PCON*CONFAC)
      TTJM  = TTJM  * RZOF * (PCON*CONFAC)
      TVIR  = TVIR  * RZOF * (ECON*CONFAC)
      TVT   = TVT   * RZOF * (ECON*CONFAC)
      TRTE  = SSTKE * TWTH / (KB*NAV*ECON)
      ROTE  = SSRKE * TWTH / (KB*NAV*ECON)
      PRINT 688,NOFST,NT
  688 FORMAT(1H1,'  RUN AVERAGED QUANTITIES. ',I8,'-TIME STEPS FOR
THIS
     &,' SEGMENTS. OF WHICH ',I5,'-STEPS USED FOR EQUILIBRATION.'//)
      PRINT 689,SSTKE,TRTE,SSRKE,ROTE,TQEK, TQTE, RQTE, TPE, TPR, TQP,
     &TTEN,QTOTE,TTMO,TTJM,TVIR,TVT,TTRTE
  689 FORMAT(1X,' < KIN.TRA.EN. > = ',G12.5,20X,' < TRA.TEMP. > = ',
     &G12.5,//,1X,' < KIN.ROT.EN. > = ',G12.5,20X,' < ROT.TEMP. > = ',
     &G12.5,//,1X,' < (KIN.TOT.EN.)**2 > = ',G12.5,/,1X,' < (TRA.TEMP.)
     &,'**2 > = ',G12.5,/1X,' < (ROT.TEMP.)**2 > = ',G12.5,/,1X,
     &' < POT.EN. > = ',G12.5,/,1X,' < PRESSURE > = ',G12.5,20X,
     &' < (PRESSURE)**2 > = ',G12.5,//,1X,' < TOTAL ENERGY > = ',G12.5,
     &20X,' < (TOT.EN.)**2 > = ',G12.5,//,1X,' < C.O.M. IMPULSE > = ',
     &G12.5,20X,' < ANG.MOM. > = ',G12.5,//,1X,
     &' < VIRIAL > = ',G12.5,' < VIR.*TEMP. > = ',G12.5,
     &' < TRA.TEMP*ROT.TEMP > = ',G12.5/)
      PRINT  999,(TIND(IJ),IJ=1,6)
      R = -DELGR/TWO
      DO 247 L1=1,100
      R = R + DELGR
      DO 245 L2=1,6
  245 G(L2,L1)=G(L2,L1)*RZOF*GRFAC/(BIND(L2)*R**2)
  247 PRINT 1999,L1,R,(G(J,L1),J=1,6)
 7000 CONTINUE
      STOP
      END
      SUBROUTINE LATBCC(A)
      IMPLICIT REAL*8 (A-H,O-Z)

      DIMENSION
     &XC(108),YC(108),ZC(108),XCO(108),YCO(108),ZCO(108),
     &XCN(108),YCN(108),ZCN(108),VXC(108),VYC(108),VZC(108)
     &,EX(3,108),EY(3,108),EZ(3,108),IN(6)
     &,JX(108),JY(108),JZ(108)
      COMMON /CMT/ XC,YC,ZC,XCO,YCO,ZCO,
     &XCN,YCN,ZCN,VXC,VYC,VZC
      COMMON /CMO/ EX,EY,EZ
      COMMON /CMJ/ JX,JY,JZ,IN,TM,KB,NAV
```

```
                                                    COMMON          /PHY/
TEMP,VOL,DT,BOXL,FACTOR,CONFAC,CUT,RTKTM,RKTF,FF,DTF
      COMMON /N/ NOM,NOMM1,NORM,NT,NOFST,NTINC,INOF
      COMMON /NTR/ TRIG
      LI=0
      DO 603 L1=1,25
      DO 603 L2=1,25
      DO 603 L3=1,25
      LM1=L1-8
      LM2=L2-8
      LM3=L3-8
      XAA=(LM1-LM2+LM3)*A/2.D0-1.D0+A/4.D0+(RAND(0)-0.5D0)*A/8.D0
      YAA=(LM1+LM2-LM3)*A/2.D0-1.D0+A/4.D0+(RAND(0)-0.5D0)*A/8.D0
      ZAA=(-LM1+LM2+LM3)*A/2.D0-1.D0+A/4.D0+(RAND(0)-0.5D0)*A/8.D0
      IF(DABS(XAA).GT.1.0D0.OR.DABS(YAA).GT.1.0D0.OR.DABS(ZAA).GT.1.0D0
     &  GO TO 603
      LI=LI+1
      XCN(LI)=XAA
      YCN(LI)=YAA
      ZCN(LI)=ZAA
603   CONTINUE
      PRINT 33,RTKTM,RKTF,TM
 33   FORMAT(1X,G12.5,1X,G12.5,1X,G12.5)
      DO 3 IC=1,NOM
      DO 2 L=1,3
      EX(L,IC)=0.0D0
      EY(L,IC)=0.0D0
 2    EZ(L,IC)=0.0D0
      EX(1,IC)=1.0D0
      EY(2,IC)=1.0D0
      EZ(3,IC)=1.0D0
      VXC(IC)=GRAND(0)*RTKTM*DTF
      VYC(IC)=GRAND(0)*RTKTM*DTF
      VZC(IC)=GRAND(0)*RTKTM*DTF
      AJ1=GRAND(0)*DSQRT(RKTF*DFLOAT(IN(1)))
      AJ2=GRAND(0)*DSQRT(RKTF*DFLOAT(IN(2)))
      AJ3=GRAND(0)*DSQRT(RKTF*DFLOAT(IN(3)))
      JX(IC)=AJ1*EX(1,IC)+AJ2*EX(2,IC)+AJ3*EX(3,IC)
      JY(IC)=AJ1*EY(1,IC)+AJ2*EY(2,IC)+AJ3*EY(3,IC)
 3    JZ(IC)=AJ1*EZ(1,IC)+AJ2*EZ(2,IC)+AJ3*EZ(3,IC)
C     NOTE:VX,VY,VZ, ARE MULTIPLIED BY DT,JX,JY,JZ, ARE NOT
      PRINT 66, LI,A
      66 FORMAT(1H1,' STARTING FROM A RANDOM QUASI-BCC LATTICE
CONFIGURATI
     &N',//,10X,I5,'-RETICOLAR SITES',F10.4,'-LATTICE CONST.'//)
      DO 5 IC=1,NOM
```



```
   5  PRINT 610,IC,XCN(IC),YCN(IC),ZCN(IC)
 610  FORMAT(10X,I4,3(4X,D10.4))
      CALL ZERO(A)
      CALL TSCAL(1,ET,ER)
      RETURN
      END
      SUBROUTINE LATFCC(A)
      IMPLICIT REAL*8 (A-H,O-Z)
      REAL*8 IN(6),JX(108),JY(108),JZ(108)
      DIMENSION
     &XC(108),YC(108),ZC(108),XCO(108),YCO(108),ZCO(108),
     &XCN(108),YCN(108),ZCN(108),VXC(108),VYC(108),VZC(108)
     &,EX(3,108),EY(3,108),EZ(3,108)

      COMMON /CMT/ XC,YC,ZC,XCO,YCO,ZCO,
     &XCN,YCN,ZCN,VXC,VYC,VZC
      COMMON /CMO/ EX,EY,EZ
      COMMON /CMJ/ JX,JY,JZ,IN,TM,KB,NAV
                                                    COMMON          /PHY/
TEMP,VOL,DT,BOXL,FACTOR,CONFAC,CUT,RTKTM,RKTF,FF,DTF
      COMMON /N/ NOM,NOMM1,NORM,NT,NOFST,NTINC,INOF
      COMMON /NTR/ TRIG
      LI=0
      DO 603 L1=1,25
      DO 603 L2=1,25
      DO 603 L3=1,25
      LM1=L1-8
      LM2=L2-8
      LM3=L3-8
      XAA=(LM1+LM3)*A/2.D0 -1.D0  +  A/4.D0  +  (RAND(0)-0.5D0)*A/8.D0
      YAA=(LM1+LM2)*A/2.D0 -1.D0  +  A/4.D0  +  (RAND(0)-0.5D0)*A/8.D0
      ZAA=(LM2+LM3)*A/2.D0 -1.D0  +  A/4.D0  +  (RAND(0)-0.5D0)*A/8.D0
      IF(DABS(XAA).GT.1.0D0.OR.DABS(YAA).GT.1.0D0.OR.DABS(ZAA).GT.1.0D0
     &  GO TO 603
      LI=LI+1
      XCN(LI)=XAA
      YCN(LI)=YAA
      ZCN(LI)=ZAA
603   CONTINUE
      PRINT 33,RTKTM,RKTF,TM
 33   FORMAT(1X,G12.5,1X,G12.5,1X,G12.5)
      PRINT *, IN(1),IN(2),IN(3)
      DO 3 IC=1,NOM
      DO 2 L=1,3
      EX(L,IC)=0.0D0
      EY(L,IC)=0.0D0
```

```
2   EZ(L,IC)=0.0D0
    EX(1,IC)=1.0D0
    EY(2,IC)=1.0D0
    EZ(3,IC)=1.0D0
    VXC(IC)=GRAND(0)*RTKTM*DTF
    VYC(IC)=GRAND(0)*RTKTM*DTF
    VZC(IC)=GRAND(0)*RTKTM*DTF
    AJ1=GRAND(0)*DSQRT(RKTF*IN(1))
    AJ2=GRAND(0)*DSQRT(RKTF*IN(2))
    AJ3=GRAND(0)*DSQRT(RKTF*IN(3))
    JX(IC)=AJ1*EX(1,IC)+AJ2*EX(2,IC)+AJ3*EX(3,IC)
    JY(IC)=AJ1*EY(1,IC)+AJ2*EY(2,IC)+AJ3*EY(3,IC)
3   JZ(IC)=AJ1*EZ(1,IC)+AJ2*EZ(2,IC)+AJ3*EZ(3,IC)
C   NOTE:VX,VY,VZ, ARE MULTIPLIED BY DT,JX,JY,JZ, ARE NOT
    PRINT 66, LI,A
 66 FORMAT(1H1,' STARTING FROM FCC LATTICE CONFIGURATION ',/,
   &10X,I5,'-RETICOLAR SITES',F10.4,'-LATTICE CONST.'//)
    DO 5 IC=1,NOM
  5 PRINT 610,IC,XCN(IC),YCN(IC),ZCN(IC)
610 FORMAT(10X,I4,3(4X,E10.4))
    CALL ZERO(A)
    CALL TSCAL(1,ET,ER)
    RETURN
    END
    SUBROUTINE LATSCC(A).
    IMPLICIT REAL*8 (A-H,O-Z)
    DIMENSION
   &XC(108),YC(108),ZC(108),XCO(108),YCO(108),ZCO(108),
   &XCN(108),YCN(108),ZCN(108),VXC(108),VYC(108),VZC(108)
   &,EX(3,108),EY(3,108),EZ(3,108)
   &,JX(108),JY(108),JZ(108),IN(6)

    COMMON /CMT/ XC,YC,ZC,XCO,YCO,ZCO,
   &XCN,YCN,ZCN,VXC,VYC,VZC
    COMMON /CMO/ EX,EY,EZ
    COMMON /CMJ/ JX,JY,JZ,IN,TM,KB,NAV
                                          COMMON /PHY/
TEMP,VOL,DT,BOXL,FACTOR,CONFAC,CUT,RTKTM,RKTF,FF,DTF
    COMMON /N/ NOM,NOMM1,NORM,NT,NOFST,NTINC,INOF
    COMMON /NTR/ TRIG
    LI=0
    DO 603 L1=1,25
    DO 603 L2=1,25
    DO 603 L3=1,25
    LM1=L1-8
    LM2=L2-8
```



```
    LM3=L3-8
    XAA=LM1*A-1.D0+A/2.D0+(RAND(0)-0.5D0)*A/8.D0
    YAA=LM2*A-1.D0+A/2.D0+(RAND(0)-0.5D0)*A/8.D0
    ZAA=LM3*A-1.D0+A/2.D0+(RAND(0)-0.5D0)*A/8.D0
    IF(DABS(XAA).GT.1.0D0.OR.DABS(YAA).GT.1.0D0.OR.DABS(ZAA).GT.1.0D0
   & GO TO 603
    LI=LI+1
    XCN(LI)=XAA
    YCN(LI)=YAA
    ZCN(LI)=ZAA
603 CONTINUE
    PRINT 33,RTKTM,RKTF,TM
 33 FORMAT(1X,G12.5,1X,G12.5,1X,G12.5)
    DO 3 IC=1,NOM
    DO 2 L=1,3
    EX(L,IC)=0.0D0
    EY(L,IC)=0.0D0
2   EZ(L,IC)=0.0D0
    EX(1,IC)=1.0D0
    EY(2,IC)=1.0D0
    EZ(3,IC)=1.0D0
    VXC(IC)=GRAND(0)*RTKTM*DTF
    VYC(IC)=GRAND(0)*RTKTM*DTF
    VZC(IC)=GRAND(0)*RTKTM*DTF
    AJ1=GRAND(0)*DSQRT(RKTF*IN(1))
    AJ2=GRAND(0)*DSQRT(RKTF*IN(2))
    AJ3=GRAND(0)*DSQRT(RKTF*IN(3))
    JX(IC)=AJ1*EX(1,IC)+AJ2*EX(2,IC)+AJ3*EX(3,IC)
    JY(IC)=AJ1*EY(1,IC)+AJ2*EY(2,IC)+AJ3*EY(3,IC)
3   JZ(IC)=AJ1*EZ(1,IC)+AJ2*EZ(2,IC)+AJ3*EZ(3,IC)
C   NOTE:VX,VY,VZ, ARE MULTIPLIED BY DT,JX,JY,JZ, ARE NOT
    PRINT 66, LI,A
    66 FORMAT(1H1,' STARTING FROM A RANDOM QUASI-SCC LATTICE
CONFIGURATI
   &N',//,10X,I5,'-RETICOLAR SITES',F10.4,'-LATTICE CONST.'//)
    DO 5 IC=1,NOM
  5 PRINT 610,IC,XCN(IC),YCN(IC),ZCN(IC)
610 FORMAT(10X,I4,3(4X,E10.4))
    CALL ZERO(A)
    CALL TSCAL(1,ET,ER)
    RETURN
    END
    FUNCTION GRAND(N)
    IMPLICIT REAL*8 (A-H,O-Z)
    COMMON/RANDNO/R3(127),R1,I2
    COMMON /NTR/ TRIG
```

```
      PI=4.D0*DATAN(1.D0)
      GRAND=DSQRT(-2.*DLOG(R1))*DCOS(2.D0*PI*R2)
      RETURN
      END
      SUBROUTINE ZERO(Z)
      IMPLICIT REAL*8 (A-H,O-Z)
      REAL*8 JX(108),JY(108),JZ(108),IN(6)
      DIMENSION
     &XC(108),YC(108),ZC(108),XCO(108),YCO(108),ZCO(108),
     &XCN(108),YCN(108),ZCN(108),VXC(108),VYC(108),VZC(108)
     &,EX(3,108),EY(3,108),EZ(3,108)

      COMMON /CMT/ XC,YC,ZC,XCO,YCO,ZCO,
     &XCN,YCN,ZCN,VXC,VYC,VZC
      COMMON /CMO/ EX,EY,EZ
      COMMON /CMJ/ JX,JY,JZ,IN,TM,KB,NAV
                                                COMMON        /PHY/
     &TEMP,VOL,DT,BOXL,FACTOR,CONFAC,CUT,RTKTM,RKTF,FF,DTF
      COMMON /N/ NOM,NOMM1,NORM,NT,NOFST,NTINC,INOF
      SVX=0.0D0
      SVY=0.0D0
      SVZ=0.0D0
      SXX=0.0D0
      SXY=0.0D0
      SXZ=0.0D0
      DO 3 IC=1,NOM
C  NOTE:VX,VY,VZ, ARE MULTIPLIED BY DT,XX,XY,XZ, ARE NOT
      SVX=SVX+VXC(IC)
      SVY=SVY+VYC(IC)
      SVZ=SVZ+VZC(IC)
    3 CONTINUE
      RNOM=1.0D0/(DFLOAT(NOM))
C SET THE MEAN VALUES TO ZERO
      SVX=SVX*RNOM
      SVY=SVY*RNOM
      SVZ=SVZ*RNOM
      SJX=0.0D0
      SJY=0.0D0
      SJZ=0.0D0
      PRINT 66
   66 FORMAT(1H ,' TOTAL TRASLATIONAL MOMENTA AND C.O.M. POS.',
     &' SET TO ZERO ')
      DO 4 IC=1,NOM
      VXC(IC)=VXC(IC)-SVX
      VYC(IC)=VYC(IC)-SVY
      VZC(IC)=VZC(IC)-SVZ
```



```
      XC(IC)=XCN(IC)-VXC(IC)
      YC(IC)=YCN(IC)-VYC(IC)
      ZC(IC)=ZCN(IC)-VZC(IC)
      SXX=SXX+XC(IC)
      SXY=SXY+YC(IC)
      SXZ=SXZ+ZC(IC)
      SJX=SJX+JX(IC)
      SJY=SJY+JY(IC)
      SJZ=SJZ+JZ(IC)
    4 CONTINUE
      SXX=SXX*RNOM
      SXY=SXY*RNOM
      SXZ=SXZ*RNOM
      SJX=SJX*RNOM
      SJY=SJY*RNOM
      SJZ=SJZ*RNOM
      DO 44 IC=1,NOM
      XC(IC)=XC(IC)-SXX
      YC(IC)=YC(IC)-SXY
      ZC(IC)=ZC(IC)-SXZ
      XCN(IC)=XCN(IC)-SXX
      YCN(IC)=YCN(IC)-SXY
      ZCN(IC)=ZCN(IC)-SXZ
      JX(IC)=JX(IC)-SJX
      JY(IC)=JY(IC)-SJY
      JZ(IC)=JZ(IC)-SJZ
   44 CONTINUE
      RETURN
      END
      SUBROUTINE TSCAL(MODE,TTEMP,RTEMP)
      IMPLICIT REAL*8 (A-H,O-Z)
      REAL*8 JX(108),JY(108),JZ(108),IN(6),KB,NAV
      DIMENSION
     &XC(108),YC(108),ZC(108),XCO(108),YCO(108),ZCO(108),
     &XCN(108),YCN(108),ZCN(108),VXC(108),VYC(108),VZC(108)
     &,EX(3,108),EY(3,108),EZ(3,108),OM(6)

      COMMON /CMT/ XC,YC,ZC,XCO,YCO,ZCO,
     &XCN,YCN,ZCN,VXC,VYC,VZC
      COMMON /CMO/ EX,EY,EZ
      COMMON /CMJ/ JX,JY,JZ,IN,TM,KB,NAV
                                                COMMON        /PHY/
     &TEMP,VOL,DT,BOXL,FACTOR,CONFAC,CUT,RTKTM,RKTF,FF,DTF
      COMMON /N/ NOM,NOMM1,NORM,NT,NOFST,NTINC,INOF
      KB=1.3807D-00
      NAV=6.0223D+23
```

```
      ELSQ=2.3071138D+05
      IF(MODE.NE.1) GO TO 1
      TTEMP=0.0D0
      RTEMP=0.0D0
      DO 2 I=1,NOM
      TTEMP=TTEMP+VXC(I)**2+VYC(I)**2+VZC(I)**2
      DO 3 L=1,3
    3 OM(L)=(EX(L,I)*JX(I)+EY(L,I)*JY(I)+EZ(L,I)*JZ(I))/IN(L)
      RTEMP=RTEMP+0.5D0*(IN(1)*OM(1)**2+IN(2)*OM(2)**2+IN(3)*OM(3)**2)
    2 CONTINUE
      PRINT 3456,KB,NAV,TM,IN(1),IN(2),IN(3)
 3456 FORMAT (7G14.6)


      TTEMP=TTEMP*0.5D0*TM/DTF**2
      TTEMP=2.0D0*TTEMP/(3.0D0*NOM*KB)
      RTEMP=RTEMP*2.0D0/(3.0D0*NOM*KB*FF)
    1 UT=DSQRT(TEMP/TTEMP)
      UR=DSQRT(TEMP/RTEMP)
      DO 413 I=1,NOM
      VXC(I)=UT*VXC(I)
      VYC(I)=UT*VYC(I)
      VZC(I)=UT*VZC(I)



      XC(I)=XCN(I)-VXC(I)
      YC(I)=YCN(I)-VYC(I)
      ZC(I)=ZCN(I)-VZC(I)
      JX(I)=UR*JX(I)
      JY(I)=UR*JY(I)
  413 JZ(I)=UR*JZ(I)
      PRINT 412,TTEMP,RTEMP
  412 FORMAT(1X,' TEMPERATURE SCALING. OLD TEMPERATURES : ',
     &1X,' TR.TEMP=',G12.5,' RO.TEMP=',G12.5)
      RETURN
      END
      SUBROUTINE RANGE(PSI,PELR,CUT,NOM,ACR,EP,BSIGSQ)
      IMPLICIT REAL*8 (A-H,O-Z)
      REAL*8 PSI,PELR,EP(36),ACR(36),BSIGSQ(36),
     &CUT,CUTSQ,A,PGR
      CUTSQ=CUT**2
      PGR=(DACOS(-1.0D0))
      PSI=0.0D0
      PELR = 0.0D0
      DO 19 J=1,25
```



```
      A=(BSIGSQ(J)/CUTSQ)**3
      PSI=PSI+EP(J)*(A-2.0D0/3.0D0*A*A)
      PELR=PELR+EP(J)*(A*A/3.0D0-A)/3.0D0
   19 ACR(J)=EP(J)*(2.0D0*A*A-A)/CUTSQ
      PSI=PSI*2.0D0*PGR*(DFLOAT(NOM*NOM))*CUT**3
      PELR= PELR*PGR*(DFLOAT(NOM*NOM))*CUT**3
      RETURN
      END
      SUBROUTINE KINET(NAV,FACTOR,M,TM,IN,RI)
      IMPLICIT REAL*8 (A-H,O-Z)
      REAL*8 FACTOR,NAV,TM,DCH,DCCL,IN(6),RI(6),M(6)
     \,ROOT3
      D1=1.0
      D2=1.0
      DOC=1.0
      M(1)=1.0D0
      M(2)=16.0D0
      M(3)=1.0D0
      M(4)=0.0D0
      M(5)=0.0D0
      TM=0.0D0
      DO 15 I=1,5
      M(I)=M(I)/(NAV*1.0D-24)
   15 TM=TM+M(I)
      PI=3.1415927
      ZET=PI*54.5/180.0
      X1=DSIN(ZET)
      Y1=-8.0/9.0*DCOS(ZET)
      Z1=0.00
      X2=0.00
      Y2=DCOS(ZET)/9.0
      Z2=0.00
      X3=-DSIN(ZET)
      Y3=Y1
      Z3=0.00
      IN(1)=M(1)*(X1*X1+Z1*Z1)+M(2)*(X2*X2+Z2*Z2)     AM(3)*(X3*X3+Z3*Z3)
                                  IN(2)=M(1)*(X1*X1+Y1*Y1)+M(2)*(X2*X2+Y2*Y2)
AM(3)*(X3*X3+Y3*Y3)
      IN(3)=M(1)*(Y1*Y1+Z1*Z1)+M(2)*(Y2*Y2+Z2*Z2)     AM(3)*(Y3*Y3+Z3*Z3)
C  MOMENTS OF INERTIA IN BOX UNITS
C  IN(3) IS PARALLEL TO Z-AXIS ,IN(2) PARALLEL TO 3-4 VECTOR,
C  IN(1) PARALLEL TO 1-2 VECTOR DOC=SIST. FROM CENTRAL ATOM TO
COM
      IN(1)=IN(1)*FACTOR**2/(NAV*1.0D-24)
      IN(2)=IN(2)*FACTOR**2/(NAV*1.0D-24)
      IN(3)=IN(3)*FACTOR**2/(NAV*1.0D-24)
```

```
   DO 18 L=1,3
   IN(L+3)=IN(L)
18  RI(L)=1.0D0/IN(L)
   PRINT 20,IN(1),IN(2),IN(3),RI(1),RI(2),RI(3),FACTOR


20 FORMAT(1X//2X,' INERTIA(1,2,3) =',3G12.5,' INV.MOM.INE.(1,2,3) ='
  &,3G12.5,1X//2X,' FACTOR =',G12.5,1X//)


   RETURN
   END
   SUBROUTINE LENJO(SIG,EPS,BSIG,BSIGSQ,EP,KB,FACTOR)
   IMPLICIT REAL*8 (A-H,O-Z)
   REAL*8 SIG(6,6),EPS(6,6),BSIG(36),BSIGSQ(36),EP(36)
  &,KB,FACTOR
   SIG(1,1)=2.25
   SIG(2,2)=2.8
   SIG(3,3)=2.25
   SIG(4,4)=0.0
   SIG(5,5)=0.0
   EPS(1,1)=21.1
   EPS(2,2)=58.4
   EPS(3,3)=21.1
   EPS(4,4)=0.0
   EPS(5,5)=0.0
   SIG(1,2)=0.5*(SIG(1,1)+SIG(2,2))
   SIG(1,3)=0.5*(SIG(1,1)+SIG(3,3))
   SIG(1,4)=0.0
   SIG(1,5)=0.0
   EPS(1,2)=DSQRT(EPS(1,1)*EPS(2,2))
   EPS(1,3)=DSQRT(EPS(1,1)*EPS(3,3))
   EPS(1,4)=DSQRT(EPS(1,1)*EPS(4,4))
   EPS(1,5)=DSQRT(EPS(1,1)*EPS(5,5))
   SIG(2,1)=SIG(1,2)
   SIG(2,3)=0.5*(SIG(2,2)+SIG(3,3))
   SIG(2,4)=0.0
   SIG(2,5)=0.0
   EPS(2,1)=EPS(1,2)
   EPS(2,3)=DSQRT(EPS(2,2)*EPS(3,3))
   EPS(2,4)=DSQRT(EPS(2,2)*EPS(4,4))
   EPS(2,5)=DSQRT(EPS(2,2)*EPS(5,5))
   SIG(3,1)=SIG(1,3)
   SIG(3,2)=SIG(2,3)
   SIG(3,4)=0.0
   SIG(3,5)=0.0
```



```
   EPS(3,1)=EPS(1,3)
   EPS(3,2)=EPS(2,3)
   EPS(3,4)=DSQRT(EPS(3,3)*EPS(4,4))
   EPS(3,5)=DSQRT(EPS(3,3)*EPS(5,5))
   SIG(4,1)=SIG(1,4)
   SIG(4,2)=SIG(2,4)
   SIG(4,3)=SIG(3,4)
   SIG(4,5)=0.0
   EPS(4,1)=EPS(1,4)
   EPS(4,2)=EPS(2,4)
   EPS(4,3)=EPS(3,4)
   EPS(4,5)=DSQRT(EPS(4,4)*EPS(5,5))
   SIG(5,1)=SIG(1,5)
   SIG(5,2)=SIG(2,5)
   SIG(5,3)=SIG(3,5)
   SIG(5,4)=SIG(4,5)
   EPS(5,1)=EPS(1,5)
   EPS(5,2)=EPS(2,5)
   EPS(5,3)=EPS(3,5)
   EPS(5,4)=EPS(4,5)
   DO 14 I=1,5
   I5=5*(I-1)
   DO 14 J=1,5
   IJ=I5+J
   BSIG(IJ)=FACTOR*SIG(I,J)
   BSIGSQ(IJ)=BSIG(IJ)**2
   EP(IJ)=KB*EPS(I,J)
14  CONTINUE
   RETURN
   END
   SUBROUTINE ATPOS(NATM,FACTOR)
   IMPLICIT REAL*8 (A-H,O-Z)
   DIMENSION
  &     XAT(648),YAT(648),ZAT(648),XA(648),YA(648)
  &,ZA(648),XC(108),YC(108),ZC(108),XCO(108),YCO(108),ZCO(108)
  &,XCN(108),YCN(108),ZCN(108),VXC(108),VYC(108),VZC(108)
  &,EX(3,108),EY(3,108),EZ(3,108)

   COMMON /ATT/ XAT,YAT,ZAT,XA,YA,ZA
   COMMON /CMT/ XC,YC,ZC,XCO,YCO,ZCO,
  &XCN,YCN,ZCN,VXC,VYC,VZC
   COMMON /CMO/ EX,EY,EZ
   COMMON /N/ NOM,NOMM1,NORM,NT,NOFST,NTINC,INOF
   TWO=2.0D0
   ROOT2=70.5*3.1415927/180.0
   FACTOR=0.13508
```

```
      PI=3.1415927
      ZET=PI*54.5/180.0
      X1=DSIN(ZET)
      Y1=-8.0/9.0*DCOS(ZET)
      Z1=0.00
      X2=0.00
      Y2=DCOS(ZET)/9.0
      Z2=0.00
      X3=-DSIN(ZET)
      Y3=Y1
      Z3=0.00
      X4=0.00
      Y4=(1.0/9.0+0.8)*DCOS(ZET)
      Z4=0.8*DSIN(ZET)
      X5=0.0
      Y5=Y4
      Z5=-Z4
      DO 369 IC=1,NOM
      IA=NATM*(IC-1)+1
      XAT(IA)=FACTOR*(X1*EX(3,IC)+Y1*EX(1,IC)+Z1*EX(2,IC))
      YAT(IA)=FACTOR*(X1*EY(3,IC)+Y1*EY(1,IC)+Z1*EY(2,IC))
      ZAT(IA)=FACTOR*(X1*EZ(3,IC)+Y1*EZ(1,IC)+Z1*EZ(2,IC))
      XAT(IA+1)=FACTOR*(X2*EX(3,IC)+Y2*EX(1,IC)+Z2*EX(2,IC))
      YAT(IA+1)=FACTOR*(X2*EY(3,IC)+Y2*EY(1,IC)+Z2*EY(2,IC))
      ZAT(IA+1)=FACTOR*(X2*EZ(3,IC)+Y2*EZ(1,IC)+Z2*EZ(2,IC))
      XAT(IA+2)=FACTOR*(X3*EX(3,IC)+Y3*EX(1,IC)+Z3*EX(2,IC))
      YAT(IA+2)=FACTOR*(X3*EY(3,IC)+Y3*EY(1,IC)+Z3*EY(2,IC))
      ZAT(IA+2)=FACTOR*(X3*EZ(3,IC)+Y3*EZ(1,IC)+Z3*EZ(2,IC))
      XAT(IA+3)=FACTOR*(X4*EX(3,IC)+Y4*EX(1,IC)+Z4*EX(2,IC))
      YAT(IA+3)=FACTOR*(X4*EY(3,IC)+Y4*EY(1,IC)+Z4*EY(2,IC))
      ZAT(IA+3)=FACTOR*(X4*EZ(3,IC)+Y4*EZ(1,IC)+Z4*EZ(2,IC))
      XAT(IA+4)=FACTOR*(X5*EX(3,IC)+Y5*EX(1,IC)+Z5*EX(2,IC))
      YAT(IA+4)=FACTOR*(X5*EY(3,IC)+Y5*EY(1,IC)+Z5*EY(2,IC))
      ZAT(IA+4)=FACTOR*(X5*EZ(3,IC)+Y5*EZ(1,IC)+Z5*EZ(2,IC))
  369 CONTINUE
      DO 30 IC=1,NOM
      I5=NATM*(IC-1)
      DO 31 IA=1,NATM
      K=I5+IA
      XA(K)=XC(IC)+XAT(K)
      XA(K)=XA(K)-TWO*(DFLOAT(IDINT(XA(K))))
      YA(K)=YC(IC)+YAT(K)
      YA(K)=YA(K)-TWO*(DFLOAT(IDINT(YA(K))))
      ZA(K)=ZC(IC)+ZAT(K)
      ZA(K)=ZA(K)-TWO*(DFLOAT(IDINT(ZA(K))))
   31 CONTINUE
```



```
   30 CONTINUE
      RETURN
      END
      SUBROUTINE GRAF(F,F1,F2,KMAX,IK,IL)
C
C
C  PLOTTING 3 CURVES F,F1,F2
C  KMAX= NUMBER OF POINTS
C  IK   = 0 (NORMALIZATION AT FIRST POINT), = 1 ( NO NORMALIZATION
C  IL   = 0 ( 'F' CURVE ONLY ), = 1 ('F'&'F1' CURVES), = 2 ( ALL CURVES
C
C
      IMPLICIT REAL*8 (A-H,O-Z)
      DIMENSION F(200),F1(200),F2(200),O(101)
      DATA B/1H /,TA/1HI/,T1/1H*/,T2/1H+/,T3/1H#/
      FF1=F(1)
      FF11=F1(1)
      FF21=F2(1)
      X=0.D0
      DO 1 I=1,KMAX
      IF(IK.EQ.0) F(I)=F(I)/FF1
      X1=DABS(F(I))
      IF(X1.GT.X)X=X1
      IF(IL.EQ.0)GOTO 1
      IF(IK.EQ.0) F1(I)=F1(I)/FF11
      X1=DABS(F1(I))
      IF (IL.EQ.1) GOTO 1
      IF (IK.EQ.0) F2(I)=F2(I)/FF21
      X1=DABS(F2(J))
      IF(X1.GT.X)X=X1
    1 CONTINUE
      DELT=X /50.D0
      DO 2 I=1,KMAX
      DO 3 J=1,101
    3 O(J)=B
      O(1)=TA
      O(51)=TA
      O(101)=TA
      M=(F(I)+X )/DELT+1.5D0
      O(M)=T1
      IF(IL.EQ.0)GOTO 4
      M=(F1(I)+X )/DELT+1.5D0
      O(M)=T2
      IF(IL.EQ.1) GO TO 4
      M=(F2(I)+X)/DELT+1.5D0
```

```
      O(M)=T3
    4 CONTINUE
      IF (IL.EQ.2) PRINT 997,I,F(I),F1(I),F2(I),O
      IF(IL.EQ.1) PRINT 998,I,F(I),F1(I),O
      IF(IL.EQ.0) PRINT 999,I,F(I),O
    2 CONTINUE
  997 FORMAT(1H ,I3,3(1X,G9.3),1X,101A1)
  998 FORMAT(1H ,I5,2(1X,G10.3),1X,101A1)
  999 FORMAT(1H ,I5,D15.7,101A1)
      RETURN
      END
      SUBROUTINE CHARGE(CHA,BCHA,ELSQ,FACTOR,TWFO)
      IMPLICIT REAL*8 (A-H,O-Z)
      DIMENSION CHA(6),BCHA(36)
      CHA(1)=0.23
      CHA(2)=0.00
      CHA(3)=0.23
      CHA(4)=-0.23
      CHA(5)=-0.23
      DO 14 I=1,5
      I5=5*(I-1)
      DO 14 J=1,5
      IJ=I5+J
      BCHA(IJ)=CHA(I)*CHA(J)*ELSQ*FACTOR/TWFO
   14 CONTINUE
      RETURN
      END
c               RANDOM NUMBER GENERATOR
C
      FUNCTION RAND(N)
      IMPLICIT REAL*8 (A-H,O-Z)
      COMMON /RANDNO/ R3(127),R1,I2
      DATA S,T,RMC/0.D0, 1.D0, 1.D0/
      DATA IW/-1/
      IF((R1.LT.1.D0).AND.(N.EQ.0)) GO TO 60
      IF (IW.GT.0) GO TO 30
   10 IW = IW + 1
      T = 0.5D0*T
      R1 = S
      S = S + T
      IF ((S.GT.R1).AND.(S.LT.1D0)) GO TO 10
      IKT = (IW - 1)/12
      IC = IW - 12*IKT
      ID = 2**(13 - IC)
      DO 20 I = 1, IC
   20 RMC = 0.5D0*RMC
```



```
      RM = 0.015625D0*0.015625D0
   30 I2 = 127
      IR = MOD(IABS(N), 8190) + 1
   40 R1 = 0.D0
      DO 50 I = 1, IKT
      IR = MOD(17*IR, 8191)
   50 R1 = (R1 + DFLOAT(IR/2))*RM
      IR = MOD (17*IR, 8191)
      R1 = (R1 + DFLOAT(IR/ID))*RMC
      R3(I2) = R1
      I2 = I2 - 1
      IF (I2.GT.0) GO TO 40
   60 IF (I2.EQ.0) I2 = 127
      T = R1 + R3(I2)
      IF (T.GE.1D0) T = (R1 - 0.5D0) + (R3(I2) - 0.5D0)
      R1 = T
      R3(I2) = R1
      I2 = I2 - 1
      RAND = R1
      RETURN
      END
      SUBROUTINE DATE(DAT)
      IMPLICIT REAL*8 (A-H,O-Z)
      RETURN
      END
      SUBROUTINE TIME(TRIG)
      IMPLICIT REAL*8 (A-H,O-Z)
      RETURN
      END
      SUBROUTINE SECOND(PTIME)
      IMPLICIT REAL*8 (A-H,O-Z)
      RETURN
      END
```

Code for Computation of Cross Correlation Functions

The following is a program for the efficient computation of cross correlation functions of all types written by Keith Refson and the present author. It uses running time averaging over N time steps and M molecules, and is capable of computing a c.c.f. over 6,000 time steps and 108 molecules in about one minute of IBM 3090 time.

```
      PROGRAM  CRLATE
      PARAMETER (NSL=1000,MAXMOL=108,MAXCCF=1000)
      PARAMETER (IR=0,IV=1, IJ=2, IE=3 ,IF=4 ,IT=5, IJ1=6,
     1          IED=7, IW=8 , IP=9 , ITOTR=10)
      REAL X(0:3*MAXMOL*NSL-1,2)
```

```
                                                                    REAL*8
RCCF(0:MAXCCF),ACCF(0:MAXCCF),DENOM,DENOM1,DENOM2,DOT
      LOGICAL LINTER,LPLOT,FIRST
      NAMELIST /ACFCCF/ NSLICE,NCF,ID1,ID2,IX1,IX2,NMOLS,NBYTE,
     1          FIRST, NSLT, LINTER, NORM, LPLOT, TSLICE, ITOUT
      COMMON /BYTE/ NBYTE
      DATA NSLICE, NCF, ID1, ID2, IX1, IX2, NMOLS,
     1    NSLT, LINTER, NORM, LPLOT, TSLICE, ITOUT
     2    / 900,200, 1, 1, 0, 0, 108, 1000, F, 0, F, 0., 6/
      INDX(NMOL,IX,ISL) = NMOL - 1 + (IX-1)*NMOLS + ISL*3*NMOLS
      NBYTE=8
      FIRST=.FALSE.  C C C
      READ(4,ACFCCF)

OPEN(UNIT=80,ACCESS='DIRECT',RECL=3*NMOLS*NBYTE,ACTION='READ')
      IF(IX1 .EQ. 0) IX2  = 0
      IF( IX1.LT.0 .OR. IX1.GT.3 .OR. IX2.LT.0 .OR. IX2.GT.3) THEN
        WRITE(6,*) ' Invalid values of ccf components IX1, IX2'
        STOP
      ELSE IF(IX1 .EQ. 0) THEN
        NORM  = 0
      ELSE
        IF(NORM .NE. 1 .AND. NORM .NE. 2) THEN
          WRITE(6,*) ' Invalid normalisation type - must be 1 or 2'
          STOP
        END IF
      END IF
      IF(ID1 .EQ. ID2 .AND. NORM .EQ. 2) NORM  = 0 C C C
      DENOM  = 0.D0
      DENOM1  = 0.D0
      DENOM2  = 0.D0
      DO 600 I=0,NCF
600     ACCF(I)  = 0:D0

      IF(ID1 .EQ. ID2) THEN

        CALL READAT(X(0,1),ID1,NCF,0,NSLT,NMOLS)
        DO 2000 IBLOCK  = NCF, NSLICE-1, NSL-NCF
          NN  = MIN(NSL-NCF,NSLICE-IBLOCK)
          CALL READAT(X(3*NMOLS*NCF,1),ID1,NN,IBLOCK,NSLT,NMOLS)
          WRITE(6,*) ' ****** DATA READ IN'

          CALL CCF(X,X,NMOLS,NN+NCF,RCCF,NCF,IX1,IX2)
          DO 1000 ICF  = 0,NCF
1000        ACCF(ICF)  = ACCF(ICF)  + RCCF(ICF)
```



```
          IF(NORM .EQ. 0) THEN C                WRITE(6,*) ' CORRELATION
FROM',IBLOCK-NCF,' FOR',NN
          DENOM  = DENOM  + DOT(X,X,3*NMOLS*NN) C          WRITE(6,*)
' DENOM=',DENOM
        ELSE IF(NORM .EQ. 1) THEN
          DO 2108 ISL=0,NN
            DENOM1=DENOM1
     1       +DOT(X(INDX(1,IX1,ISL),1),X(INDX(1,IX1,ISL),1),NMOLS)
            DENOM2=DENOM2
     1       +DOT(X(INDX(1,IX2,ISL),1),X(INDX(1,IX2,ISL),1),NMOLS)
2108        CONTINUE
        END IF

C       WRITE(6,*) ' MOVING',NCF,' FROM',NSL-NCF,' TO',0
        CALL MOVE(X(3*NMOLS*(NSL-NCF),1),X,3*NMOLS*NCF)
2000    CONTINUE

      ELSE IF(IX1.GE.1 .AND. IX1.LE.3 .AND. IX2.GE.1 .AND. IX2.LE.3)THE

        CALL READAT(X(0,1),ID1,NCF,0,NSLT,NMOLS)
        CALL READAT(X(0,2),ID2,NCF,0,NSLT,NMOLS)
        DO 4000 IBLOCK  = NCF, NSLICE-1, NSL-NCF
          NN  = MIN(NSL-NCF,NSLICE-IBLOCK)
          CALL READAT(X(3*NMOLS*NCF,1),ID1,NN,IBLOCK,NSLT,NMOLS)
          CALL READAT(X(3*NMOLS*NCF,2),ID2,NN,IBLOCK,NSLT,NMOLS)
          WRITE(6,*) ' ****** DATA READ IN'

          CALL CCF(X(0,1),X(0,2),NMOLS,NN+NCF,RCCF,NCF,IX1,IX2)
          DO 3000 ICF  = 0,NCF
3000        ACCF(ICF)  = ACCF(ICF)  + RCCF(ICF)

          IF(NORM .EQ. 1) THEN
            DO 4108 ISL=0,NN
              DENOM1=DENOM1
     1         +DOT(X(INDX(1,IX1,ISL),1),X(INDX(1,IX1,ISL),1),NMOLS)
              DENOM2=DENOM2
     1         +DOT(X(INDX(1,IX2,ISL),2),X(INDX(1,IX2,ISL),2),NMOLS)
4108          CONTINUE
          ELSE IF(NORM .EQ. 2)THEN
            DENOM1=DENOM1+DOT(X(0,1),X(0,1),3*NMOLS*NN)
            DENOM2=DENOM2+DOT(X(0,2),X(0,2),3*NMOLS*NN)
          END IF

          CALL MOVE(X(3*NMOLS*(NSL-NCF),1),X(0,1),3*NMOLS*NCF)
          CALL MOVE(X(3*NMOLS*(NSL-NCF),2),X(0,2),3*NMOLS*NCF)
4000    CONTINUE
```

```
      ELSE
        WRITE(6,*) ' IX1(2) > 3 OR IX1(2) < 0 ', IX1,IX2
        STOP
      END IF

C     CALL READAT(R,IR,NSLICE,NT,NMOLS)

C       NMOLN=NMOLS C       CALL COMPCT(V,R,NMOLS,NMOLN,NSLICE) C
WRITE(6,*) ' ****** COMPACTED'

C   CALL FOR 'DOT PRODUCT' ACF
      IF(NORM .NE. 0) DENOM = SQRT(DENOM1*DENOM2)
      WRITE(ITOUT,100) DENOM,ACCF(0)
  100 FORMAT(' DENOMINATOR = ',1P,D16.8,'    <V(0).V(0)> = ',D16.8)
      DO 1080 I=0,200
 1080   ACCF(I) = ACCF(I)/DENOM

      CALL PRINT(ACCF,ID1,ID2,IX1,IX2,NCF,ITOUT)
      IF(LPLOT) THEN
       IF(FIRST) THEN
         REWIND 9
         ENDFILE 9
       ENDIF
      REWIND 9
      DO 98 I=1,10000
      READ (9,END=99)
   98 CONTINUE
   99 BACKSPACE 9
      WRITE (9) ACCF,NCF,TSLICE,NMOLS,ID1,ID2,IX1,IX2
      REWIND 9
      ENDIF
      STOP
      END

      FUNCTION CCFNOR(X1,X2,IC1,IC2,NMOL,NSL)
        REAL*4 X1(1:NMOL,1:3,0:NSL-1),X2(1:NMOL,1:3,0:NSL-1)
        REAL*8 X1X1,X2X2, CCFNOR, DOT
        X1X1 = 0.D0
        X2X2 = 0.D0
        DO 6 ISL = 0,NSL-1
          X1X1 = X1X1+DOT(X1(1,IC1,ISL),X1(1,IC1,ISL),NMOL)
          X2X2 = X2X2+DOT(X2(1,IC2,ISL),X2(1,IC2,ISL),NMOL)
    6   CONTINUE
        CCFNOR = SQRT(X1X1*X2X2)
        RETURN
```



```
      END

      SUBROUTINE READAT(X,IX,NSL,NSL0,NSLMAX,NMOL)
        REAL*4 X(0:3*NMOL*NSL-1)
        PARAMETER (MAXMOL=108)
        REAL*8 BUFF(0:3*MAXMOL-1)
        COMMON /BYTE/ NBYTE C       WRITE(6,*) ' READING SLICES ',NSL0,'
TO ',NSL+NSL0-1

        IF(NMOL .GT. MAXMOL) THEN
          WRITE(6,*) 'READ BUFFER TOO SMALL -INCREASE NMOL'
          STOP
        END IF

        J0 = 0 C       WRITE(6,*) ' READING RECORDS',IX*NSLMAX+NSL0+1,'
TO', C   1                          IX*NSLMAX+NSL+NSL0
        IF(NBYTE .EQ. 8)THEN
          DO 1000 IREC=IX*NSLMAX+NSL0+1,IX*NSLMAX+NSL+NSL0
            CALL RBLOCK(BUFF,IREC,2*NMOL)
            DO 1010 J=3*NMOL-1,0,-1
              X(J+J0) = BUFF(J)
 1010         CONTINUE
            J0 = J0 + 3*NMOL
 1000     CONTINUE
        ELSE
          DO 2000 IREC=IX*NSLMAX+NSL0+1,IX*NSLMAX+NSL+NSL0
            CALL RBLOCK(X(J0),IREC,NMOL)
            J0=J0+3*NMOL
 2000     CONTINUE
        END IF
        RETURN
      END

      SUBROUTINE RBLOCK(BUFF,IREC,NMOLS)
        REAL*4 BUFF(0:3*NMOLS-1)
        READ(UNIT=80,REC=IREC) BUFF
        RETURN
      END

C       FUNCTION DOT(A,B,N) C       REAL*4 A(N),B(N) C       REAL*8
SUM,DOT C       SUM = 0.0D0 C       DO 1000 I = 1,N C       SUM = SUM
+ A(I)*B(I) C1000    CONTINUE C       DOT=SUM C       RETURN C    END

      SUBROUTINE MOVE(FROM,TO,LEN)
        REAL*4 FROM(LEN),TO(LEN)
        DO 1000 I=1,LEN
```

```
1000      TO(I) = FROM(I)
      RETURN
    END

    SUBROUTINE CCF(X,Y,NMOL,NSL,RCCF,NCCF,IX1,IX2)
      PARAMETER (NMOLS=108,NSLICE=900,NT=1000)
      REAL*4 X(1:NMOL,1:3,0:NSL-1),Y(1:NMOL,1:3,0:NSL-1)
      REAL*8 DOT,RCCF(0:NCCF)

      DO 1020 I=0,NCCF
        RCCF(I) = 0.0
1020  CONTINUE
      IF(IX1 .LE. 0 .OR. IX2 .LE. 0) THEN
        IX=1
        JX=1
        N=3
      ELSE IF(IX1 .LE. 3 .AND. IX2 .LE. 3) THEN
        IX = IX1
        JX = IX2
        N=1
      ELSE
        WRITE(6,*) IX1, ' AND ',IX2 ,' ARE INVALID COMPONENTS'
        STOP
      END IF

      DO 1000 IT0 = 0,NSL-NCCF-1
        IF(MOD(IT0,10).EQ.0) WRITE(6,*) ' WORKING ON SLICE', IT0
        DO 1010 IDT = 0,NCCF
          RCCF(IDT) = RCCF(IDT) + DOT(X(1,IX,IT0),
     1                          Y(1,JX,IT0+IDT),N*NMOL)
1010      CONTINUE
1000    CONTINUE
      RETURN
    END

    SUBROUTINE COMPCT(X,R,NMOL,NMOLN,NSL)
      PARAMETER(NMOLS=108,NSLICE=900)
      PARAMETER (CUBE=0.5)
      REAL R(1:NMOL,1:3,0:NSL-1),X(NMOLS*3*NSLICE)
      INTEGER MOL(NMOLS)
      LOGICAL IN
      INDX(IM,IK,IS) = (IS*3+IK-1)*NMOL+IM

      NLIST=0
      DO 1000 ISL=0,NSL-1
        DO 1010 IMOL=1,NMOL
```



```
          IF(  ABS(R(IMOL,1,ISL)).LT.CUBE
     A       .AND.ABS(R(IMOL,2,ISL)).LT.CUBE
     B       .AND.ABS(R(IMOL,3,ISL)).LT.CUBE) THEN
            DO 2000 ILIST=1,NLIST
              IF(IMOL .LE. MOL(ILIST)) GOTO 2600
2000          CONTINUE
            NLIST = NLIST + 1
            MOL (NLIST) = IMOL
            WRITE(6,200) ISL,(MOL(IL),IL=1,NLIST)
2600        IF(IMOL.NE.MOL(ILIST)) THEN
              NLIST=NLIST+1
              DO 3000 IL1=NLIST,ILIST,-1
3000            MOL(IL1)=MOL(IL1-1)
              MOL(ILIST)=IMOL
              WRITE(6,200) ISL,(MOL(IL),IL=1,NLIST)
            END IF
          END IF
1010    CONTINUE
1000  CONTINUE

      WRITE(6,100) NLIST,(MOL(ILIST),ILIST=1,NLIST)
 100  FORMAT(' NUMBER OF MOLECULES WHICH ENTER INNER CUBE =
',I6/(12I6)
 200  FORMAT(' LIST UPDATED AT TIMESLICE',I5,/' NEW LIST....',(10I6))
      IX=0
      DO 4000 ISL = 0,NSL-1
        DO 4010 I = 1,3
          DO 4020 IMOL = 1,NMOL
            IN = .FALSE.
            DO 4030 ILIST = 1,NLIST
              IF(IMOL .EQ. MOL(ILIST)) IN = .TRUE.
4030          CONTINUE
            IF(.NOT. IN) THEN
              IX = IX + 1
                    X(IX) = X(INDX(IMOL,I,ISL)) C                    WRITE(6,*)
IX,INDX(IMOL,I,ISL)
            END IF
4020      CONTINUE
4010    CONTINUE
4000  CONTINUE
      NMOLN=NMOL-NLIST
      RETURN
      END

      SUBROUTINE PRINT(RCF,IX,IY,IC1,IC2,NRCF,ITOUT)
        REAL*8 RCF(0:NRCF)
```

```
      CHARACTER*1 XYZ(1:3)
      CHARACTER*127 DESCR
      CHARACTER*15 WHICH(0:9)
      DATA WHICH /'R(123)  ','V(123)  ','VXW(123)     ','RXW(123)
     1           ,'(RXW)XW','VXW(L)','FXW(L)       ','TQXV(L)     ',
     1            'W(123)       ','RXW(L)       '/
      DATA XYZ /'X','Y','Z'/

      IF (IX .EQ. IY .AND. IC1 .EQ. 0 .AND. IC2 .EQ. 0) THEN
        DESCR=WHICH(IX)//' AUTOCORRELATION FUNCTION'
      ELSE
       DESCR=WHICH(IX)//'('//XYZ(IC1)//')-'//WHICH(IY)//'('//XYZ(IC2
     1  //') CROSS-CORRELATION FUNCTION'
      END IF
      WRITE(ITOUT,*) DESCR
      WRITE(ITOUT,100) RCF
  100  FORMAT(1P,(1X,5D16.8))
      RETURN
    END
```

VIBRONIC INTERACTIONS IN POLYNUCLEAR MIXED-VALENCE CLUSTERS

I. B. BERSUKER and S. A. BORSHCH

Laboratory of Quantum Chemistry, Institute of Chemistry, Academy of Sciences of SSRM, Kishinev, USSR

CONTENTS

Advances in Chemical Physics, Volume LXXXI, Edited by I. Prigogine and Stuart A. Rice.
ISBN 0-471-54570-8